# $SO_2$ and $O_2$ separation by using ionic liquid absorption


## S.L. Rabie

**BEng (Chem. Eng.) (North-West University)**


Dissertation submitted for the degree of *Master in Chemical Engineering*

**North-West University Potchefstroom Campus**

Supervisor: Dr. M. Le Roux

November 2012

Innovation through diversity ®

NORTH-WEST UNIVERSITY ®
YUNIBESITI YA BOKONE-BOPHIRIMA
NOORDWES-UNIVERSITEIT
POTCHEFSTROOM CAMPUS

# Declaration

I, S.L. Rabie, hereby declare that the dissertation entitled: "**$SO_2$ and $O_2$ separation by using ionic liquid absorption**", submitted in fulfilment of the requirements for the degree M.Eng is my own work, except where acknowledged in the text, and has not been submitted to any other tertiary institution in whole or in part.

Signed at Potchefstroom.

S.L. Rabie

Date

# Acknowledgements

The author would hereby wish to acknowledge and thank everyone who played a major part in the completion of this project, and in particular:

- Dr. Marco le Roux for his guidance and suggestions during the course of the project.
- Mr. Jan Kroeze and Mr. Adrian Brock for helping with the design, building and repair of the equipment.
- Miss Eleanor de Koker for placing all the orders.
- HySA for providing the funding for the project.
- Mr. Max Tietz for his help with the experiments and analysis of the data.
- Prof. Hein Neomagus for giving advice on the thermodynamics of the process.
- Prof. Schalk Vorster for proof reading the report.
- My friend Jean du Toit for his support during the three years of this project.

# Abstract

In order to reduce the amount of pollution that is generated by burning fossil fuels alternative energy sources should be explored. Hydrogen has been identified as the most promising replacement for fossil fuels and can be produced by using the Hybrid Sulphur (HyS) cycle. Currently the $SO_2/O_2$ separation step in the HyS process has a large amount of knock out drums. The aim of this study was to investigate new technology to separate the $SO_2$ and $O_2$. The technology that was identified and investigated was to separate the $SO_2$ and $O_2$ by absorbing the $SO_2$ into an ionic liquid.

In this study the maximum absorption, absorption rate and desorption rate of $SO_2$ from the ionic liquid [BMIm][$MeSO_4$] with purities of 95% and 98% was investigated. These ionic liquid properties were investigated for pure $O_2$ at pressures ranging from 1.5 to 9 bar(a) and for pure $SO_2$ at pressures from 1.5 to 3 bar(a) at ambient temperature. Experiments were also carried out where the composition of the feed-stream to the ionic liquid was varied with compositions of 0, 25, 50, 75 and 100 mol% $SO_2$ with $O_2$ as the balance. For each of these compositions the temperature of the ionic liquid was changed from 30$^o$C to 60$^o$C, in increments of 10$^o$C.

The absorption rate of $SO_2$ in the ionic liquid increased when the mole percentage $SO_2$ in the feed stream was increased. When the temperature of the ionic liquid was decreased the maximum amount of $SO_2$ that the ionic liquid absorbed increased dramatically. However, the absorption rate was not influenced by a change in the absorption temperature.

The experimental results for the maximum $SO_2$ absorption were modelled with the Langmuir absorption model. The model fitted the data well, with an average standard deviation of 17.07% over all the experiments. In order to determine if the absorption reaction was endothermic or exothermic the Clausius-Clapeyron equation was used to calculate the heat of desorption for the desorption step. The heat of desorption data indicated that the desorption of $SO_2$ from this ionic liquid was an endothermic reaction because the heat of desorption values was positive. Therefore the absorption reaction was exothermic.

From the pressure-change experiments the results showed that the mole percentage of $O_2$ gas that was absorbed into the ionic liquid was independent of the pressure of the $O_2$ feed.

On the other hand, there was a clear correlation between the mole percentage $SO_2$ that was absorbed into the ionic liquid and the feed pressure of the $SO_2$. When the feed pressure of the $SO_2$ was increased the amount of $SO_2$ absorbed also increased, this trend was explained with Fick's law.

In the study the effect of the ionic liquid purity on the $SO_2$ absorption capacity was investigated. The experimental results for the pressure experiments showed that the 95% and 98% pure ionic liquid absorbed about the same amount of $SO_2$. During the temperature experiments the 95% pure ionic liquid absorbed more $SO_2$ than the 98% pure ionic liquid for all but two of the experiments. However the 95% pure ionic liquid also absorbed small amounts of $O_2$ at 30 and 40$^oC$ which indicated that the 95% pure ionic liquid had a lower selectivity than the 98% pure ionic liquid. Therefore, the 95% pure ionic liquid had better $SO_2$ absorption capabilities than the 98% pure ionic liquid.

These result showed that the 98% pure ionic liquid did not absorb more $SO_2$ than the 95% pure ionic liquid, but it did, however, show that the 98% pure ionic liquid had a better selectivity towards the $SO_2$. Hence, it can be concluded that even with the $O_2$ that is absorbed it would be economically more advantageous to use the less expensive 95% pure ionic liquid rather than the expensive 98% pure ionic liquid, because the $O_2$ would not influence the performance of the process negatively in such low quantities.

**Keywords:** Sulphur dioxide ($SO_2$), Oxygen ($O_2$), Separation, Ionic Liquid, Absorption

# Opsomming

Om die hoeveelheid besoedeling wat veroorsaak word deur die verbranding van fossielbrandstof te verminder, moet alternatiewe bronne van energie ondersoek word. Waterstof is geïdentifiseer as die belowendste alternatief vir fossiel brandstowe en kan vervaardig word met die “Hybrid Sulphur” (HyS)-siklus. Huidig het $SO_2$/$O_2$-skeidingsprosesse in die HyS-siklus ’n groot aantal proses eenhede. Vir hierdie studie was die doel om nuwe tegnologie wat gebruik kan word om die $SO_2$ en die $O_2$ te skei, te ondersoek. Die tegnologie wat geïdentifiseer is om $SO_2$ en die $O_2$ te skei, is die absorpsie van die $SO_2$ in ioniese vloeistowwe.

Gedurende hierdie studie is die maksimum absorpsie, absorpsietempo en die desorpsietempo van die ioniese vloeistowwe [BMIm][$MeSO_4$] met suiwerhede van 95% en 98% ondersoek. Hierdie eienskappe van die ioniese vloeistowwe is ondersoek vir suiwer $O_2$ by drukke wat gewissel het van 1,5 tot 9 bar(a) en vir suiwer $SO_2$ by drukke van 1,5 tot 3 bar(a) by kamertemperatuur. Eksperimente is ook uitgevoer waar die samestelling van die voerstroom verander is na 0, 25, 50, 75 en 100 mol% $SO_2$ met $O_2$ as die balans. Vir elkeen van hierdie samestellings is die temperatuur van die ioniese vloeistowwe na 30, 40, 50 en 60$^oC$ verander.

Die absorpsietempo in die ioniese vloeistowwe het toegeneem met verhoging van die mol% $SO_2$ in die voerstroom. Die maksimum hoeveelheid $SO_2$ wat die ioniese vloeistowwe geabsorbeer het, het dramaties toegeneem as die temperatuur van die ioniese vloeistowwe verlaag is. Daarenteen was die absorpsietempo nie beïnvloed deur die verandering in temperatuur nie.

Die resultate van die maksimum $SO_2$-absorpsie is gemodelleer met die Langmuir-absorpsiemodel. Die model het die eksperimentele data goed gepas en daar was 'n gemiddelde standaardafwyking tussen die model en die data van 17.07% vir al die eksperimente. Om te bepaal of die absorpsie reaksie endotermies of eksotermies is, was die Clausius-Clapeyron vergelyking gebruik om die desorbsie hitte te bepaal. Hierdie data het aangedui dat die desorbsie van $SO_2$ in hierdie ioniese vloeistof ‘n endotermiese reaksie was

aangesien die desorpsie hitte waardes positief was. Dus was die absorpsie reaksie dan eksotermies.

Vir die druk-eksperimente het die resultate getoon dat die mol% $O_2$ wat in die ioniese vloeistowwe geabsorbeer is, onafhanklik is van die $O_2$-voerdruk. Daarteenoor was daar 'n duidelike korrelasie tussen die mol% $SO_2$ wat in die ioniese vloeistowwe geabsorbeer is en die voerdruk van die $SO_2$. Met die verhoging van die voerdruk van die $SO_2$, het die hoeveelheid $SO_2$ wat geabsorbeer is ook toegeneem. Hierdie tendens kon met behulp van Fick se wet verduidelik word.

In die projek is die effek van die ioniese vloeistowwe se suiwerheid op die $SO_2$-absorpsievermoë ondersoek. Die resultate vir die druk-eksperimente het getoon dat die 95% en 98%-suiwer ioniese vloeistowwe omtrent dieselfde hoeveelhede $SO_2$ geabsorbeer het. In die temperatuur-eksperimente het die 95%-suiwer ioniese vloeistowwe meer $SO_2$ geabsorbeer as die 98%-suiwer ioniese vloeistowwe in veertien van die sestien gevalle. Die 95%-suiwer ioniese vloeistowwe het egter ook klein hoeveelhede $O_2$ geabsorbeer by 30 en 40$^{o}$C, wat toon dat die 95%-suiwer ioniese vloeistowwe 'n laer selektiwiteit het as die 98%-suiwer ioniese vloeistowwe. Dit dui daarop dat die 95%-suiwer ioniese vloeistowwe ‘n beter $SO_2$-absorpsievermoë het as die 98%-suiwer ioniese vloeistowwe.

Hierdie resultate het gewys dat die 98%-suiwer ioniese vloeistowwe nie meer $SO_2$ absorbeer as die 95%-suiwer ioniese vloeistowwe nie. Dit het egter bewys dat die 98%-suiwer ioniese vloeistowwe 'n beter selektiwiteit vir $SO_2$ het. Dus, sal dit ekonomies baie meer voordelig wees om die 95%-suiwer ioniese vloeistowwe eerder as die 98%-suiwer ioniese vloeistowwe te gebruik, want die $O_2$ wat geabsorbeer word sal nie die proses negatief beïnvloed teen sulke lae hoeveelhede nie.

**Sleutelwoorde:** Swaweldioksied ($SO_2$), Suurstof ($O_2$), Skeiding, Ioniese Vloeistowwe, Absorpsie

# Table of contents

# List of figures

# List of tables

# List of symbols

| Symbol | Unit | Description |
|---|---|---|
| $C_A$ | $Mol/m^3$ | Molar concentration of A |
| $D_{AB}$ | $m^2/s$ | Diffusion coefficient |
| H | bar | Henry's constant |
| $\Delta H_{des}$ | kJ/mol | Heat of desorption |
| $J_{Az}$ | $kg/s \cdot m^2$ | Molar flux of A in z direction |
| k | 1/bar | The dissolution constant |
| $k_b$ | $m^2\ kg\ s^{-2}K^{-1}$ | Boltzmann constant |
| $k_F$ | - | Freundlich constant |
| MW | g/mol | Molecular weight |
| m | g | Mass |
| $N_A$ | $mol^{-1}$ | Avogadro's number |
| N | - | Number of data points |
| n | mol | Amount of mole |
| $n_F$ | - | Freundlich exponent |
| P | bar | Pressure |
| p | - | Number of fitted parameters |
| q | mol $SO_2$/mol IL | Amount of $SO_2$ absorbed into the ionic liquid |
| $q_{max}$ | mol $SO_2$/mol IL | Maximum amount of $SO_2$ absorbed into the ionic liquid |
| R | J/mol·K | Gas constant |
| r | Å | Radius of a diffusing particle |
| T | $^oC$ | Temperature |
| V | $m^3$ | Volume |
| x | - | Mole fraction |
| $y_{exp}$ | - | Experimental value |
| $y_{calc}$ | - | Value predicted by the model |
| ρ | $g/cm^3$ | Density |
| η | mPa·s | Viscosity |

# Abbreviations

| Abbreviation | Meaning |
|---|---|
| [BMIm][$MeSO_4$] | 1-Butyl-3-Methylimidazolium methyl sulphate |
| CI | Confidence interval |
| FPR | Forward pressure regulator |
| GC | Gas chromatograph |
| IFP | Institut français du pétrole |
| IL | Ionic liquid |
| SD | Standard deviation |
| SRNL | Savannah River National Laboratory |
| UHP | Ultra-high purity |

# Chapter 1

# Introduction

## 1.1 Background

Fossil fuels currently meet most of the world's energy requirements; for example by burning coal to generate electricity, using oil to manufacture petrol to power cars and using gas to heat homes. According to Shafiee & Topal (2009:186) there are enough coal reserves remaining worldwide for the next 107 years and enough natural gas reserves left for the next 37 years. The US geological survey estimates that there is a total of 2.6 trillion barrels of oil left in the world, whilst at present about 30.6 billion barrels of oil is used per year around the world. When the annual growth rate and the population increase is taken into account, the oil reserves may last for only 25 more years; although oil shale and tar sands could add another 30 years to that estimation (Lattin & Utgikar, 2007:3230). These facts, as well as the fact that the burning of fossil fuels pollutes the atmosphere, suggest that it is very important to explore alternative energy sources as soon as possible.

Currently the automotive sector consumes the bulk of available oil. In 2004, the US utilized 20 million barrels of oil per day with 13 million of the total being used by the transportation sector (Lattin & Utgikar, 2007:3230). Biodiesel, electricity, ethanol, hydrogen, methanol, natural gas, propane and solar energy are all examples of alternative fuels that have been applied commercially as a replacement for petroleum. Of all these alternatives, hydrogen has one of the best chances of being implemented on a commercial scale. The main reasons why hydrogen is one of the most likely alternative fuels to be used on a large scale are energy security and low levels of pollution. Hydrogen is one of the most abundant elements in the universe and it is a clean fuel (when hydrogen is combusted the only by-product is water vapour). Therefore, hydrogen is a very attractive alternative to petroleum as a fuel source for the future. It is very important to keep in mind that hydrogen is not an energy source but rather an energy carrier; thus it has to be manufactured just like electricity (Johnston *et al.*, 2005:571).

## 1.2 HyS cycle

### 1.2.1 Background and history

In Section 1.1 it was stated that the world has to minimize its dependence on fossil fuel to reduce pollution. Hydrogen was identified as the most promising replacement. Currently hydrogen is produced by reacting natural gas, naphtha or coal with steam to form hydrogen. This process, however, produces carbon dioxide. New processes are being developed to produce hydrogen from water by only using heat or a combination of heat and electricity. These new developments are known as thermochemical water-splitting cycles (Gorensek *et al.*, 2009:2).

Thermochemical cycles are made up of a series of connected chemical reactions. These reactions result in the dissociation of water into hydrogen and oxygen. In these thermochemical cycles the only consumable is water; all other reagents are recycled in the cycle and reused, bar minor losses. There are two types of thermochemical cycles: Pure thermochemical cycles and hybrid thermochemical cycles. The difference between the two is that the pure thermochemical cycle only requires heat to drive the reactions. On the other hand, a hybrid cycle has at least one electrochemical step. The Hybrid Sulphur (HyS) cycle is a hybrid thermochemical cycle because of the electrolysis step in the process (Gorensek *et al.*, 2009:2).

The HyS Cycle, also known as the Westinghouse Sulphur Cycle or the Ispra Mark 11 Cycle, was developed in the early 1970s by Westinghouse Electric Corporation. By 1978, all the basic chemistry steps for the HyS cycle were successfully demonstrated. A closed-loop integrated laboratory bench scale model was successfully operated and produced 120 litres of hydrogen per hour. Research continued on equipment design and optimization, materials of construction, integration with a nuclear/solar heat source, process optimization, and economics, until 1983. However, due to the fact that hydrogen could be produced from steam reforming of natural gas at low prices, as well as the lack of interest in developing advanced nuclear reactors and high temperature solar receivers at that time, the program was stopped (Summers *et al.*, 2005:2).

In 2002, a study was carried out to review all thermochemical hydrogen production cycles and find the leading contenders. The cycles were reviewed and ranked according to (Brown *et al.*, 2003:2-3):

- Minimum number of chemical reactions.
- Minimum number of separation steps.
- Minimum number of elements in the cycle.
- Using abundant elements in the earth's crust, oceans and atmosphere.
- Minimum number of expensive materials of construction by avoiding corrosive chemical systems
- Minimum flow of solids.
- Maximum heat input temperature
- High number of papers from many authors and institutions.
- Tests at moderate or large scale.
- High efficiency and the availability of cost data.

In the study 115 cycles were identified and evaluated, and the HyS cycle was ranked as number one (Summers *et al.*, 2005:2). Currently the HyS process is being developed by the Savannah River National Laboratory (SRNL) in the USA and forms part of the Nuclear Hydrogen Initiative (NHI) (Gorensek *et al.*, 2009:2). It was also identified by the North-West University, which form part of the HySA initiative, as the thermochemical cycle of choice.

### 1.2.2 Process description

The HyS cycle is one of the simplest thermochemical cycles because it only has liquid reagents and consists of just two reaction steps. These steps are the decomposition of sulphuric acid and the $SO_2$-depolarised electrolysis of water. Figure 1.1 shows a schematic representation of the HyS cycle.

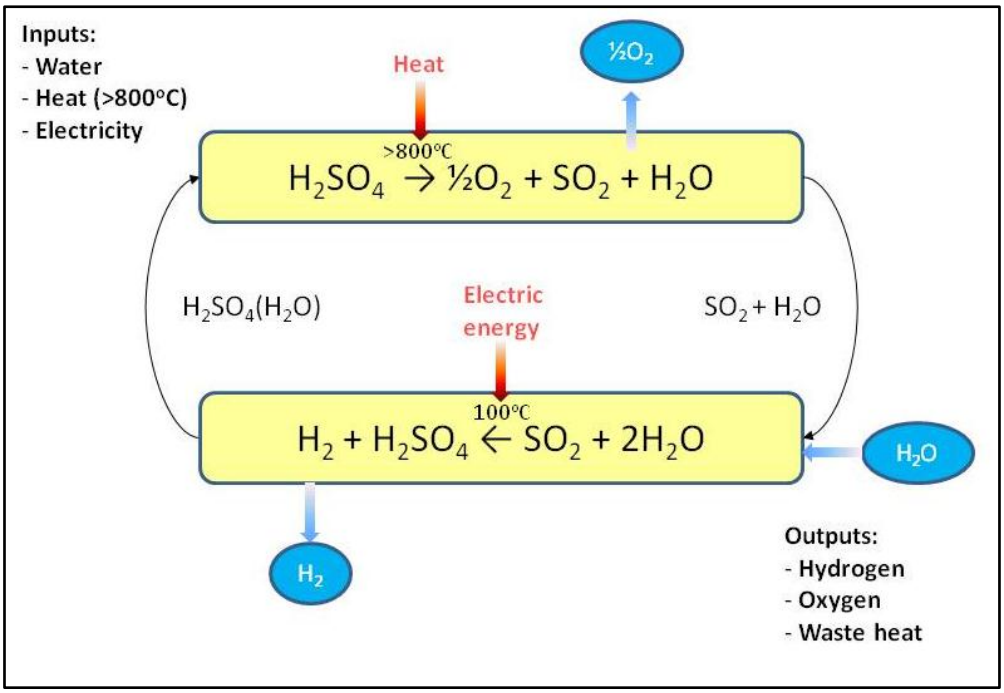


**Figure 1.1: HyS Cycle (Gorensek *et al.*, 2009:15)**

Figure 1.1 shows that the first step in the process is the decomposition of sulphuric acid at high temperatures. This decomposition reaction is common to all sulphur cycles. The second step in the HyS process is the $SO_2$-depolarised electrolysis of water. After the first step, $O_2$ is removed from the stream and the $SO_2$ and $H_2O$ are combined with make-up water, which is then fed to the anode of the electrolyser where the electrolysis takes place (Gorensek *et al.*, 2009:15). $H_2$ is produced at the cathode while $H_2SO_4$ is formed at the anode. Sulphuric acid is now recycled back to step one and $H_2$ is removed as the main product (Leybros *et al.*, 2010:1020). Figure 1.2 shows the HyS flow sheet proposed by SRNL.

Figure 1.2 shows the proposed flow sheet put forward by SRNL for the HyS process. Large numbers of knock-out drums and heat exchangers are required in the process to adjust the temperature and pressure of the reagents between the major process steps. It also serves to separate the volatile reagents like the $SO_2$ and $O_2$ from the less volatile reagents like the water and the sulphuric acid. The stream table shows that the $SO_2$ absorber uses about 5.92 kmol $H_2O$ per second (383 616 litre $H_2O$ per hour). From this data the $SO_2$ stream exiting the $SO_2$ absorber contained 0.019 mol% $O_2$ and the oxygen product stream contained no $SO_2$ after the $O_2$ drying step (Gorensek *et al.*, 2009:43).

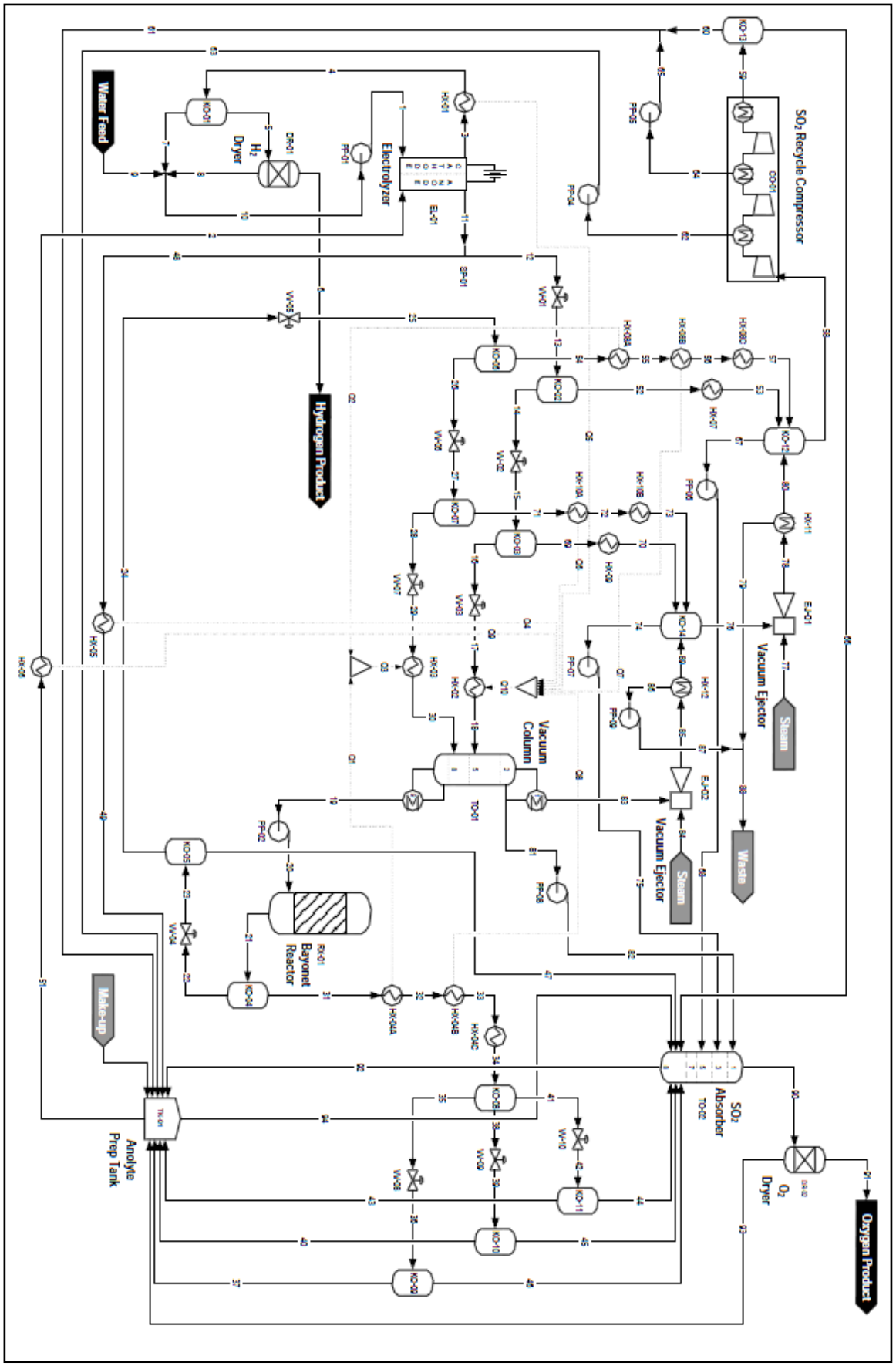


**Figure 1.2: Proposed HyS flow sheet (Gorensek *et al.*, 2009:43)**

For this study only the part where the $O_2$ is separated from the $SO_2$ before the $SO_2$ is sent to the second reaction will be considered. During the start-up phase of the Hydrogen research initiative at the NWU, Le Roux and Hattingh (2010:8) studied alternative separating methods for separating $SO_2$ and $O_2$ in the HyS process. The aim of this investigation was to identify different separation methods that could be introduced to the HyS process in an attempt to eliminate the large amount of knock out drums and columns. Four alternative methods were identified by which the $O_2$ and $SO_2$ can be separated. These methods are distillation, gas scrubbing, gas absorption into ionic liquids and membrane separation. After careful consideration, the method chosen for further study in this project was gas absorption into ionic liquids. Each of these methods will be discussed in more detail in Section 2.1 and some advantages and disadvantages will be given for each. An in-depth study will be performed to determine the influence of changing process conditions on the separation of $SO_2$ and $O_2$.

## 1.3 Problem statement

The problem statement for this study entails an investigation into the possibility of using ionic liquids of different purities to separate mixtures of $SO_2$ and $O_2$. Part of the study will include the influence of different process conditions like temperature, pressure and feed concentration on the separability of the gas mixtures.

## 1.4 Objectives

The separation of $O_2$ and $SO_2$ is an important part of the HyS process and was discussed in Section 1.2.2 above. It takes place between the decomposition of sulphuric acid and the $SO_2$-depolarised electrolysis of water (see Figure 1.2) and removes the $SO_2$ from the co-product, $O_2$. Hereafter, the purified $SO_2$ is send to the second reaction. In this study, ionic liquids will be used to absorb the $SO_2$ and then separate it from the $O_2$. Thereafter, the $SO_2$ is desorbed from the ionic liquid by temperature swing desorption.

The following conditions will be changed during the experimentation phase:

- Pressure of the $SO_2$ and $O_2$ fed to the system
- Absorption temperature of the ionic liquid
- Feed composition of the $SO_2$ and $O_2$
- Purity of the ionic liquid

During the course of this study the following questions will be answered:

- How will the absorption temperature influence the maximum absorption and absorption rates of $SO_2$ and $O_2$ into the ionic liquids?
- Will the feed composition of $SO_2$ and $O_2$ have an influence on the maximum absorption and the absorption rate of $SO_2$ and $O_2$ into the ionic liquids?
- What will the effect of the feed pressure of both the $SO_2$ and $O_2$ have on the absorption capabilities of the ionic liquid?
- Does the $SO_2$ absorbed into the ionic liquid desorb at a temperature higher than 120$^{o}$C?
- Will a more pure ionic liquid have a higher maximum absorption and absorption rate? In other words, is a more pure ionic liquid better at separating $SO_2$ and $O_2$ than a less pure, but more cost friendly, ionic liquid?

## 1.5 Outline

In this report a literature study will be conducted in Chapter 2, in which more information will be given on $SO_2/O_2$ separation, ionic liquids, industrial applications of ionic liquids and future applications of ionic liquids.

In Chapter 3 the materials, equipment and the experimental procedure as well as the expected results of the experiments will be discussed.

Chapter 4 contains the results and discussion of the experiments performed to study the effect of temperature on the $SO_2$ absorption, as well as the modelling of the experimental data.

In Chapter 5 the results obtained from the experiments on the effect of pressure on the $SO_2$ absorption into ionic liquid will be examined and the data discussed.

Finally, in Chapter 6 the final conclusions about the study and recommendations for future research will be made.

# Chapter 2

# Literature study

From Figure 1.2 in Chapter 1 it was concluded that the process to separate the $SO_2$ and the $O_2$ proposed by Gorensek *et al.* (2009:43) requires a large number of process units. It was decided to investigate the possibility of using a new technology to do the separation. The method that was decided upon was to use ionic liquids to separate the $SO_2$ and the $O_2$. This chapter will consider:

- Different methods of $SO_2/O_2$ separation (including ionic liquid absorption).
- Ionic liquids.
- Some industrial applications for ionic liquids.
- Future applications of ionic liquids.

## 2.1 $SO_2/O_2$ Separation

When $SO_2$ and $O_2$ were compared with one another, it was found that the largest differences in properties are their phase-change temperatures and the solubility of the components. For these property differences, the most applicable separation methods are:

- Distillation
- Membrane separation
- Gas absorption

Gas absorption will be divided into two processes for this study, namely gas absorption into water and gas absorption into ionic liquids. These two processes are both good separation methods for $SO_2$ and $O_2$ in the HyS process. This section will describe these four separation methods and give a process description, attention to the applicability of each method in the HyS process and list some advantages and disadvantages.

### 2.1.1 Distillation

**Process description**

Distillation is the most widely used separation technique in industry. Distillation consists of multiple contacts between liquid and vapour phases flowing counter-currently. At each contact the two phases are mixed to promote rapid partitioning of species by mass transfer. Thereafter, the phases are separated again. At each of these contact points, the lighter (more volatile) component will enter the vapour phase while the heavier (less volatile) component will enter the liquid phase. Thus the vapour flowing up the column is increasingly enriched with the lighter component, while the liquid flowing down is enriched with the heavier component (Seader & Henley, 2006:8).

Figure 2.1 shows a schematic representation of a distillation column with all the major accessories included. The feed is introduced at a certain point on the column (often near the middle), depending on the components in the feed. (Seader & Henley, 2006:8).

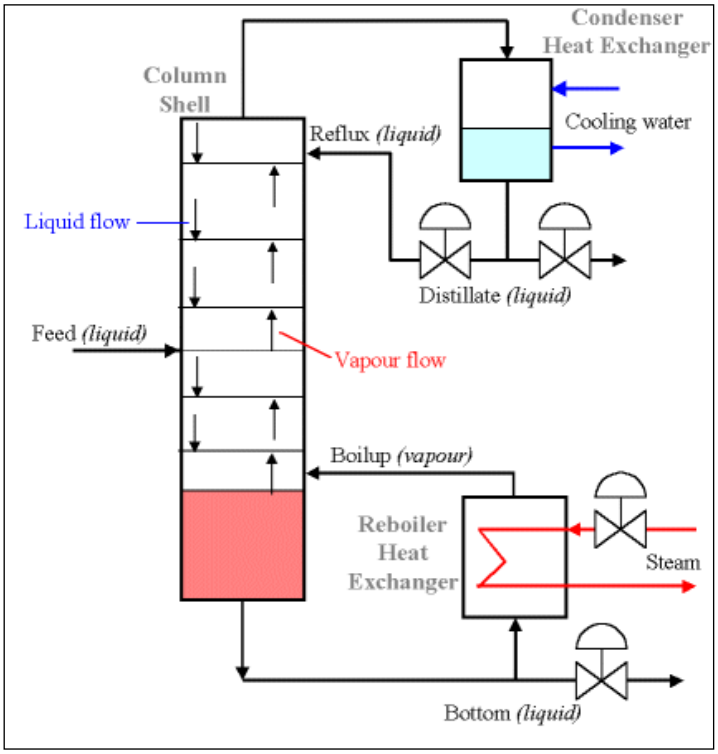


**Figure 2.1: Schematic representation of a distillation column (Le Roux and Hattingh, 2010:10)**

**Applicability**

In 1977, with the original design of the HyS process, Brecher *et al.* (1977:3) suggested that the $SO_2$ and $O_2$ should be separated by low temperature (cryogenic) distillation. The boiling points for $SO_2$ and $O_2$ are -10$^{o}$C and -183$^{o}$C, respectively (Perry & Green, 1997:2-25). Because of the large difference in boiling points these gases can be flashed into two streams. When the temperature is above the dew point of $O_2$ and below the dew point of $SO_2$, an $O_2$-rich top stream and a $SO_2$-rich bottom stream will be produced.

**Advantages and disadvantages**

Distillation is a well-known separation technique in the chemical industry. Table 2.1 gives some of the advantages and disadvantages of using distillation to separate $SO_2$ and $O_2$ (Le Roux and Hattingh, 2010:12).

**Table 2.1: Advantages and disadvantages of distillation**

| **Advantages** | **Disadvantages** |
|---|---|
| Known technology | Expensive |
| Easy to design | Hard to operate |
| Large operating window | Best operation at cryogenic conditions |
| Can theoretically be separated in one stage | Not all VLE data are available |

### 2.1.2 Membrane separation

**Process description**

Membranes act as selective barriers between two components or phases. A gas mixture is separated with a membrane due to the differences in the rates of permeation through the membrane. In other words, some of the gases pass through the membrane quickly while others move more slowly (Mulder, 1998:309). As can be seen from Figure 2.2, the feed stream is split into a permeate stream that passes through the membrane and a retentate stream that does not pass through. The characteristics of the membrane and the properties of the components will determine how fast the rate of separation is.

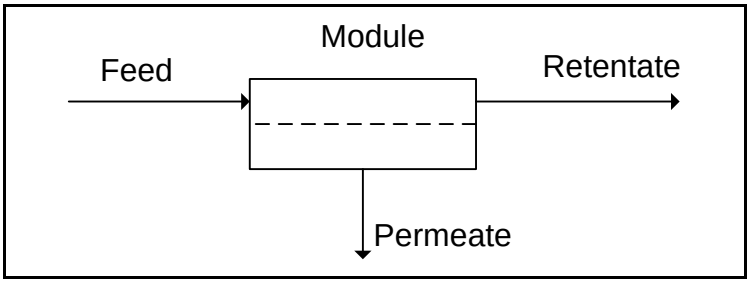


**Figure 2.2: Representation of a simple membrane process**

For a pair of gases like $O_2/N_2$, there are two parameters that characterise the membrane separation performance. These are the permeability coefficient and the selectivity of the gases. There exists a trade-off between these two parameters, for example a more permeable membrane will be less selective and vice versa. Because of this trade-off an upper limit for the performance of the system exists (Seo *et al.*, 2006:4501).

**Applicability**

Not much work has been done on the separation of $SO_2$ and $O_2$ with membranes. Most of the published results do not show much promise. The reason for the difficulty in separation is the similarity in the kinetic diameter of the two gases (Dong & Long, 2004:13). Polymer membranes have not developed to such an extent that it can aid in this separation, because many polymers will decompose at temperatures higher than 150$^o$C (Orme *et al.*, 2009:4089).

Dong & Long (2004:9) developed a membrane that gives a favourable ideal selectivity of 491 for $O_2$ over $SO_2$. These results were obtained at 20$^o$C and 10 bar. The membrane was reported to be a calcined B-AI-ZSM-5 zeolite made by using porous glass disks as a base.

**Advantages and disadvantages**

There are several advantages that membrane separation provides over conventional separation techniques like distillation. Some of the most important advantages and disadvantages of membrane separation are listed in Table 2.2 (Dong & Long, 2004:10, Perry & Green, 1997:22-38, Seader & Henley, 2006:713).

**Table 2.2: Advantages and disadvantages of membrane separation**

| Advantages | Disadvantages |
|---|---|
| Operates close to ambient temperature and pressure | For gas separation it can still be classified as a new technology |
| Low energy consumption | Very low permeation rates will require large surface areas |
| Simplicity in the separation method | The influence that the process conditions will have on the separation still needs to be investigated |
| Does not need any additives or phase changes | |
| Can separate azeotropes | |
| It is a kinetic and not equilibrium process | |
| It is easy to up-scale the process | |
| Gives a high sharpness of separation | |

### 2.1.3 Gas absorption

During the process of gas absorption a mixture of different gases comes into contact with a liquid called the absorbent or solvent. One or more of the components of the gas mixture is then dissolved into the liquid by means of mass transfer. Gas absorption can be used to recover valuable chemicals, remove impurities, contaminants, pollutants or catalyst poisons from gas mixtures and can be used to separate gas mixtures. This means that the product required at the end of the process may be either the component that was absorbed into the absorbent, or the component that was not absorbed. Because the absorbed component is also of interest, it is important to choose a solvent that desorbs (strips) the component quickly and efficiently. Desorption or stripping is the opposite of absorption and is the process whereby the absorbed component is removed from the liquid into which it has been absorbed (Seader & Henley, 2006:193).

When absorption of a gas into a liquid takes place without any chemical reaction and only the solubility of the gas into the liquid has an effect on the absorption, it is known as physical absorption. On the other hand if a reaction does take place when the gas is absorbed into the liquid, it is known as chemical absorption (Tondeur et al., 2008:311).

Choosing the correct solvent for use in a specific process is very important. A good solvent must have the following properties to ensure a good separation (Seader & Henley, 2006:201):

- High solubility for the solute
- Low volatility
- Low viscosity
- Stable
- Non-corrosive
- Non-foaming when in contact with the solute
- Non-toxic
- Not flammable
- Easy availability

#### 2.1.3.1 Gas absorption into water

**Process description**

The process description for the absorption into water is similar to the process description of absorption in general. This was discussed in Section 2.1.3, where a general overview of absorption was given.

Form literature the absorption of gas into water utilizes a physical absorption process (Seader & Henley, 2006:195).

**Applicability**

The solubility of $SO_2$ in water is 1 500 times more than the solubility of $O_2$ in water (Le Roux and Hattingh, 2010:13). $SO_2$ has a solubility in water of 0.078 mol $SO_2$/mol $H_2O$ at 30$^oC$ (Perry & Green, 1997:2-124). Gorensek *et al.* (2009:43) also incorporated this into the concept design of the HyS process, as can be seen in Figure 1.2. Jonker (2009:54) investigated the possibility of scrubbing the stream from the decomposition reactor in the HyS process with water. The assumption was made that only $SO_2$, $O_2$ and $H_2O$ were present in the feed to the scrubber, which meant that the remaining acid in the stream from the reactor had to be removed before the scrubber. The acid can be removed by a single knock-out drum directly after the reactor. After this, the stream is cooled and decompressed to 21 bar and 40$^oC$. At these conditions the stream would consist of a $SO_2$-rich liquid and a saturated vapour mixture. Therefore, a second knock-out drum is needed to separate the

two phases before feeding to the scrubber. The knock-out drum is FL-01 in Figure 2.3. Figure 2.3 shows the proposed flow diagram for the separation of $SO_2$ and $O_2$ by absorbing the $SO_2$ into water (Jonker, 2009:55). Jonker (2009:43) found that feed composition, temperature and pressure have notable influences on the efficiency of the separation.

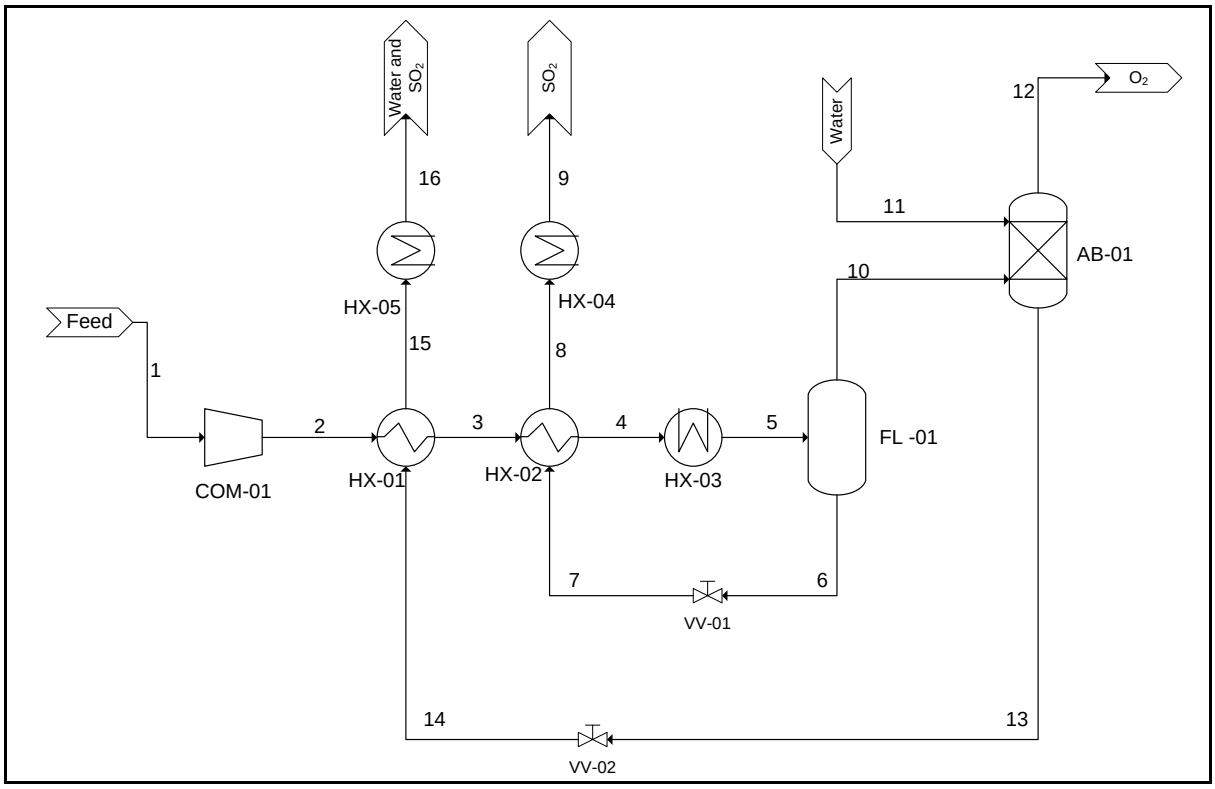


**Figure 2.3: Proposed $SO_2$/$O_2$ separation by means of a water scrubber (Jonker, 2009:55)**

**Advantages and disadvantages**

This is, again, a proven technology that is used to remove $SO_2$ from flue gas. Table 2.3 shows some of the advantages and disadvantages of the design (Le Roux and Hattingh, 2010:15, Perry & Green, 1997:2-124, Lee *et al.*, 2008:6035).

**Table 2.3: Advantages and disadvantages of $SO_2$ absorption into water**

| Advantages | Disadvantages |
|---|---|
| Known technology | Expensive |
| Easy to design | Hard to operate |
| Water has high $SO_2$ solubility | Normally only used to remove impurities |
| Desorption of $SO_2$ not necessary | Possible environmental hazard |
| Can use recycled process water | A pre-separation step is needed |
| | Lower $SO_2$ solubility than ionic liquid. |

#### 2.1.3.2 Gas absorption into an ionic liquid

**Process description**

The process description and equipment used in the process of gas absorption into an ionic liquid, and for the absorption into water, are similar. A detailed description of these points was given in Section 2.1.3.

From literature there are three different opinions as to what type of process the absorption of $SO_2$ into an ionic liquid are. These opinions are that the absorption is a:

- Physical process (Huang *et al.*, 2006a:4029, Ren *et al.*, 2010:2179).
- Combination of a physical and chemical process (Ren *et al.*, 2010:2179)
- Chemical process (Shiflett & Yokozeki, 2010:1375).

Huang *et al.* (2006b:4028) used H NMR spectra together with FT-IR spectra to show that no new chemical bonds formed and only molecular $SO_2$ were observed after the absorption into the ionic liquids, which indicates that the $SO_2$ is physically absorbed into the ionic liquids. Ren *et al.* (2010:2179) compared the viscosity, conductivity and density of two groups of ionic liquids (normal ionic liquids and task-specific ionic liquids) and concluded that the way normal ionic liquids absorb $SO_2$ is purely physical, but the task-specific ionic liquids uses a combination of both chemical and physical absorption. Finally, Shiflett & Yokozeki, (2010:1370) used an equation of state model to calculate excess (Gibbs, enthalpy and entropy) functions as well as Henry's law constants, which indicated that the ionic liquids used chemical absorption to absorb the $SO_2$ into the ionic liquid. This shows that it is not that easy to determine with absolute certainty which absorption process is always applicable.

**Applicability**

Ionic liquids are made up of cations and anions. It is regarded as solvents of the future due to its ability to absorb large amounts of certain gases and its regeneration ability. It is also considered to be "green" solvents because it has very low volatility, which means that almost no solvent will be lost due to evaporation (Wong *et al.*, 2002:1089). Ionic liquids will be discussed in more detail in Section 2.1.3.3 of this chapter.

In 2008, Lee *et al.* (2008:6034) suggested that the ionic liquid 1-Butyl-3-Methylimidazolium methyl sulphate [BMIm][$MeSO_4$] should be used as an absorbent for $SO_2$ in the production of hydrogen via thermochemical cycles. [BMIm][$MeSO_4$] was selected as the most appropriate

absorbent for thermochemical cycles from a number of tested ionic liquids, because of its thermal stability, high $SO_2$ absorption and high initial absorption rate (Lee *et al.*, 2008:6035). Figure 2.4 shows the chemical structure of [BMIm][$MeSO_4$].

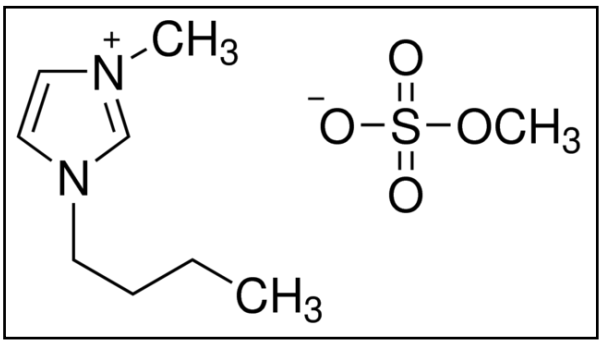

**Figure 2.4: Chemical structure of [BMIm][$MeSO_4$] (Sigma-Aldrich, 2012)**

Lee *at al.* (2008:6033) shows that [BMIm][$MeSO_4$] is thermally stable up to a temperature of 300$^o$C. It was also shown that [BMIm][$MeSO_4$] absorbed large amounts of $SO_2$ up to 1.38 mol $SO_2$/mol IL at 35$^o$C and ambient pressure. It has the highest initial absorption rate and it can desorb $SO_2$ completely reversibly. The ionic liquid thus has very good regeneration abilities, and can be used several times without losing any of its capacity to absorb $SO_2$. Figure 2.5 shows that after three times the ionic liquid still had the same absorption capacity (Lee *et al.*, 2008:6035).

In the previous section the three absorption types were discussed. For the chosen ionic liquid, [BMIm][$MeSO_4$], it seems as if physical absorption would be the preferred mechanism. This decision was made because [BMIm][$MeSO_4$] is a normal ionic liquid and not a task-specific one, which according to Huang *et al.* (2006b:4029) and Ren *et al.* (2010:2179) means that $SO_2$ is physically absorbed into the ionic liquid.

For the experiments in Figure 2.5 the absorption was done at 50$^o$C and desorption at 130$^o$C, 100$^o$C, and 70$^o$C. Figure 2.5 shows that for a constant temperature the amount of $SO_2$ absorbed remains the same even after three repeats. The figure also shows that almost all the $SO_2$ is desorbed from the ionic liquid after each of the absorption steps. The figure indicates a temperature dependency for the rate of desorption exemplified by the change in the slope of the $SO_2$-loading as a function of time and temperature (see Figure 2.5) which will be discussed in the influence of process conditions (Lee *et al.*, 2008:6034).

One of the main reasons why ionic liquids are not used more often in industry is because they are expensive. The cost of the ionic liquid [BMIm][$MeSO_4$] ranges from R1 100.00/100g to R10 000.00/100g, depending on the purity of the liquid (Sigma-Aldrich, 2011)

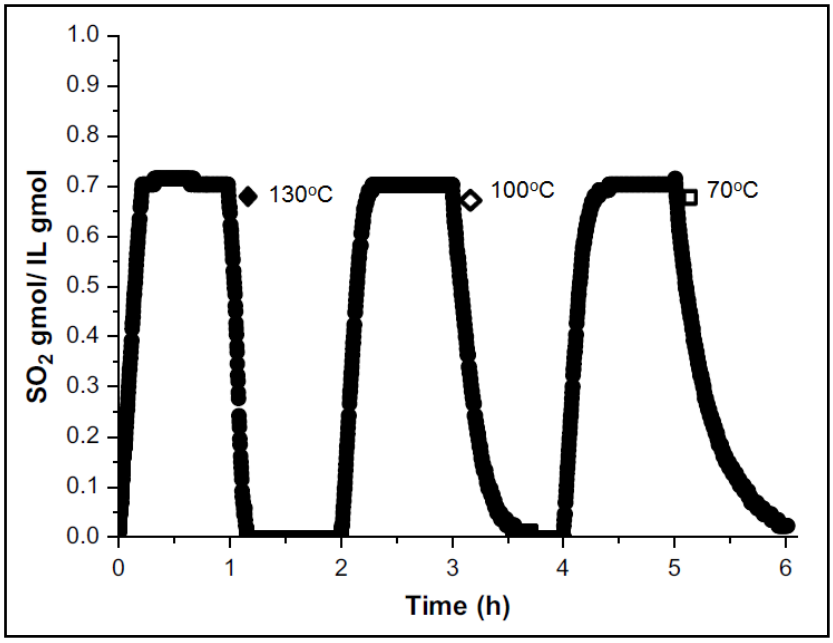


**Figure 2.5: $SO_2$ absorption and desorption cycles using [BMIm][$MeSO_4$] (Lee *et al.*, 2008:6035)**

Kim *et al.* (2008:5) proposed a separation technique for $SO_2$ and $O_2$ very similar to the Linde Solinox process. This technique consists of a separation and regeneration cycle for the separation of $SO_2$ and $O_2$. It uses temperature swing absorption technology and is designed specifically for thermochemical cycles. Figure 2.6 shows a flow diagram for this separation process.

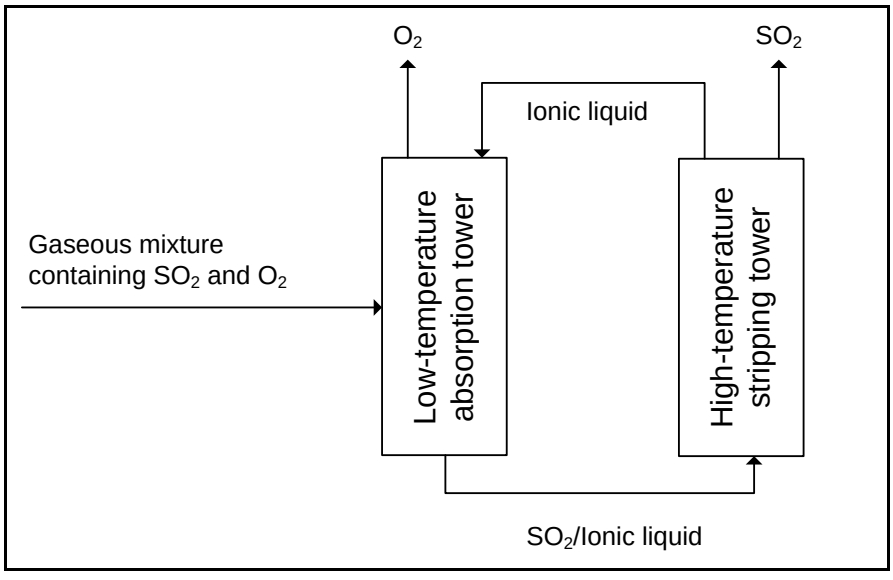


**Figure 2.6: Ionic liquid absorption and desorption (Kim *et al.* 2007:1)**

Figure 2.6 shows that an $SO_2$ and $O_2$ stream is fed to the bottom of the low temperature absorption tower. Here the gas will come in contact with the ionic liquid stream from the striping tower counter-currently. In the absorption tower the $SO_2$ will be absorbed into the ionic liquid; this step will take place between 20$^oC$ and 50$^oC$. The $O_2$ stream will leave at the top of the absorber and the $SO_2$-rich ionic liquid will leave at the bottom of the tower, to be fed into the high-temperature stripping tower. The $SO_2$ will be stripped from the ionic liquid by increasing the temperature to between 120$^oC$ and 200$^oC$. This will produce a depleted ionic liquid stream that is recycled back to the absorption tower and a 98% to 99% pure $SO_2$ stream that will be sent to the next processing step. With this setup an $SO_2$ recovery of 85% to 95% can be achieved, depending on the process conditions (Jonker, 2009:31).

**Influence of process conditions**

The size of the stripping section of the process is temperature-dependent. From Figure 2.5 it can be seen that the rate at which the ionic liquid desorbs the $SO_2$, decreases as the temperature is decreased. It may also be noted in the figure that the amount of gas desorbed was the same at all three temperatures, but the time for desorption of the $SO_2$ was not. Desorption at 130$^oC$ took just 600 seconds, but at 70$^oC$ it took more than 3600 seconds (Lee *et al.*, 2008:6034). This data illustrate that by desorbing the $SO_2$ at higher temperatures like 130$^oC$, the throughput of the process can be increased. In Section 4.2.2 the absorption rate will be considered to see how the absorption step can be shortened by changing the process conditions.

Figure 2.7 shows the effects of temperature and $SO_2$ partial pressure on the absorption capacity of the ionic liquid used by (Lee *et al.*, 2008:6035).

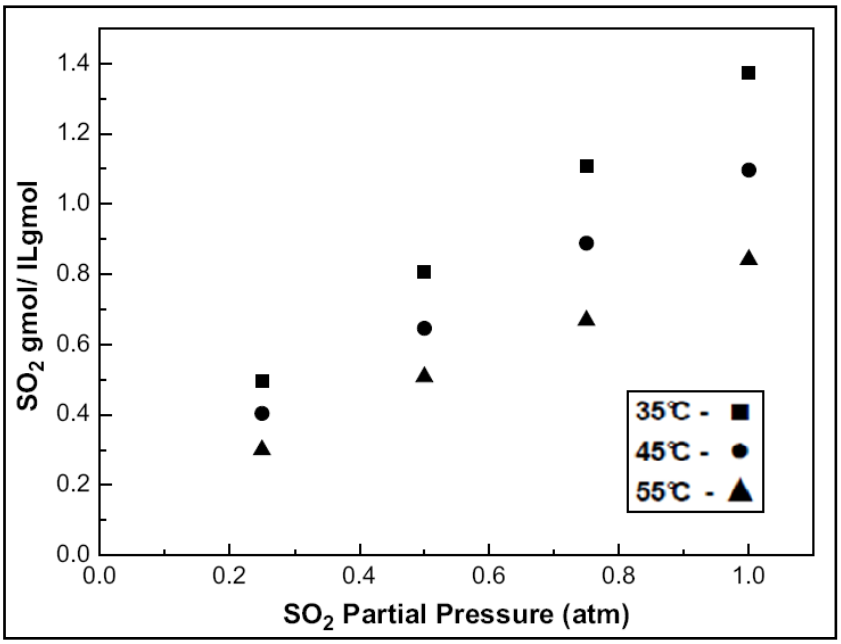


**Figure 2.7: $SO_2$ solubility at various temperatures and $SO_2$ partial pressures (Lee *et al.*, 2008:6035)**

Figure 2.7 shows that when the temperature is decreased and the partial pressure of $SO_2$ is increased, the amount of $SO_2$ absorbed into the ionic liquid increases (Lee *et al.*, 2008:6034).

**Advantages and disadvantages**

The use of ionic liquids is a new technology, even if it is based and operated on well-known absorption principles. Table 2.4 shows some advantages and disadvantages of $SO_2$ absorption into ionic liquids (Perry & Green, 1997:2-124, Lee *et al.*, 2008:6035).

**Table 2.4: Advantages and disadvantages of $SO_2$ absorption into ionic liquids**

| Advantages | Disadvantages |
|---|---|
| Based on well-known technology | Ionic liquid is new to this application |
| Ionic liquid has high $SO_2$ solubility | The solvent has an environmental and health risk |
| $SO_2$ can be desorbed easily with temperature swing | The ionic liquid is expensive |
| "Green" technology | |
| Almost no loss of solvent | |
| $SO_2$ desorbs almost completely | |
| Higher $SO_2$ solubility than water | |

#### 2.1.3.3 Absorption modelling

It is very important to be able to predict what the absorption capabilities of the solvent will be under conditions that are outside the range used in the study. To do this the results obtained from the experiments will be modelled using one of the isotherms discussed below. The fitting of the model will be discussed in Section 4.3.

**Langmuir isotherm**

The Langmuir equation was derived from simple mass-action kinetics, assuming chemisorption. This equation also assumes that the surface of the pores of the adsorbent is homogeneous and that the forces acting between the adsorbed molecules are negligible. It is restricted to type I isotherms which corresponds to unimolecular adsorption and has a maximum limit in the amount adsorbed. Although the equation was originally devised for only chemisorptions, it has been widely applied to physical adsorption as well (Seader & Henley, 2006:559).

The Langmuir equation can be expressed as follows for an absorption system (Locati *et al.*, 2009:456):

$$\boldsymbol{q} = \frac{\boldsymbol{q_{max} kP}}{\boldsymbol{1 + kP}} \qquad \text{Equation 2.1}$$

Where:

q – Amount of $SO_2$ absorbed into the ionic liquid (mol $SO_2$/mol IL).

$q_{max}$ – Maximum amount of $SO_2$ absorbed into the ionic liquid (mol $SO_2$/mol IL).

k – The dissolution constant.

P – The partial pressure of $SO_2$ in the feed gas stream

Figure 2.8 shows data of the dissolution of $CO_2$ into the ionic liquid [BMIm][$BF_4$], and the fitted Langmuir model.

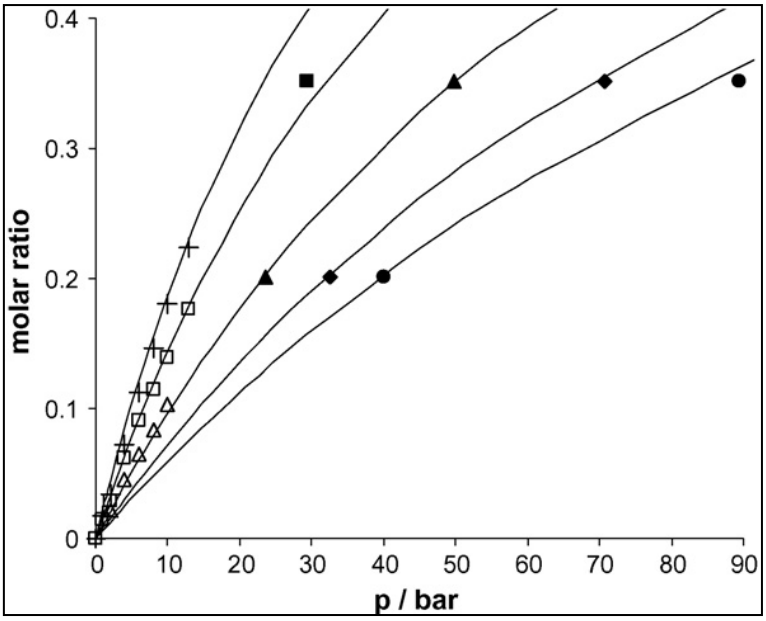


**Figure 2.8: $CO_2$ dissolution into ionic liquid [BMIm][$BF_4$] with fitted Langmuir model (Locati *et al.*, 2009:455)**

Locati *et al.* (2009:456) observed that the solvation energy does not change much when the molar fraction of the $CO_2$ is chanced from zero to 0.2. Locati *et al.* (2009:456) then anticipated that the solvation mechanism would not change in this range, which can be described by a Langmuir type dissolution mechanism. Hence the data in Figure 2.8 is fitted with the Langmuir model. Figure 2.8 show that the Langmuir model fits the above data well, although no reference to the error of the fitted model was given in the paper. However, it can visually be concluded that this model is valid to describe gas absorption into ionic liquids.

**Henry's law**

The solubility of a gas into a liquid is normally described in terms of Henry's law, provided that the solubility of the gas into the liquid is low and no chemical absorption takes place (Anthony *et al.*, 2002:7317). For gases with a high solubility into the liquid, Henry's law may not be applicable, even if the partial pressure of the gas is low (Seader & Henley, 2006:145). Equation 2.2 shows Henry's law (Anthony *et al.*, 2002:7317):

$$\boldsymbol{H = lim_{x \to 0} \frac{P}{x}} \qquad \text{Equation 2.2}$$

Where:

H – Henry's constant

P – Pressure of the gas

x – Mole fraction of the gas dissolved in the ionic liquid phase.

Thus if a graph of pressure versus mole fraction forms a straight line, Henry's law is applicable for that system. Figure 2.9 shows data of the solubility of $C_2H_4$ in the ionic liquid [bmim][$PF_6$] at three temperatures.

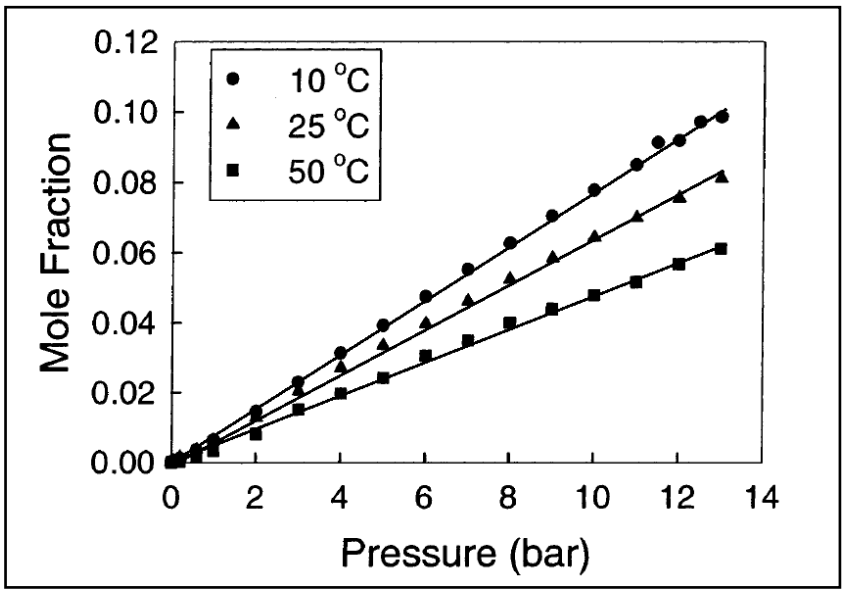


**Figure 2.9: $C_2H_4$ solubility in [BMIm][$PF_6$] at 10, 25 and 50°C (Anthony *et al.*, 2002:7317)**

From Figure 2.9 it may be seen that the data forms a straight line on the mole fraction versus pressure graph, therefore Henry's law is applicable for this data. A plot of the Henry's law model is represented by the three solids lines in the above figure.

**Freundlich isotherm**

The Freundlich isotherm is derived by assuming a heterogeneous sorbent with a nonuniform distribution of the heat of adsorption (Seader & Henley, 2006:561). This isotherm also assumes that there are many types of sites that act simultaneously, each site with a different free energy of sorption and that there is a large amount of sites available for adsorption (García-Zubiri *et al.*, 2009:11). Equation 2.3 shows the Freundlich equation:

$$q = k_F P^{\frac{1}{n_F}} \qquad \text{Equation 2.3}$$

Where:

q – Amount of $SO_2$ absorbed into the ionic liquid (mol $SO_2$/mol IL).

P – The partial pressure of $SO_2$ in the feed gas stream.

$k_F$ – Freundlich constant

$n_F$ – Freundlich exponent

Figure Figure 2.10 shows data of the adsorption of 2,2,4-trimethylpentane on a hydrocarbon adsorber at three different temperatures. The figure also shows the fitting of the Freundlich as well as the Langmuir isotherms to the data.

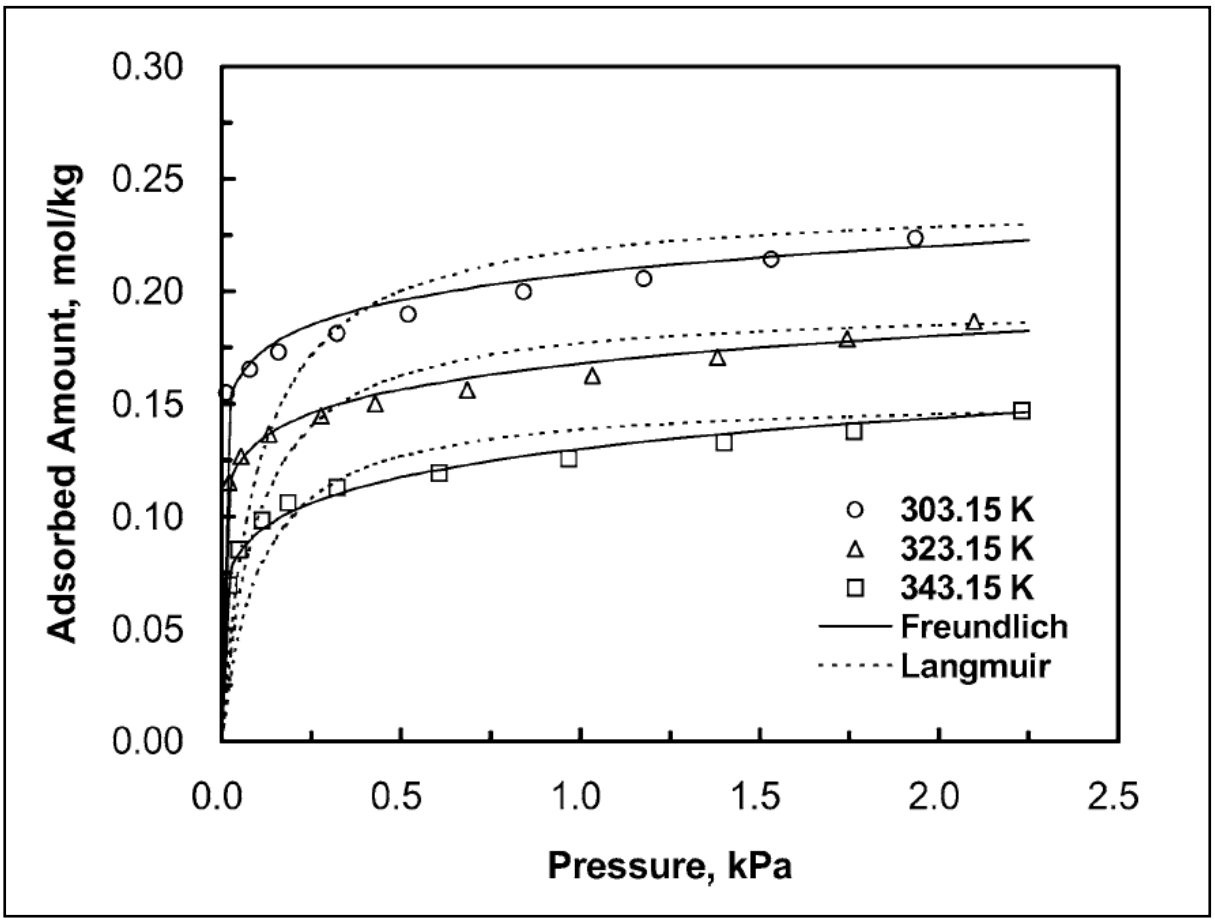


**Figure 2.10: Adsorption isotherms of 2,2,4-trimethylpentane on a hydrocarbon adsorber (Kim, 2004:292)**

Figure 2.10 shows the diference between the Freundlich and the Langmuir isotherms for one set of data. The reason that the Freundlich isotherm fits the data better than the Langmuir isotherm can be attributed to the heterogeneity of the adsorber. One of the limitations of the Freundlich isotherm is that it assumes there is no adsorption limit (García-Zubiri *et al.*, 2009:11).

## 2.2 Ionic liquid

Ionic liquids have been around for over a century. In 1888 ethanol ammonium nitrate, with a melting point of 52-55$^{o}$C, was reported. In 1914 the room-temperature ionic liquid ethyl ammonium nitrate was first synthesized. During the rest of the century the progress was slow, but recently the interest in ionic liquids has increased dramatically to a point where the

number of publications on ionic liquids has increased from below 50 in 1995 to just over 1 600 in 2008. In 2004 the first publicly announced industrial application of ionic liquids the Biphasic Acid Scavenging utilizing Ionic Liquids (BASIL) process was used by BASF. Ionic liquids also have a large number of other potential industrial applications, such as: catalytic reactions, gas separations, liquid-liquid extractions, electrochemistry, fuel cells, biotechnology especially for biocatalysts, synthesis of RNA and DNA oligomers and have been used to synthesize novel polymers and nanomaterials (Ren, 2009).

The general definition of ionic liquids is that they are a special class of molten salts existing in the liquid state below $100^oC$, and have a large temperature range within which they are stable liquids (Pereiro *et al.*, 2007:377). Ionic liquids consist of anions and cations and are named as [cation][anion] (Ren, 2009:3). One of the most important features of ionic liquids is the fact that, by changing the cation and anion on the molecule, the properties of the liquid can be changed to suit certain conditions and criteria. It has been estimated that there are up to $10^{14}$ different combinations of ionic liquids (Ren, 2009:7). The properties of the ionic liquids are determined by the anion and cation functional groups used on the ionic liquid. Thus, an ionic liquid having specific properties can be constructed. Some of the properties important for this study are the solubility of $SO_2$, viscosity of the ionic liquid, stable temperature range, purity of ionic liquid and its volumetric properties (Ren, 2009:8). Ionic liquids also have negligible vapour pressures, which means that they do not evaporate at room temperature making them potential “green” solvents (Manan *et al.*, 2009:2005).

### 2.2.1 Ionic liquid properties

The interaction between the structure and properties of ionic liquids must be known before ionic liquids can be selected for certain processes. Prior research shows that the anion of the ionic liquid has an influence on most of its properties. For the cation, the alkyl chain length and functional alkyl chain added are also of some importance to the properties of the ionic liquid. In this section, some of the different types of ionic liquids, the melting points and thermal stabilities, volumetric properties and viscosities of ionic liquids will be discussed (Ren, 2009:7).

#### 2.2.1.1 Types of ionic liquids

As stated above, ionic liquids are made up of anions and cations bonded together. There are many different ionic liquid types and these are normally defined by the cation of the ionic

liquid. The four most common types of ionic liquids are imidazolium, pyridinium, ammonium, and phosphonium. Figure 2.11 shows the chemical structures of these four cations.

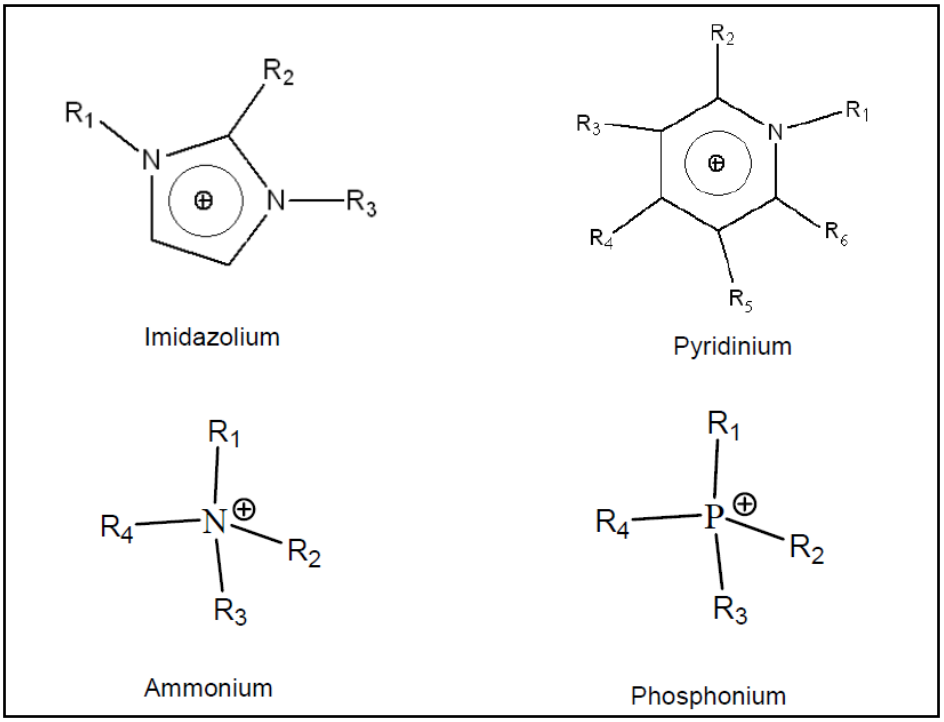


**Figure 2.11: Common cations used in ionic liquids (Camper, 2006:3)**

It is important to understand how ionic liquids are named. One of the most common ionic liquids is the imidazolium type ionic liquid. Its cation is a 1-alkyl-3-methylimidazolium, which is abbreviated as [RMIm]. The R represents the different alkyl chain lengths. The R can be replaced by the first letter of the alkyl chain, for example [EMIm] refers to 1-Ethyl-3-methylimidazolium, and [BMIm] refers to 1-Butyl-3-methylimidazolium. The anions in the ionic liquid are abbreviated as their molar formulas. Thus 1-Butyl-3-methylimidazolium tetrafluoroborate will be abbreviated as [BMIm][BF4] and 1-Hexyl-3-methylimidazolium methyl sulphate will be [HMIm][MeSO4] (Ren, 2009:3).

#### 2.2.1.2 Melting point and thermal stability

Ionic liquids normally consist of large and unsymmetrical ions; consequently they usually have low melting points. Therefore, small and symmetrical ions like halide anions have higher melting points and large amide anions like [$Tf_2N$] have lower melting points (Ren, 2009:8). The alkyl chain length also influences the melting point. At first the melting point decreases as the alkyl chain increases (but only to a certain length). From 8-10 carbon

atoms in the alkyl chain, the melting point increases when the alkyl chain increases. This happens due to the difficulty of ion packing (Huddleston *et al.*, 2001:159).

The thermal stability of an ionic liquid is an important property when it is being used as an absorbent, because the absorption normally takes place at low temperatures and desorption at high temperatures. For this reason the very wide liquid range of ionic liquids is an essential feature. The ionic liquids have such a wide liquid range that the only other solvents that can perhaps match them are liquid polymers (Anderson, 2008:2). The factor that has the largest influence on the thermal stability of ionic liquids is the anion used in the ionic liquid. The influence of the cation on the thermal stability is negligible in comparison with the anion. Therefore, before choosing an ionic liquid it is important to know what the conditions in the process will be to insure that the liquid is stable within that temperature range.

#### 2.2.1.3 Volumetric properties

The two main volumetric properties are compressibility and expansion upon absorption of the ionic liquid. It was found that the general trend for ionic liquids is to become more compressible when the temperature is increased. On the other hand, when the pressure is increased the ionic liquid becomes less compressible. It should be noted that the data used to draw this conclusion had very large standard deviations and the compressibility under changing pressure could be considered constant. The isothermal compressibilities of ionic liquids are similar to those of water and high-temperature molten salts. They are less compressible than organic solvents because there are very strong Coulombic interactions between the ions (Gardas *et al.*, 2007:84).

Gardas *et al.* (2007:85) also studied the isobaric expansion upon absorption of a few ionic liquids. It was found that the ionic liquid does not notably expand with an increase in temperature.

When $CO_2$ is absorbed into normal organic liquids, the volume normally increases. The classical definition of volume expansion is based on the change in the absolute volume of the liquid. Equation 2.4 shows this definition where $V_L$ is the volume of the entire liquid at a specific temperature and pressure while $V_2$ is the volume of the pure liquid at the same temperature and ambient pressure (Aki *et al.*, 2004:20363).

$$\frac{\Delta \boldsymbol{V}}{\boldsymbol{V}}\% = \frac{\boldsymbol{V_L(T,P,x1) - V_2(T,\ P_0)}}{\boldsymbol{V_2\ (T,\ P_0)}} \qquad \text{Equation 2.4}$$

Equation 2.4 was used to calculate the percentage volume expansion of all of the ionic liquids used in the study conducted by (Aki *et al.*, 2004:20363). Figure 2.12 shows the volume expansion upon absorption of the ionic liquids when $CO_2$ is absorbed, and compares them to two organic solvents.

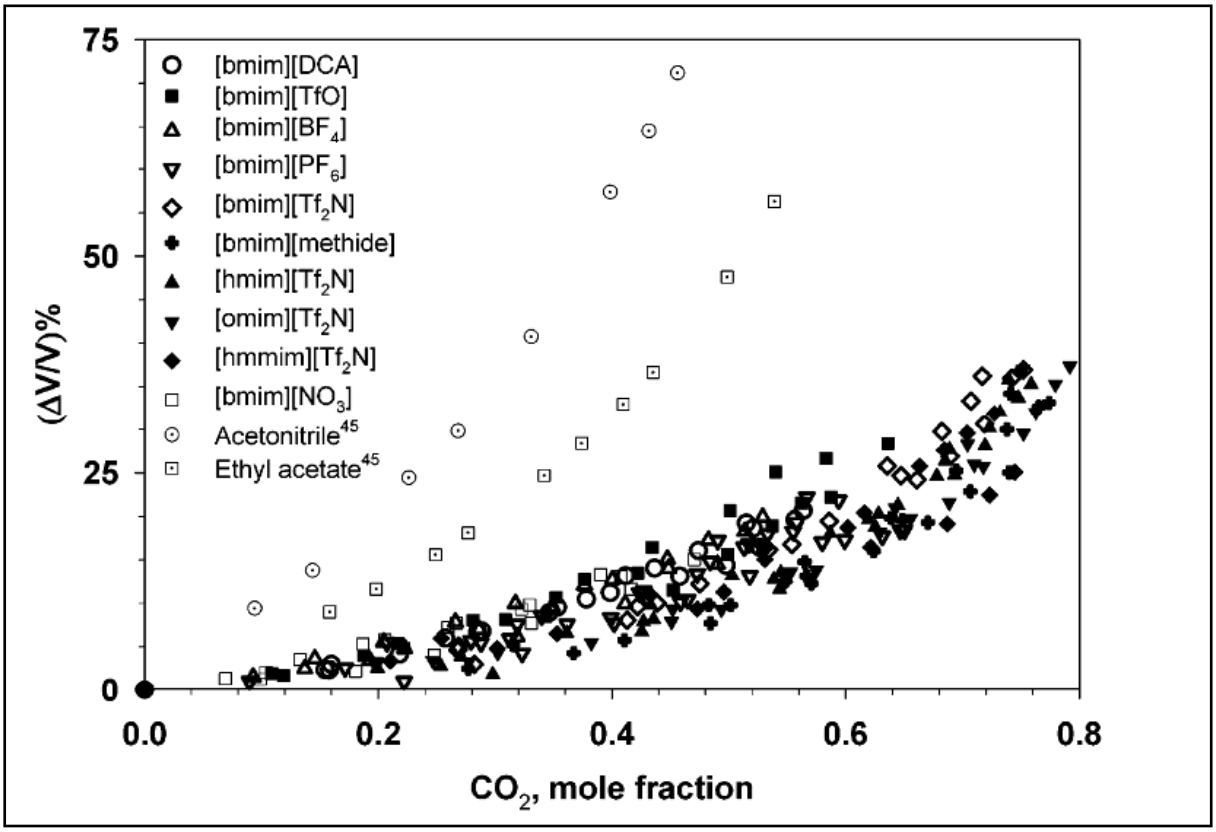


**Figure 2.12: Volume expansion upon absorption of ionic liquids and two organic solvents (Aki *et al.*, 2004:20363)**

From Figure 2.12 it can be seen that the volume expansion upon absorption is much less than that of the organic solvents. From these experiments Aki *et al.* (2004:20364) concluded that the ionic liquids expand to a very small degree when $CO_2$ is absorbed in them. This ionic liquid property is very important for the experiments that will be carried out in this study. It is important to know how the volume of the ionic liquid will change to compensate for a change in pressure or to insure that the absorption chamber is large enough to handle the liquid after it has expanded.

#### 2.2.1.4 Viscosity

The most common ionic liquids have viscosities between 10 mPa·s and 500 mPa·s. This is much higher than other common liquids like water, ethylene glycol and glycerol that have

viscosities of 0.89, 16.1, and 93.4 mPa·s, respectively (Camper, 2006:2). Temperature has a large influence on the viscosity of ionic liquids. When the temperature is increased the viscosity decreases, for example the viscosity of the ionic liquid [HMIm][PF6] deceases by about 50% when the temperature is increased by 10$^{o}$C from 20$^{o}$C to 30$^{o}$C (Ren, 2009:10). Another important influence on viscosity is the purity of the ionic liquid. Impurities like halides (from the ionic liquid syntheses process) and water (from the atmosphere) have an influence on the viscosity of ionic liquids. When the water content is increased the viscosity of the ionic liquid decreases; on the other hand, when the halide content is increased the viscosity increases (Anderson, 2008:5). The viscosity of ionic liquids will also be affected by the anion and cation chosen. The viscosity will increase when the alkyl chain length is increased. This is due to the stronger Van der Waals interactions. The symmetry of the molecule also affects the viscosity; for symmetrical molecules the viscosity will be higher than for asymmetrical molecules (Ren, 2009:10).

The viscosity of the ionic liquid will have a large influence on the gas absorption. The viscosity of the ionic liquid has to be low to insure a low pressure drop over the absorption chamber, as well as high heat and mass transfer (Seader & Henley, 2006:201). Therefore, it is important to know how the viscosity is influenced by the experimental conditions before selecting an ionic liquid.

## 2.3 Industrial application of ionic liquids

When discussing ionic liquids, the general perception is that they are not yet being applied in the industry. This assumption is incorrect and ionic liquids have been applied in industrial applications for over ten years. In this section the companies that have taken ionic liquids out of the laboratory into the plant, will be discussed, as well as the processes where the ionic liquids were applied. Table 2.5 shows some of the companies and processes that use ionic liquids in the industry.

**Table 2.5: Companies and processes that use ionic liquids in the industry**

| Company | Process description |
|---|---|
| BASF | The BASIL™ process was the first publicly announced commercial process utilising ionic liquids. It was introduced in Germany at the BASF site in Ludwigshafen in 2002. After ionic liquids were introduced into the process, the yield increased from 50 to 98% (Plechkova & Seddon, 2008:135). |
| | Ionic liquids have been used as entrainers or separation enhancers. The ionic liquid can then be used to break common azeotropes like water-tetrahydrofuran and water-ethanol. This reduces the cost of separation significantly (Plechkova & Seddon, 2008:136). |
| | For the reaction of butan-1,4-diol with phosgene BASF discovered that hydrogen chloride in ionic liquids can replace phosgene. When the reaction is repeated with hydrogen chloride in ionic liquids, the product is almost pure with 98% selectivity (Plechkova & Seddon, 2008:136). |
| Eastman Chemical Company | The BASIL™ process discussed above was the first publicly announced process utilizing ionic liquids. However, the Eastman chemical company had been running a process for the isomerisation of 3,4-epoxybut-1-ene to 2,5-dihydrofuran since December of 1996. (Plechkova & Seddon, 2008:137). |
| IFP (Institut français du pétrole) | BASF and Eastman chemical company commercialised the first processes using ionic liquids. IFP on the other hand operated the first pilot plant using ionic liquid. The Dimersol process consists of the dimerisation of alkenes, like propene and butane, to hexenes and octenes. (Plechkova & Seddon, 2008:137). |
| Air Products | A very exciting new technology was presented at the first International congress on ionic liquids by Dan Temple of Air products. This new technology can be used to store dangerous gases. It is at least twice as efficient as the normal processes that use adsorption of the gases onto solids. (Plechkova & Seddon, 2008:140). |
| LoLiTec | LoLiTec is a new company and specialises in developing applications for ionic liquids. One of the applications that they have developed is a practical and efficient way to clean high value and sensitive surfaces. Figure 2.13 shows the improvement when an ionic liquid is used to clean the spray nozzle. |

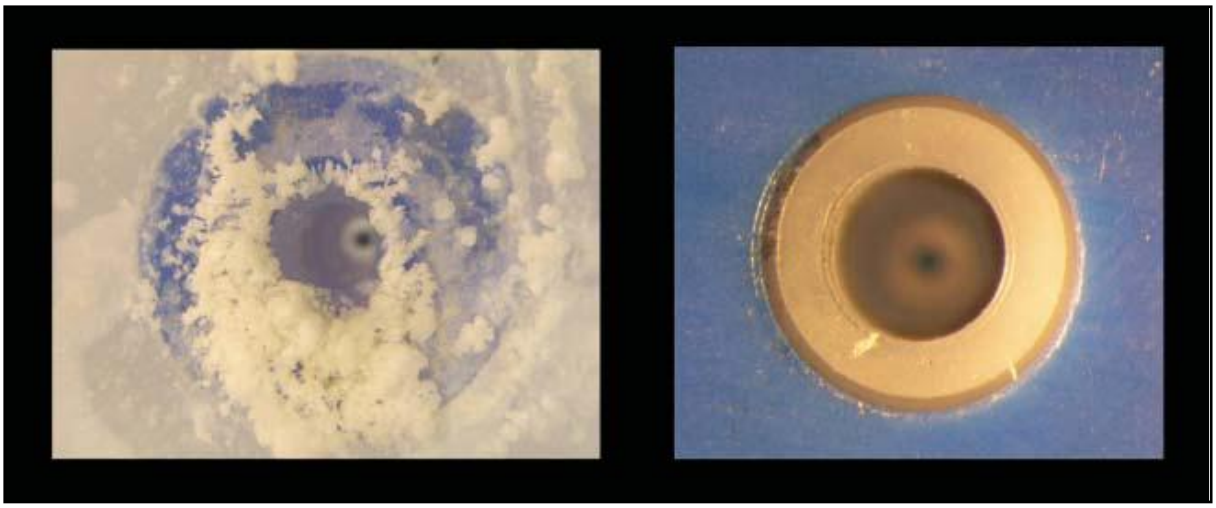

**Figure 2.13: A spay nozzle after 10 hours of operation. Nozzle for aqueous sodium chloride solutions (left) and ionic liquid (right) (Plechkova & Seddon, 2008:141)**

The companies mentioned in Table 2.5 are only a few that are researching and implementing ionic liquids in industry. Some of the other companies that were not discussed above are (Plechkova & Seddon, 2008:144):

- Degussa
- Central Glass Co. Ltd., Japan
- BP
- ExxonMobil
- Chevron and Chevron Phillips
- PetroChina
- Eli Lilly
- Pionics
- Scionix
- Linde

## 2.4 Future of ionic liquids

In the past few years the field of ionic liquids has grown remarkably quickly. The number of applications for ionic liquids and the diversity of the applications are remarkable. Figure 2.14 shows some of the applications of ionic liquids that can be expected in the future (Plechkova & Seddon, 2008:145).

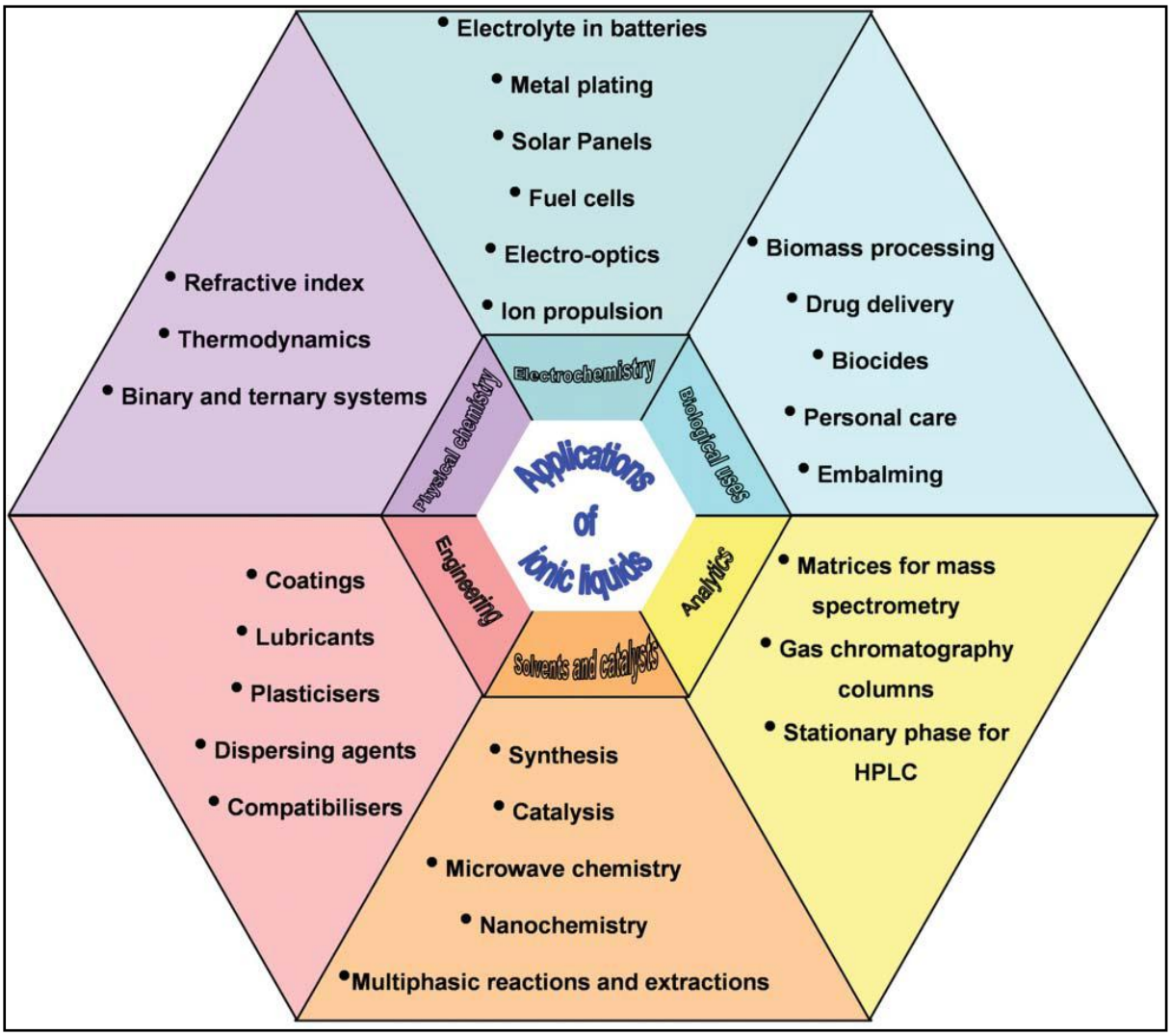


**Figure 2.14: Future applications of ionic liquids (Plechkova & Seddon, 2008:145)**

Figure 2.14 illustrates six main categories in which new applications for ionic liquids will be developed. These categories are analytics, biological uses, electrochemistry, physical chemistry, engineering and catalysts and solvents. Some of the well-known fields that ionic liquids will impact are gas chromatograph (GC) columns for chemical analysis and drug delivery in medicine, as well as the improvements of technologies like solar panels and fuel cells in the field of electrochemistry. Ionic liquids will also play a role in the field of thermodynamics in physical chemistry, as well as applications like coatings and lubricants in engineering. This study will focus on extractions in the solvents and catalyst category.

From the above description it can be seen that ionic liquids can be applied to a very broad range of topics. What makes them so interesting is the fact that they are so versatile, with almost endless possibilities. The most exciting fact is that scientists have only started to scratch the surface and that ionic liquids can potentially revolutionise some fields. The

following section looks at what results is expected to be obtained during the experiments described in Chapter 3.

## 2.5 Hypothesis

The amount of $SO_2$ absorbed and the rate at which the $SO_2$ is absorbed is influenced by the pressure, temperature, feed composition and purity of the ionic liquid.

Several hypotheses will be tested during this study:

- For low ionic liquid temperatures of 30$^oC$ the amount of $SO_2$ absorbed is more than when the temperature is increased to 60$^oC$, but the absorption rate will increase with an increase in temperature.
- If the feed composition of $SO_2$ is increased from 0 mol% $SO_2$ to 100 mol% $SO_2$, the absorption rate of $SO_2$ will also be increased.
- The absorbed $SO_2$ will desorb if the ionic liquid temperature is above 120$^oC$.
- When the feed pressure of $SO_2$ is increased from 1.5 bar (a) to 3 bar (a) and feed pressure of $O_2$ is increased from 1.5 bar (a) to 9 bar (a) the amount of each gas absorbed will increase.
- The amount of $O_2$ that is absorbed by the ionic liquid is negligibly small.
- The 98% pure ionic liquid will absorb more $SO_2$ than the 95% pure ionic liquid.

# Chapter 3

# Experimental

## 3.1 Introduction

In this chapter all the materials, such as the gases and the ionic liquids that were used, will be discussed. Then the experimental setup and equipment of both the pressure and temperature experiments will be introduced, thereafter the experimental procedures and experimental planning for both experiments will be discussed in detail. Finally the expected hypotheses for the experimental results will be given.

## 3.2 Materials used

This section discusses the different gases and the ionic liquids used in the study.

### 3.2.1 Gases

For this study two gases were used:

- Oxygen ($O_2$)
- Sulphur dioxide ($SO_2$)

Both of these gases were purchased from Afrox and used as received. The $O_2$ is ultra-high purity (UHP) $O_2$ with a purity of 99.995%. $SO_2$ is stored in liquid form and has a purity of 99.9%. The corrosive nature of $SO_2$ was kept in mind during the design of the equipment. The MSDSs of these two gases can be found in Appendix F, on the CD included.

### 3.2.2 Ionic liquids

For this study the ionic liquid 1-Butyl-3-methylimidazolium methyl sulphate [BMIm][$MeSO_4$], with purities of 95% and 98% will be used in the experiments. The 95% pure ionic liquid was obtained from Sigma-Aldrich while the 98% pure ionic liquid was purchased from Merck.

Ionic liquids are also corrosive, adding to the cost of designing the equipment. The MSDS for the ionic liquid can also be found in Appendix F.

For the experiments the temperature of the ionic liquid will be changed to determine its effect on the performance of the ionic liquid. Therefore, the effect of temperature on the density and viscosity of the ionic liquid is important and can be seen in Table 3.1 showing the density and viscosity of [BMIm][$MeSO_4$] as a function of temperature.

**Table 3.1: Density (ρ) and Viscosity (η) of [BMIm][MeSO4] as a function of temperature (Pereiro *et al.*, 2007:378)**

| Temperature ($^oC$) | ρ ($g/cm^3$) | η (mPa·s) |
|---|---|---|
| 5 | 1.22584 | - |
| 10 | 1.22244 | - |
| 15 | 1.21903 | - |
| 20 | 1.21562 | 288.99 |
| 25 | 1.21222 | 213.19 |
| 30 | 1.20881 | 160.93 |
| 35 | 1.20541 | 123.73 |
| 40 | 1.20204 | 96.83 |
| 45 | 1.19866 | 77.08 |
| 50 | 1.19534 | 62.22 |
| 55 | 1.19202 | - |
| 60 | 1.18873 | 42.24 |
| 65 | 1.18545 | - |
| 70 | 1.18219 | 29.99 |

From Table 3.1 it can be seen that the density of the ionic liquid decreases slightly and the viscosity decreases significantly when the temperature is increased. As discussed in Section 2.2.1.4 the viscosity influences the pressure drop over the absorption chamber, as well as the heat and mass transfer through the ionic liquid. Hence the temperature of the ionic liquid has a large influence on its properties and will have a large influence on the absorption characteristics of the ionic liquid. The chemical structure of the ionic liquid [BMIm][$MeSO_4$] can be seen in Figure 2.4.

### 3.3 Temperature experiments

The temperature experiments will determine the maximum amount of $SO_2$ and $O_2$ gas that will be absorbed into the ionic liquid at different temperatures. These experiments will also serve to study the rate of absorption and desorption of the $SO_2$ and $O_2$ into the ionic liquid. This will be done by determining the change in mass of the ionic liquid as the $SO_2$ and $O_2$ is absorbed and desorbed.

#### 3.3.1 Process flow diagram

In this section the process flow diagram of the temperature experiments will be discussed. Figure 3.1 shows the experimental setup for all of the equipment that has been used for the temperature experiments.

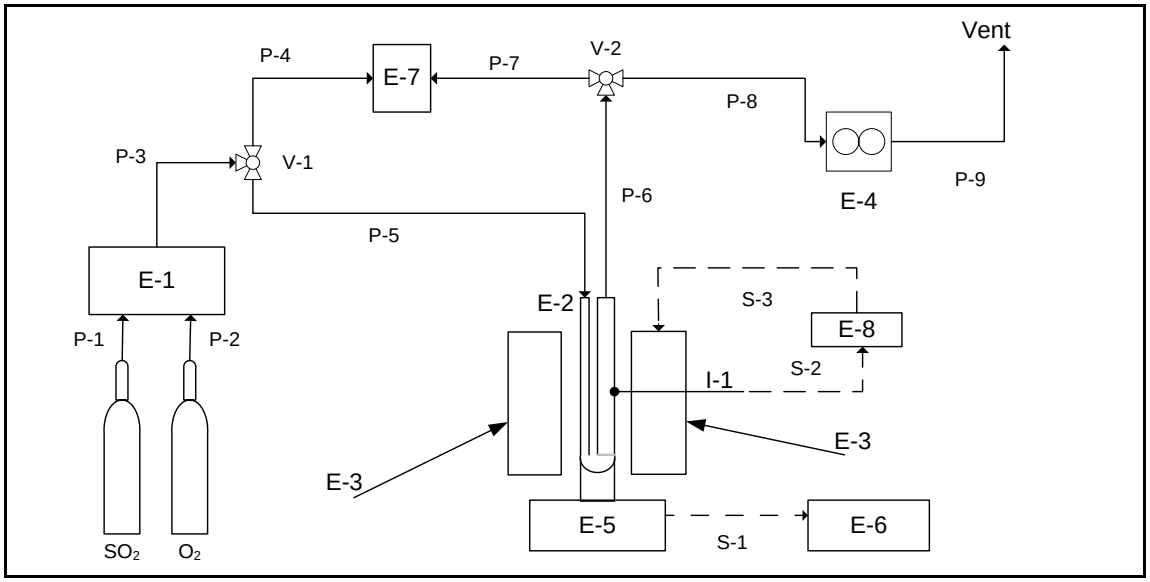


**Figure 3.1: Process flow diagram for temperature experiments**

From the above figure it can be seen that the $SO_2$ and $O_2$ gas will firstly go to mass flow controllers, E-1, where the flows will be adjusted to get the required composition for each experiment. From the mass flow controllers the gas will flow to valve V-1 where it could be sent directly to the GC (E-7) in line P-4 or to the absorption chamber (E-2) via P-5. The gas will be sent directly to the GC when the GC is calibrated. In the absorption chamber the gas will bubble through the ionic liquid while the liquid temperature is controlled by the temperature controller (E-8) and the heater (E-3) heats the chamber to maintain the correct temperature. When the ionic liquid absorbs a gas its mass increases, which will be measured by the balance (E-5) and then logged on a computer (E-6). The excess $SO_2$ and

$O_2$ will exit the absorption chamber through line P-6, after which valve V-2 can be used to direct the gas either to the GC for analysis or to the bubble flow meter (E-4) where the flow rate is determined before the gas is vented.

### 3.3.2 Equipment list

In Figure 3.1 the experimental setup for the temperature experiments is shown and in this section all the individual components will be listed, with a short description and summary of their function. Table 3.2 shows the list of equipment for the temperature experiments.

**Table 3.2: List of equipment for the temperature experiments**

| Equipment nr. | Description | Function | Picture |
|---|---|---|---|
| - | $SO_2$ and $O_2$ gas cylinders with the pressure regulators purchased from Afrox and Instrumentation Specialities | Supplies the $SO_2$ and $O_2$ gas to the setup at a certain pressure. |  |
| E-1 | Brooks Mass flow controllers | Controls the flow of gas to the setup. |   |

| | | | |
|---|---|---|---|
| E-2 | Glass absorption chamber manufactured at the North-West University | Contains the ionic liquid and is where the absorption takes place. |  |
| E-3 | Heater and stand build at the North-West University | Heats the chamber to the desired temperature and holds the heater steady around the absorption chamber. |  |
| E-4 | Bubble flow meter | Measures the gas flow that exits the absorption chamber. | N/A |
| E-5 | PGW 753i balance from ADAM, purchased from Labex | Measures the mass of the absorption chamber to determine the amount of $SO_2$ that was absorbed. |  |
| E-6 | Computer | The data from the balance is logged on the computer. | N/A |
| E-7 | HP 6890 GC | Analyses the gas that exits the absorption chamber to determine the composition of $SO_2$ and $O_2$. |  |

| | | | |
|---|---|---|---|
| E-8 | JCS-33A Shinko temperature controller, purchased from WIKA | Controls the temperature of the heater at the desired level. |  |
| V-1 and V-2 | Stainless steel three-way valves | Allows the flow of the gas to be changed. |  |
| I-1 | Thermocouple from WIKA | Measures the temperature inside the heater. |  |
| S-1 | RS-232 cable | Connects the balance to the computer. | N/A |
| S-2 | Thermocouple cable | Connects the thermocouple to the temperature controller. | N/A |
| S-3 | Electric cable | Connects the temperature controller and the heater. | N/A |
| P-2 and P-9 | 1/4” Plastic pipe | The gas flows through the pipes to the different sections of the setup. | N/A |
| P-1, P-3, P-4, P-5, P-6, P-7 and P-8 | 1/8” Stainless steel pipe | The gas flows through the pipes to the different sections of the setup. | N/A |

### 3.3.3 Experimental setup

Before the experiments can start some of the equipment have to be calibrated first. In this section the calibration of the temperature controller, the mass flow controllers, the GC, and the setting up of the balance will be discussed.

**Heater and temperature control**

The most important variable in these experiments will be the temperature of the absorption chamber. To control the temperature a JCS-33A-S/M Shinko controller will be used. To ensure optimal temperature control of the absorption chamber the temperature controller was installed and tuned.

The heater was designed in such a way as not to touch the absorption chamber at any time. Figure 3.2 shows a top view of the heater with the absorption chamber inside.

**Figure 3.2: Top view of the heater with the absorption chamber inside.**

In Figure 3.2 it can be seen that the heater does not touch the absorption chamber, thereby ensuring that it does not influence the reading of the balance on which the chamber stands. The heater is also mounted on a vertical stand on which it can be raised or lowered during the experiments.

Because of the design of the setup a thermocouple could not be placed directly inside the ionic liquid to check the temperature. Instead the thermocouple will read the temperature on the outside of the absorption chamber. Thus, because of the heat losses that occur, the temperature that the controller reads will not be the exact temperature of the ionic liquid. To correct this discrepancy, the controller was set to ten different temperatures and the temperature of the ionic liquid taken directly with another thermocouple that was inserted into the absorption chamber. This was done every 600 seconds for half an hour. It was found that after 600 seconds the temperature of the ionic liquid did not increase by more than $1^oC$. The actual temperature of the ionic liquid was plotted against the set point temperature on the controller, and is shown in Figure 3.3.

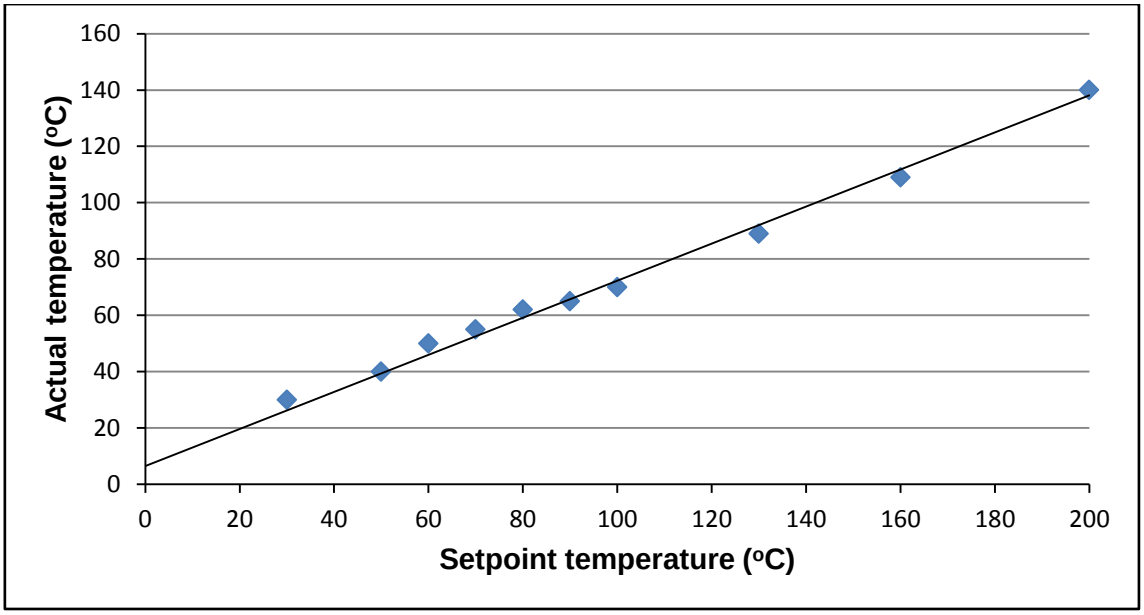


**Figure 3.3: Temperature calibration**

From the data in the above figure a linear trend line was plotted and the following equation was obtained:

$$\boldsymbol{Actual\ temperature} = \mathbf{0.658}(\boldsymbol{Set\ point\ temperature}) + \mathbf{6.501} \qquad \text{Equation 3.1}$$

This equation was used to calculate the set point temperatures of the controller for the ionic liquid to be at the required temperature. Table 3.3 shows the set point temperatures of the controller for each of the temperatures used in the experiments.

**Table 3.3: Temperature chart for temperature controller**

| Set point temperature (°C) | Actual temperature of ionic liquid (°C) |
|---|---|
| 32.2 | 30 |
| 48.0 | 40 |
| 63.8 | 50 |
| 79.7 | 60 |
| 182.5 | 125 |

From the above table it can be seen that to achieve, for example, an ionic liquid temperature of 50°C, the temperature controller must be set to 63.8°C. Table 3.3 will be used to set the temperature on the controller for all the temperature experiments.

**Mass flow controllers**

In order to control the flow and composition of the feed gas, mass flow controllers were used. For this study two Brooks mass flow controllers were used to control the flow of $SO_2$

and $O_2$ gas to the absorption chamber. Before the mass flow controllers could be used they first had to be calibrated. This was done by selecting a controller for each of the gases and then plotting the controller settings versus the gas flow rate for each of the settings. After the calibration the same gas had to be used in a specific controller every time. Figure 3.4 and Figure 3.5 show the calibration curves for $SO_2$ and $O_2$ gas, as well as the linear trend lines at 25$^{o}$C and ambient pressure.

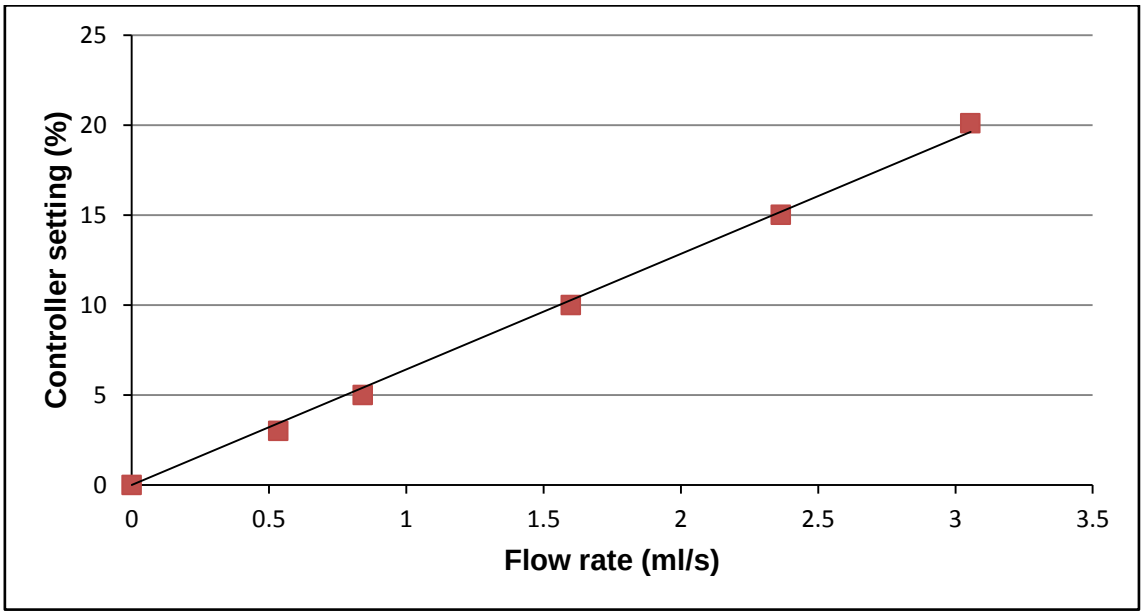


**Figure 3.4: Mass flow controller calibration curve for $SO_2$**

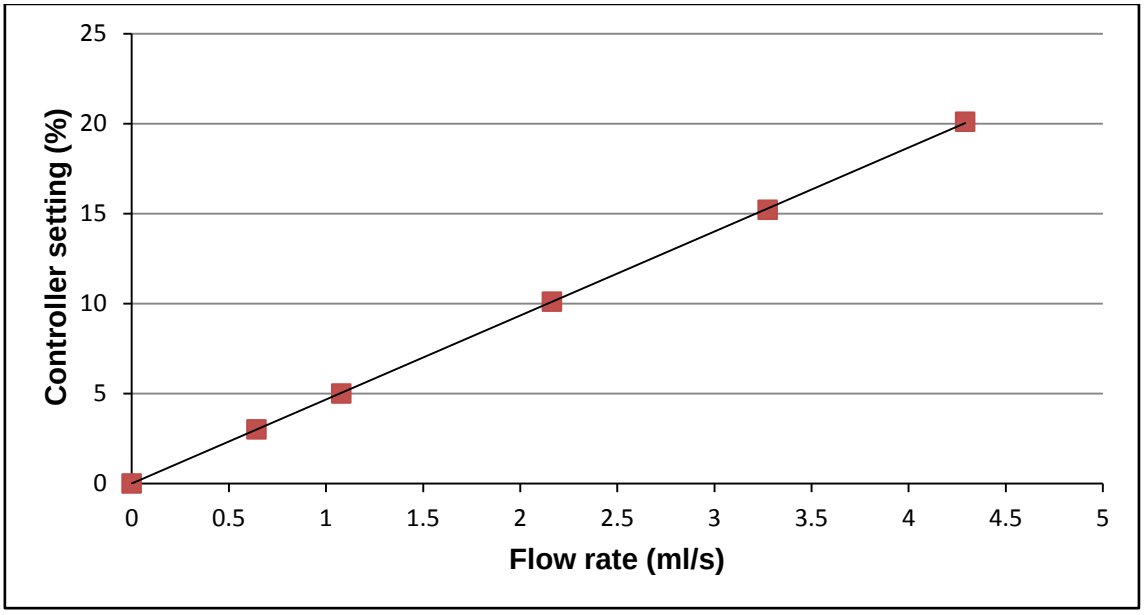


**Figure 3.5: Mass flow controller calibration curve for $O_2$**

From the above figures and linear trend lines calibration equations for $SO_2$ (Equation 3.2) and $O_2$ (Equation 3.3) was obtained:

$$\boldsymbol{Controller\ setting} = \mathbf{6.423}(\boldsymbol{Flow\ rate}) \qquad \text{Equation 3.2}$$

$$\boldsymbol{Controller\ setting} = \mathbf{4.666}(\boldsymbol{Flow\ rate}) \qquad \text{Equation 3.3}$$

These equations will now be used to calculate the specific mass flow controller settings to achieve the required gas flow rate for each of the experiments.

**Setup of balance**

The amount of $SO_2$ that is absorbed will be determined by the increase in mass of the ionic liquid in order to measure the increase in mass a very sensitive balance will be used. The balance that was chosen is the PGW 753i balance from Adam. Table 3.4 shows the technical specifications of the balance.

**Table 3.4: Balance specifications (ADAM, 2011)**

| Technical Specifications | |
|---|---|
| Model | PGW 753i |
| Maximum capacity | 750g |
| Readability | 0.001g |
| Repeatability (S.D.) | 0.001g |
| Pan size | 5.5×5.5" / 140×140mm |
| Draught shield dimensions | 158x158x80mm |
| Overall dimensions | 251×358×104mm |
| Interface | Bi-directional RS-232 |

The balance was connected to a computer with the RS-232 cable and the mass of the ionic liquid will be transmitted to the laptop where the data will be logged by the data logging program supplied with the balance. The mass of the ionic liquid was logged on the laptop every two seconds for the duration of the experiment, after which the data could be accessed and analysed.

**Gas chromatograph**

For this study the composition of the gas stream exiting the absorption chamber was analysed with a GC in order to determine how the composition of $SO_2$ and $O_2$ changed from the feed stream. For the experiments the GC used was a HP 6890 with a 6ft × 1/8'' 80/100 Hysep Q packed column bought from Sigma Aldrich. The GC analyses for all of the experiments were carried out at 65$^{o}$C with He as the carrier gas at a flow rate of 30 ml/min. After the column was installed the GC had to be calibrated.

In order to calibrate the GC the ratio of the peak areas versus the ratio of the feed stream composition to the GC had to be plotted. This was done by using the mass flow controllers to feed a specific ratio of $SO_2$ to $O_2$ gas to the GC, resulting in two peaks. Next the ratio of the areas of the two peaks were determined a number of times, and the average value used. The ratio of the peak areas versus the composition ratio of the stream to the GC is shown in Figure 3.6

From Figure 3.6 the following linear equation was obtained:

$$\boldsymbol{Gas\ composition\ ratio\ of\ stream\ to\ GC = 1.812(GC\ peak\ area\ ratio)} \quad \text{Equation 3.4}$$

This equation will be used to determine the gas composition in the gas stream after the absorption chamber, by using the area of the peaks generated by the GC.

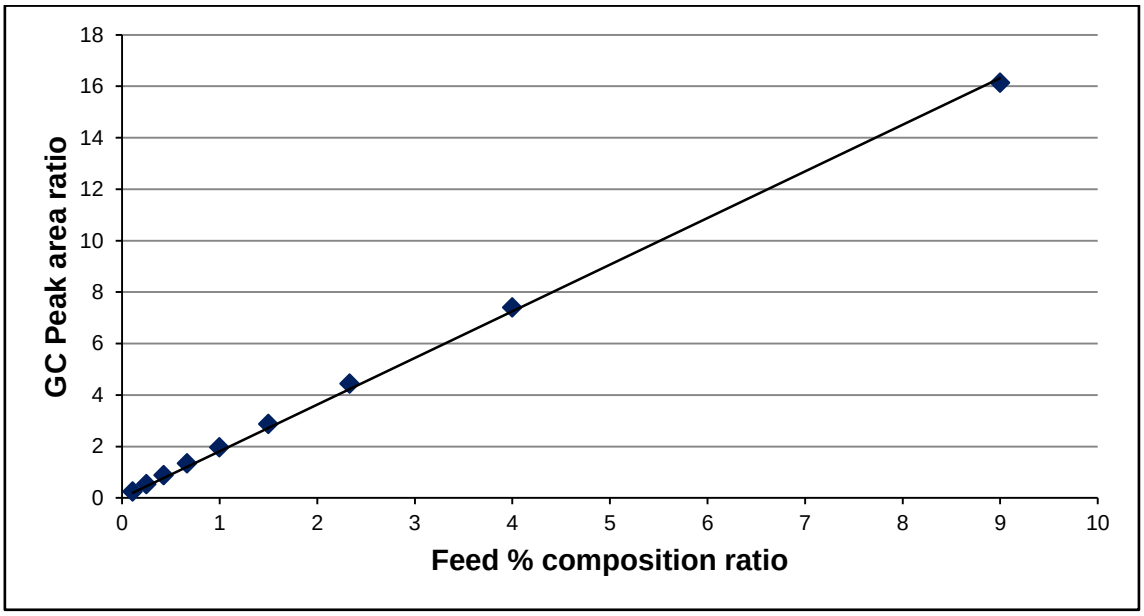


**Figure 3.6: GC calibration curve**

### 3.3.4 Experimental procedure

This section will describe the procedure that will be followed during the temperature experiments. It will cover both the absorption and desorption procedures as well as the GC analysis.

Start by turning on the GC-computer, mass flow controllers and temperature controller and setting the flow and temperature controllers to the required values. Start up the GC and the GC control software on the computer and place the absorption chamber, with the ionic liquid

inside, on the balance. Then connect all the gas pipes to the absorption chamber, allow the temperature to stabilise at the set point and open the data capturing program. After opening the gas flows to the chamber, take flow readings with E-4 at time 30s, 60s, 180s, 360s, 600s, 900s and 1200s, as well as a GC sample at time 1m40s. After the computer has taken 1 000 data points, or about 32 minutes after the experiment has been started, stop the gas flow through the mass flow controllers and change the temperature set point to the desorption temperature (125$^o$C). Open the $O_2$ gas stream at a flow of 2.5 cm$^3$/s to carry all $SO_2$ that desorbed from the ionic liquid out of the absorption chamber. As soon as the computer has taken 1 700 data points, or after approximately 56 minutes, stop the $O_2$ gas flow through the mass flow controllers and turn the heater off. Remove the absorption chamber from the balance and as soon as the heater reaches the required temperature, the next experiment can be started.

### 3.3.5 Experimental planning

For this study the temperature and the composition of the feed gas were changed. The amount of gas that was absorbed into the ionic liquid, as well as the rate of the absorption and desorption was then determined at each of the conditions. For all the experiments 3 cm$^3$ of the ionic liquid was present inside the absorption chamber to absorb the gas. Table 3.5 shows the different temperatures and compositions that were used during the study.

**Table 3.5: Experimental planning for temperature experiments**

| | **Temperature ($^o$C)** | | | |
|---|---|---|---|---|
| **Composition (mole %$SO_2$)** | **30$^o$C** | **40$^o$C** | **50$^o$C** | **60$^o$C** |
| **0% (100% $O_2$)** | 1 | 2 | 3 | 4 |
| **25%** | 5 | 6 | 7 | 8 |
| **50%** | 9 | 10 | 11 | 12 |
| **75%** | 13 | 14 | 15 | 16 |
| **100%** | 17 | 18 | 19 | 20 |

In the above table it can be seen that the temperature was varied from 30$^o$C to 60$^o$C and the feed gas composition was varied from 0 mol% $SO_2$ to 100 mol% $SO_2$. The numbers from 1 to 20 shows the number of experiments carried out. All experiments were executed twice, once with the 95% pure ionic liquid and the second time with the 98% pure ionic liquid in order to determine if the purity of the ionic liquid has an effect on the results.

### 3.4 Pressure experiments

In short, the pressure experiments will determine the amount of $SO_2$ gas that will be absorbed into the ionic liquid at different pressures. Two pressure chambers will be used and by determining the pressure difference over these two chambers after the $SO_2$ has been absorbed, the amount of $SO_2$ absorbed into the ionic liquid can be determined.

#### 3.4.1 Process flow diagram

This section will describe the process flow diagram for the pressure experiments and give a short description of the operation of the setup. Figure 3.7 shows the experimental setup for the pressure experiments, as well as all the connections and equipment used.

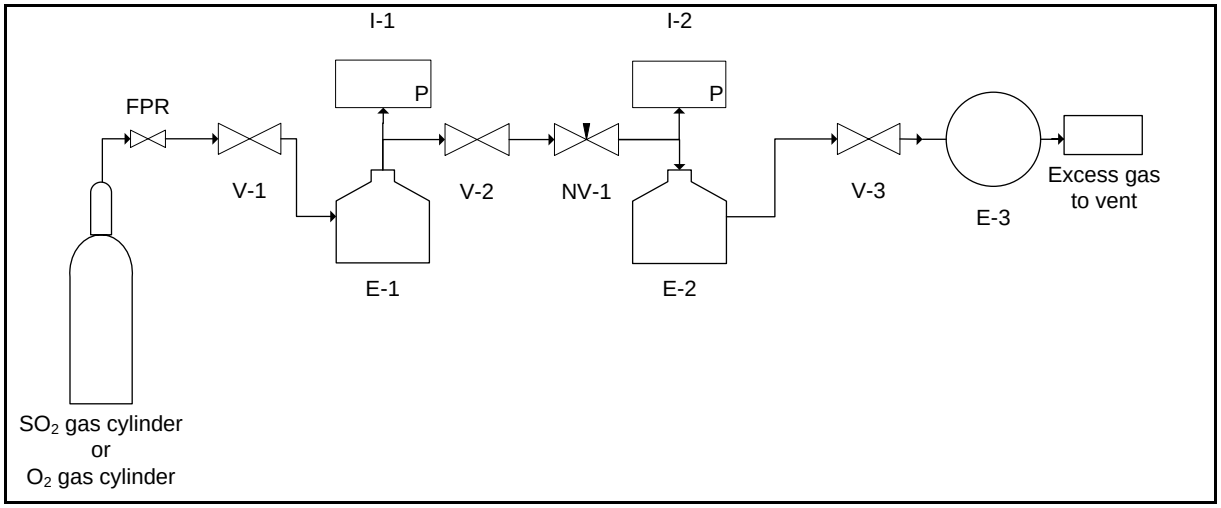


**Figure 3.7: Process flow diagram for the pressure experiments**

Figure 3.7 shows that the gas (either $SO_2$ or $O_2$) enters the setup through valve V-1, it then moves to the first pressure chamber E-1 where the pressure gauge I-1 indicates the pressure. From there it flows through valve V-2 and the needle valve NV-1, which limits the velocity of the gas into the second pressure chamber E-2, where the second pressure gauge I-2 measures the pressure. This prevents the ionic liquid, which is located in E-2, from being bubbled out of the chamber when the gas enters E-2 to fast. E-2 is also where the $SO_2$ is absorbed into the ionic liquid. After the absorption the excess gas is extracted by the vacuum pump E-3 and is vented.

### 3.4.2 Equipment list

Figure 3.7 shows how all the equipment fit together. In this section each of the individual components will be shown, together with a description and a brief summary of its function. Table 3.6 shows the list of equipment used in the pressure experiments.

**Table 3.6: List of equipment for the pressure experiments**

| Equipment Nr. | Description | Function | Picture |
|---|---|---|---|
| - | $SO_2$ and $O_2$ gas cylinder purchased from Afrox | Will supply the gas to the experimental setup. | N/A |
| FPR | $O_2$ and $SO_2$ gas pressure regulators purchased from Instrumentation Specialities | Regulates the pressure of the gas to the experimental setup. |  |
| E-1 and E-2 | The two pressure chambers in the setup, constructed from stainless steel at the North-West University. | E-1 is used to determine the amount of gas that will be available for absorption in the system. E-2 contains the ionic liquid and is where the absorption takes place. |  |
| V-1, V-2 and V-3 | Ball valves designed for corrosive gases. | Used to regulate the flow of the gas and the pressure. |  |

| | | | |
|---|---|---|---|
| NV-1 | Stainless steel needle valve | Used to regulate gas flow. | 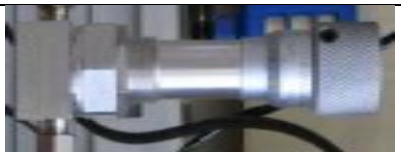 |
| I-1 and I-2 | WIKA Pressure gauges | Indicate the pressure inside the pressure chambers. |  |
| E-3 | Edwards Vacuum Pump | To extract much of the air in the setup before each experiment and to ensure that the ionic liquid discharges any water that it might have absorbed. |  |
| - | Heating plate | Used to heat the oil bath to 130-150$^{o}$C | N/A |
| - | Thermal Oil | Used as heating liquid in the oil bath | N/A |
| - | ¼'' and 1/8'' Stainless steel piping | The gas flows through the piping from the gas cylinders to the vent. | N/A |

### 3.4.3 Experimental setup

In the experimental setup the volume of the chambers is very important. Therefore, one of the first tasks was to determine the volume of the chambers and the piping connecting the chambers. It is important to also determine the volume of the piping in the setup, because the volume of the chambers is very small and the extra volume of the piping has a significant influence on the results.

In order to establish the volume of the apparatus the volume of water that can be contained by the setup was determined. The setup was first taken apart into its individual components. Then the volume for each component was measured repeatedly, and an average value was obtained. Thereafter the setup was assembled into two sections:

- Section 1 from V-1 to V-2
- Section 2 from V-2 to V-3

The volumes of these two sections were determined by measuring the volume of water that can be injected into each of the sections. The average of a number of determinations was calculated and compared with the sum of the volumes as determined dimensionally for the individual components. The two volumes were found to be equal. The final volumes for the two sections were then calculated as 18.90 ±0.01 $cm^3$ for section 1 and 21.80 ±0.01 $cm^3$ for section 2. At these small error margins the error bars on the graphs was too small to see and was therefore left out of the graphs in Chapter 5.

With the volume of the apparatus now known, the following step was to test the setup for leakages. This was done in two ways:

- Firstly, the system was pressurised to 10 bar with $O_2$ and then submerged in a water bath to check for any bubbles escaping from the setup. It was left in the system for 30 min without detecting any bubbles.
- Secondly, the system was pressurised to 10 bar with $O_2$ and then left overnight (twelve hours) to detect any pressure drop in the system. A pressure drop of less than 0.001 bar in twelve hours was deemed acceptable for these experiments. No pressure drops were detected with either of the two tests and therefore, the system was considered to be leak-free.

The final preparation step was to calibrate the pressure gauges fitted to chamber E-1 and E-2. The gauges were bought as pre-calibrated gauges, and were found to give accurate measurements within 0.001 bar.

### 3.4.4 Experimental procedure

In this section the general experimental method, as well as the detailed experimental procedures will be discussed.

#### 3.4.4.1 General method

For the pressure experiments all the experiments will be carried out at relatively low pressures (<10 bar) and at ambient temperature (25$^{o}$C). Thus, the deviation from the ideal gas law will be negligibly small (Felder & Rousseau, 2000:213). Because the volume of each section is known, as well as the pressure and temperature, the number of moles in the system can be calculated with Equation 3.5 (Ideal gas law):

$$\boldsymbol{PV = nRT} \qquad \text{Equation 3.5}$$

Where:

P – Pressure inside the chamber (1 bar = $1\times10^5$ Pa)

V – Volume of the chamber (1 $cm^3$ = $1\times10^{-6}$ $m^3$)

n – Number of moles (mol)

R – Gas constant (R = 8.314 J/mol·K)

T – Temperature (298 K)

When chamber E-1 is pressurised the number of moles of gas in the chamber will be calculated, using the ideal gas law. It is a closed system and from section 2.1.3.2 it was concluded that no chemical reactions occur, because only physical absorption takes place when $SO_2$ is absorbed into [BMIm][$MeSO_4$], therefore the number of moles of gas in the system will remain constant throughout the experiment. When valve V-2 between the chambers is opened, the volume of the system changes and consequently the pressure also changes according to the ideal gas law. However, because the ionic liquid absorbs some of the gas the drop in pressure is larger than that predicted by the ideal gas law in the absence of absorption. After the system has reached equilibrium the number of moles of gas will be calculated again, and the difference between these amounts will equal the amount of gas absorbed into the ionic liquid.

#### 3.4.4.2 Detailed experimental procedures

During these experiments dangerous chemicals will be used; therefore a few basic safety rules must be adhered to at all times. These rules are:

- All experiments have to be carried out inside a ventilation chamber
- When performing the experiments, protective clothing such as a laboratory coat, respirator, eye protection and gloves must be worn.

- The vacuum pump and the heated oil bath must also be placed in the ventilation chamber in view of the fact that the exhaust gas from the vacuum pump and the oil vapour are carcinogenic.
- The ionic liquids are corrosive and cause burns. Therefore, contact with the skin should be avoided. In the event of contact, thorough rinsing with soap and water is required.

The following sections explain two main experimental procedures that will be used during the pressure experiments. These procedures are the absorption and desorption procedures. They will indicate how the experiments must be carried out to ensure the proper working of the experimental setup.

**Absorption**

Insert the required amount of ionic liquid into chamber E-2 and seal the chamber. Start the vacuum pump and let it run for five minutes to remove as much air form the system as possible. After closing V-2 and V-3, switch off the vacuum pump and allow two minutes for the pressure readings to stabilise before taking the readings. Set the pressure regulator to the desired pressure and open V-1 to pressurise chamber E-1 to the desired pressure. Allow two minutes for the pressure gauges to stabilise before the pressure readings are taken. Next V-2 is opened to let the gas into chamber E-2. After the pressure readings on both gauges have equalised, open NV-1 to ensure that equilibrium was reached and allow ten minutes before taking the final pressure readings.

**Desorption**

After the absorption step ensure that the pressure gauge I-2 indicates a positive reading of at least 2 bar(g). This step is to insure that the ionic liquid is not spilled when the chamber is opened. For the experiments with $SO_2$, the reading will be significantly less than 2 bar(g), in order to increase the pressure just add $O_2$ until the pressure is high enough. Now open chamber E-2 and extract the ionic liquid from the bottom half of the chamber and place it in a dark glass container. Place the dark glass container in an oil bath that has been heated to between 130 and 150$^{o}$C and let the gas desorb from the liquid for 20-30 minutes (Lee *et al.*, 2008:6035). Let the gas desorb until no more bubbles can be seen on the surface of the ionic liquid. After the desorption step, remove the glass container from the oil bath and allow it to cool, after the ionic liquid has cooled to room temperature it can be used again for absorption.

### 3.4.5 Experimental planning

For this study the feed pressure of the different pure gasses and the purity of the ionic liquid will be varied to see what the effect will be on the amount of gas that will be absorbed into the ionic liquid. A summary of the experimental planning is shown in Table 3.7. During all the experiments 5 $cm^3$ of ionic liquid will be used in chamber E-2. Each of the experiments will be carried out three times to check the repeatability.

**Table 3.7: Experimental planning for the pressure experiments**

| Feed pressure (bar(a)) | 95% IL | 98% IL |
|---|---|---|
| **1.5** | Pure $SO_2$ or pure $O_2$ | Pure $SO_2$ or pure $O_2$ |
| **2.0** | Pure $SO_2$ or pure $O_2$ | Pure $SO_2$ or pure $O_2$ |
| **2.5** | Pure $SO_2$ or pure $O_2$ | Pure $SO_2$ or pure $O_2$ |
| **3.0** | Pure $SO_2$ or pure $O_2$ | Pure $SO_2$ or pure $O_2$ |
| **6.0** | Pure $O_2$ | Pure $O_2$ |
| **9.0** | Pure $O_2$ | Pure $O_2$ |

From Table 3.7 it can be seen that for the experiments at 1.5, 2.0, 2.5, and 3.0 bar(a) both pure $SO_2$ and $O_2$ gas will be used, but only $O_2$ will be used for the higher pressures of 6.0 and 9.0 bar(a). This is because at pressures higher than 3.0 bar(a) $SO_2$ will start to liquefy, which is to be expected because the vapour pressure of $SO_2$ at 25$^oC$ is about 4.0 bar(a) (Air Liquide, 2009). All the experiments were repeated with both the 95% and 98% pure ionic liquid.

# Chapter 4

# Temperature experiments – Results and discussion

## 4.1 Experimental data

In this section the raw data obtained from the experimental setup will be presented and an interpretation of the data given. For the duration of each experiment the mass of the absorption chamber containing the ionic liquid was recorded. These data points were then transferred to MSExcel® where further data analysis was done. Figure 4.1 shows the raw experimental data logged for the experiment with 95% pure ionic liquid and 100 mol% $SO_2$ at 30°C.

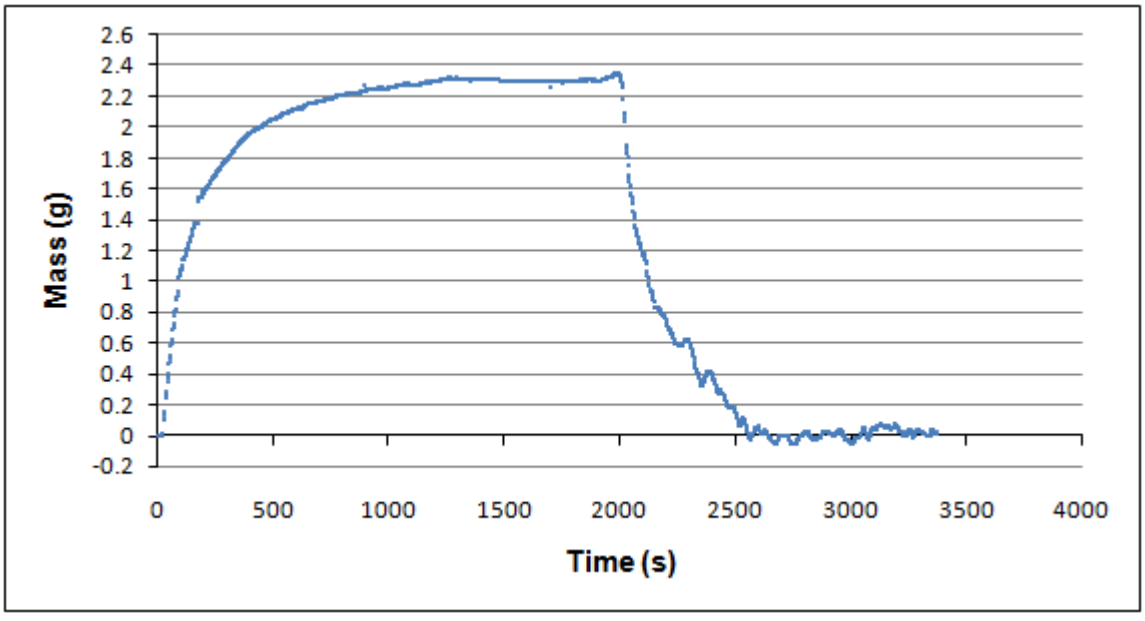


**Figure 4.1: Mass $SO_2$ absorbed in 95% IL with 100 mol% $SO_2$ at 30°C and mass $SO_2$ during desorption after 2000 seconds**

In Figure 4.1 it can be seen that there are a large number of data points, about 1 700 if a data point is taken every two seconds. This creates the illusion that the graph is presented

as a solid line, as seen in Figure 4.1. In order to show data points and not a continuous line the number of points was reduced to about 170 by recording only every tenth data point. Figure 4.2 shows the same experiment as in Figure 4.1, but with a reduced number of data points.

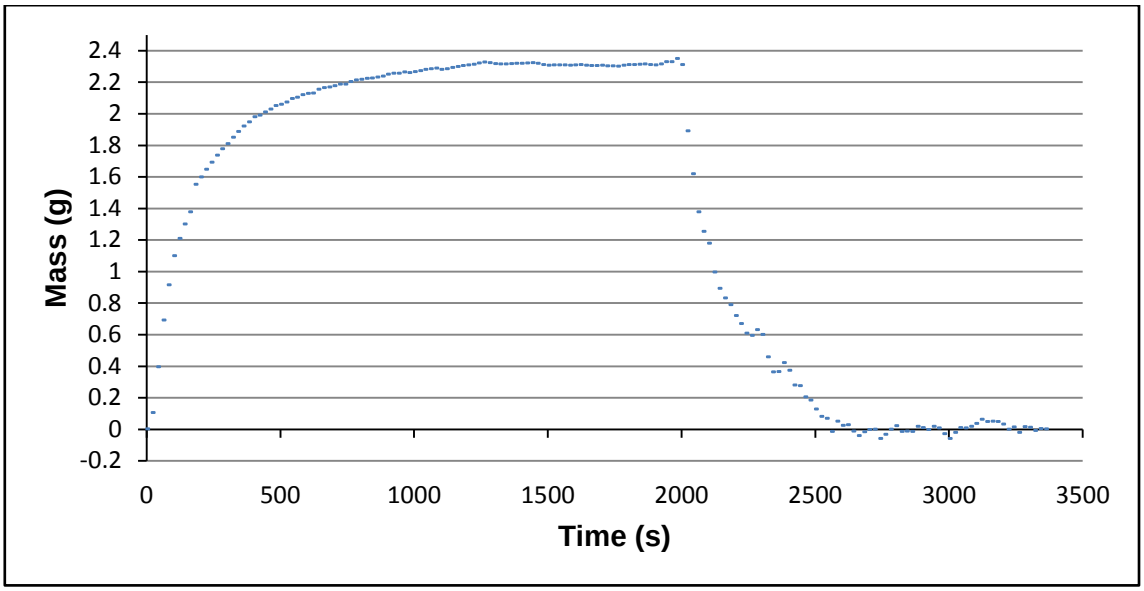


**Figure 4.2: Mass $SO_2$ absorbed in 95% IL with 100 mol% $SO_2$ at 30°C and mass $SO_2$ during desorption after 2000 seconds**

Figure 4.3 shows the mass of $SO_2$ absorbed into the 95% pure ionic liquid when 100 mol% $SO_2$ was fed to the absorption chamber at 30, 40, 50 and 60°C.

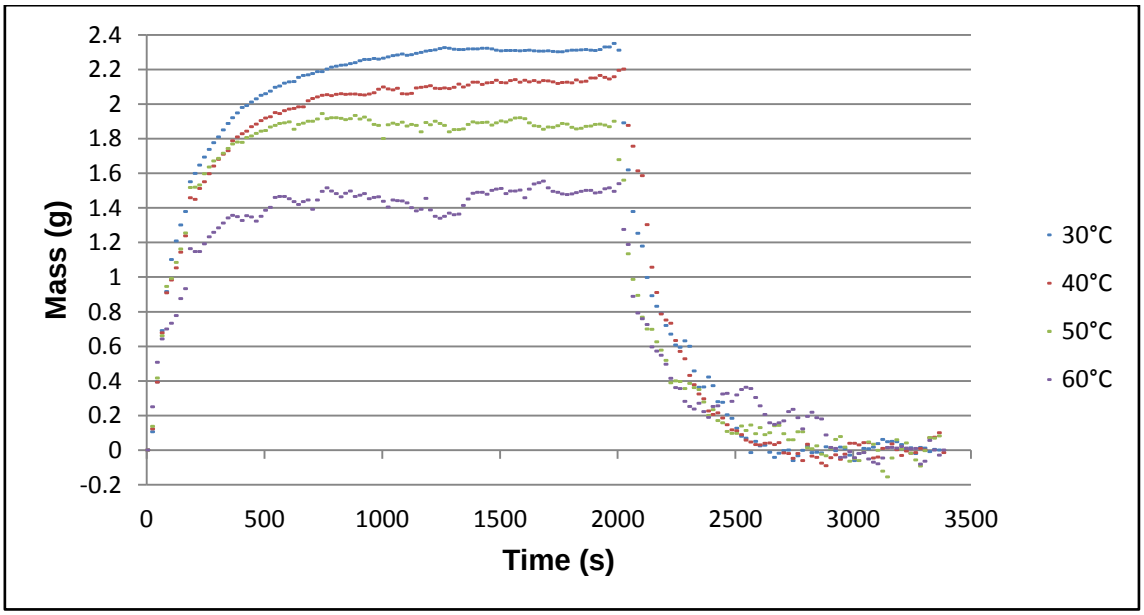


**Figure 4.3: Mass $SO_2$ absorbed in 95% IL with 100 mol% $SO_2$ at 30°C to 60°C and mass $SO_2$ during desorption after 2000 seconds**

From Figure 4.3 it may be seen that the mass of the ionic liquid decreased as the absorption temperature was increased, which indicated that the amount of $SO_2$ absorbed decreased with an increase in temperature. After about 2000 seconds the mass decreased sharply as the $SO_2$ was desorbed from the ionic liquids. Figure 4.4 shows the experimental data for the absorption of $SO_2$ into the 98% ionic liquid with 100 mol% $SO_2$ at 30, 40, 50 and 60$^oC$.

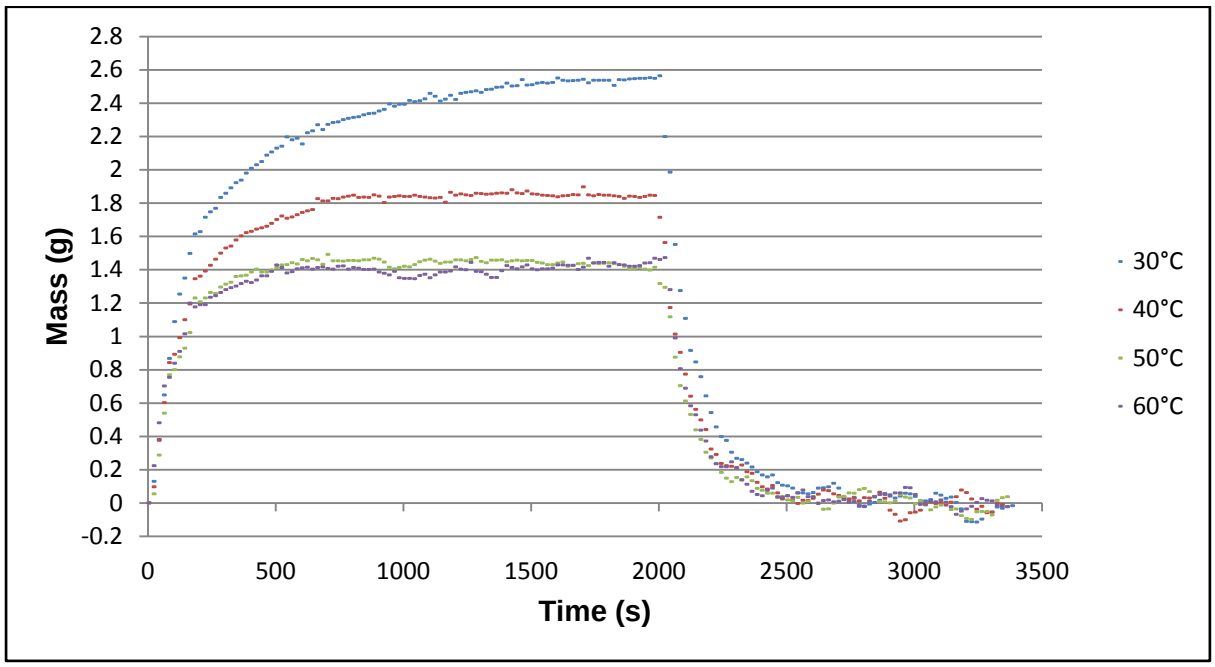


**Figure 4.4: Mass $SO_2$ absorbed in 98% IL with 100 mol% $SO_2$ at 30$^oC$ to 60$^oC$ and mass $SO_2$ during desorption after 2000 seconds**

Similar trends can be seen for both Figure 4.4 and Figure 4.3, regarding the $SO_2$ absorbed, absorption rate and desorption. In Figure 4.1 to 4.4 it can be seen that the mass of the ionic liquid increased dramatically for the first 600 seconds after which it levelled out at about 1 200 seconds. At 2 000 seconds the temperature of the absorption chamber was increased to 125$^oC$ to desorb the $SO_2$ from the ionic liquid. This caused the mass of the ionic liquid to decrease rapidly as the $SO_2$ was desorbed until about 2 600 seconds when the mass stabilised around zero.

Figure 4.3 and Figure 4.4 show that during desorption of the ionic liquid the amount of scatter in the data increased dramatically. This is because the increase in temperature caused a pressure difference between the inside and the outside of the heater whereby some air flowed out of the heater, increasing the amount of scatter in the balance data.

In the next section the maximum amount of $SO_2$ absorbed into the ionic liquid will be calculated and the influence of the absorption temperature, $SO_2$ feed composition and ionic

liquid purity on the amount of $SO_2$ absorbed as well as the absorption and desorption rates will be discussed. The effect of these three parameters on the rates of absorption and desorption will also be investigated.

## 4.2 Data analysis

After the experimental data were collected it was analysed and the maximum absorption, absorption rate and desorption rate for each experiment was calculated. In the following three sections these results will be discussed with reference to the temperature of the experiment, the composition of the feed gas and the purity of the ionic liquid.

When using the gravimetric method to determine the solubility of a gas there is a buoyancy force that has an effect on the measurement of the weight gain and has to be corrected for. This however is mostly a problem with low solubility gases, where the buoyancy correction will be a large fraction of the weight gain measured (Anderson, 2008:56). Soriano *et al.* (2008:1657) found that the buoyancy effect was significant at high pressures but negligible near atmospheric pressure. Therefore the effect of buoyancy was not taken into account in the following results.

### 4.2.1 Maximum Absorption

From the experimental data in Section 4.1 the maximum amount of $SO_2$ absorbed into the ionic liquid was calculated by taking the average of the data points between time 1 000 and 1 900 seconds. These times were chosen because it was visually determined that at these times the absorption of the $SO_2$ had levelled out and would give a good indication of the maximum amount of $SO_2$ absorbed. From this information the maximum amount (in grams) of $SO_2$ that had been absorbed in each experiment was calculated.

In order to be able to compare the data more easily with other publications these values were converted to moles $SO_2$ absorbed per mole ionic liquid by using the Equation 4.1:

$$\boldsymbol{Max\ absorption} = \frac{\frac{m_{SO2}}{MW_{SO2}}}{mol_{IL}} \qquad \text{Equation 4.1}$$

Where:

$m_{SO2}$ – Maximum mass of $SO_2$ absorbed (g)

$MW_{SO2}$ – Molar weight of $SO_2$ (g/mol)

$Mol_{SO2}$ – Mole amount of ionic liquid used in each experiment (mol)

For each experiment exactly 3 $cm^3$ of ionic liquid was used, with a density of 1.21 $g/cm^3$ at 25°C and a molar weight of 250.32 g/mol. Therefore the number of moles of ionic liquid for each experiment was 0.0145 mol.

Figure 4.5 to 4.9 show the number of moles $SO_2$ that was absorbed per mole of ionic liquid versus the temperature of the ionic liquid. Each of these five graphs shows the experimental data of a different feed gas composition of 0, 25, 50, 75 and 100 mol% $SO_2$, with the balance $O_2$. The blue bars in the graphs signify the 95% pure ionic liquid and the red bars the 98% pure ionic liquid. In Appendix D a confidence interval of 10.55% was calculated for the temperature experiments.

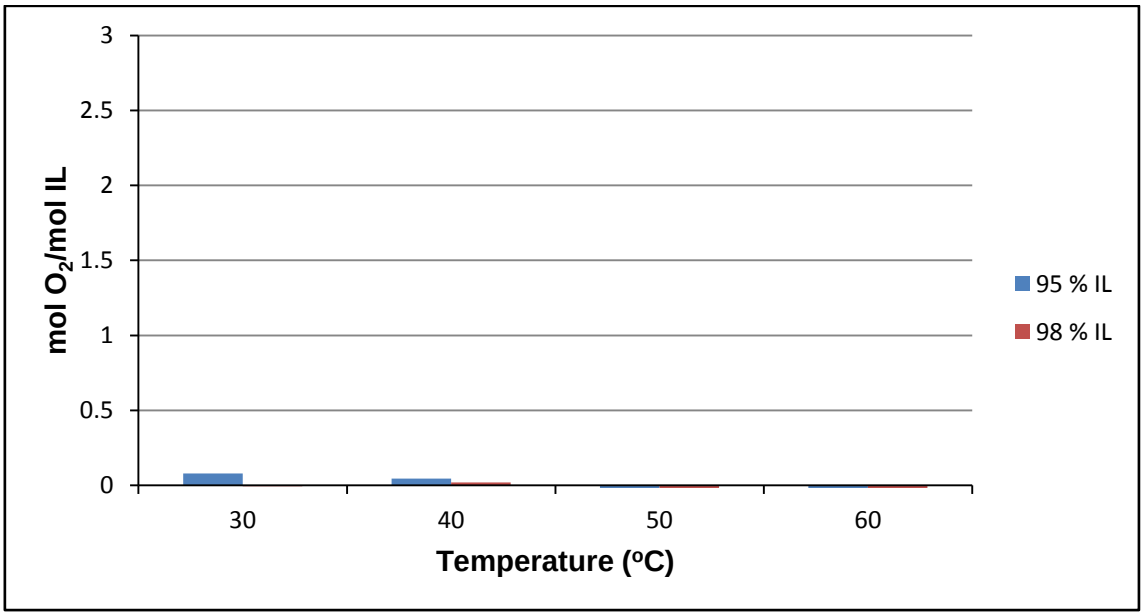


**Figure 4.5: Mol $O_2$/mol IL with 0 mol% $SO_2$**

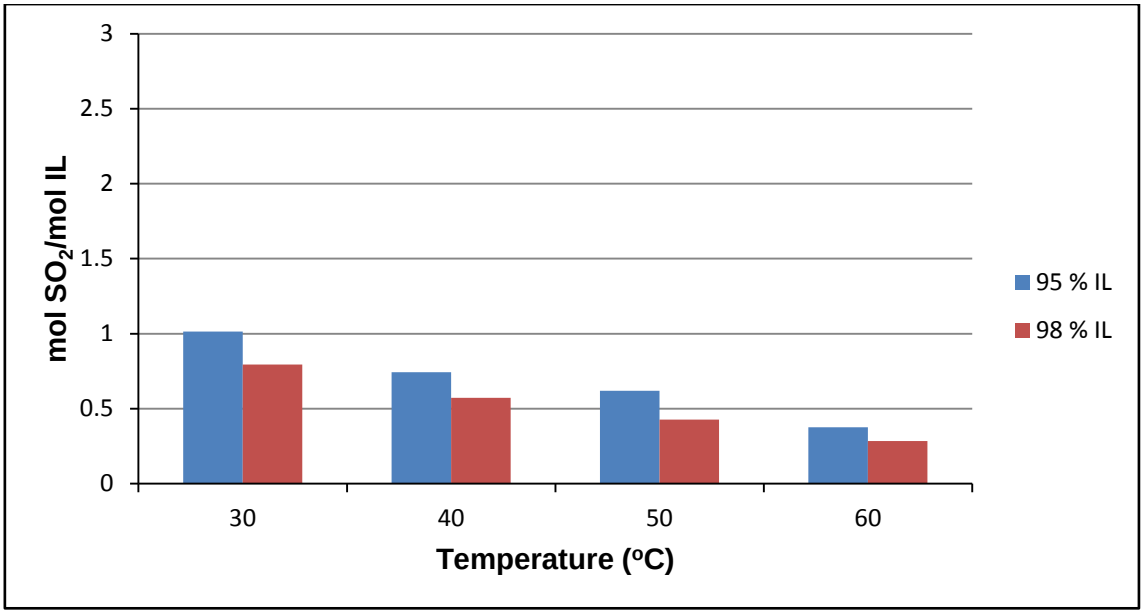


**Figure 4.6: Mol $SO_2$/mol IL with 25 mol% $SO_2$**

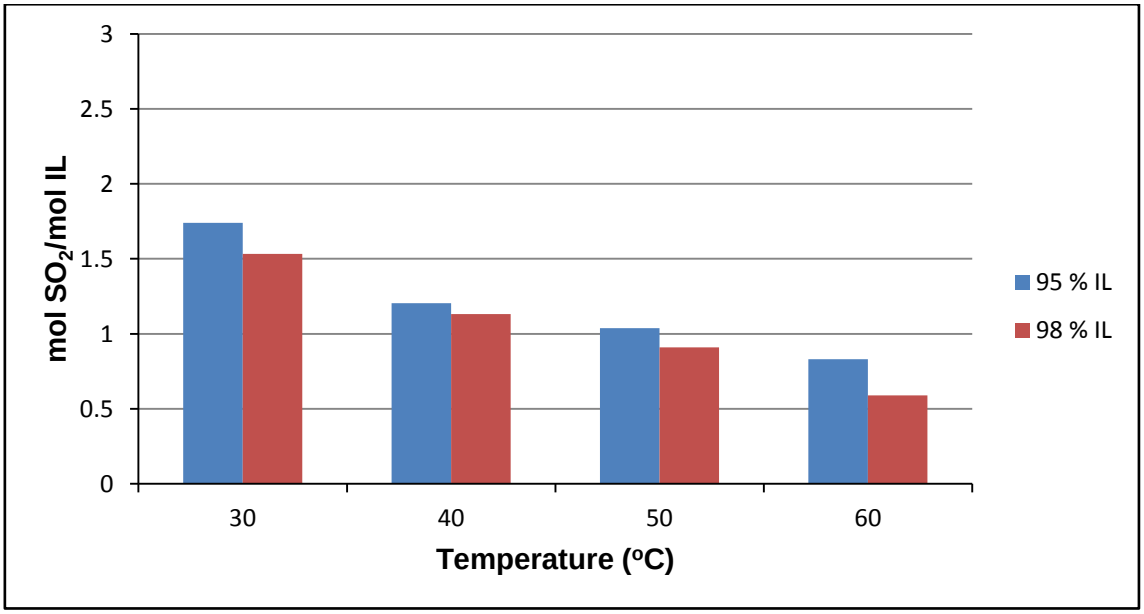


**Figure 4.7: Mol $SO_2$/mol IL with 50 mol% $SO_2$**

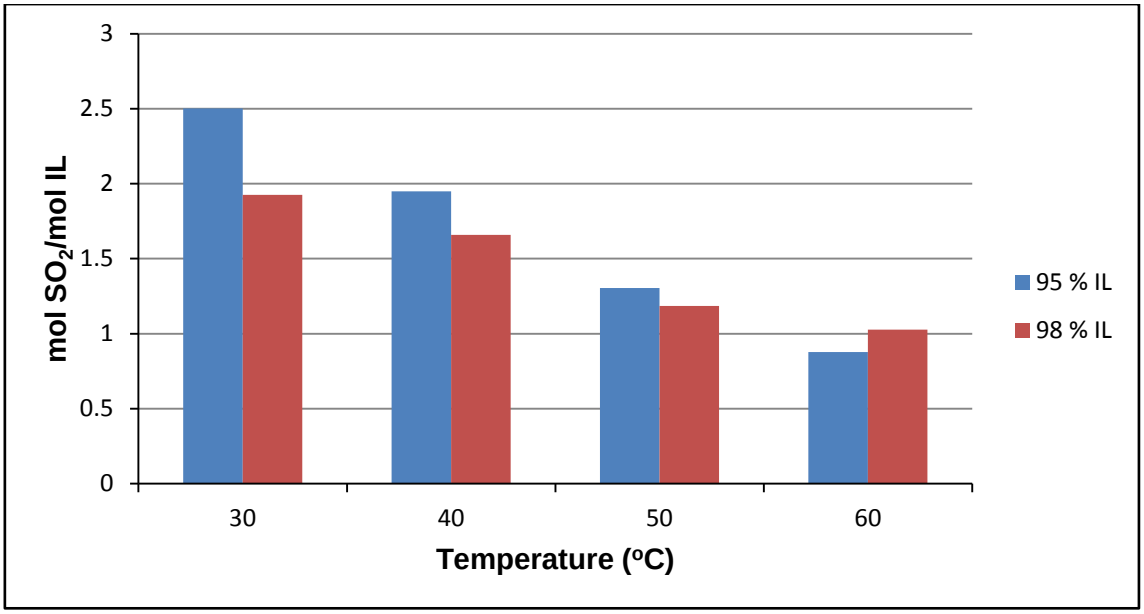


**Figure 4.8: Mol $SO_2$/mol IL with 75 mol% $SO_2$**

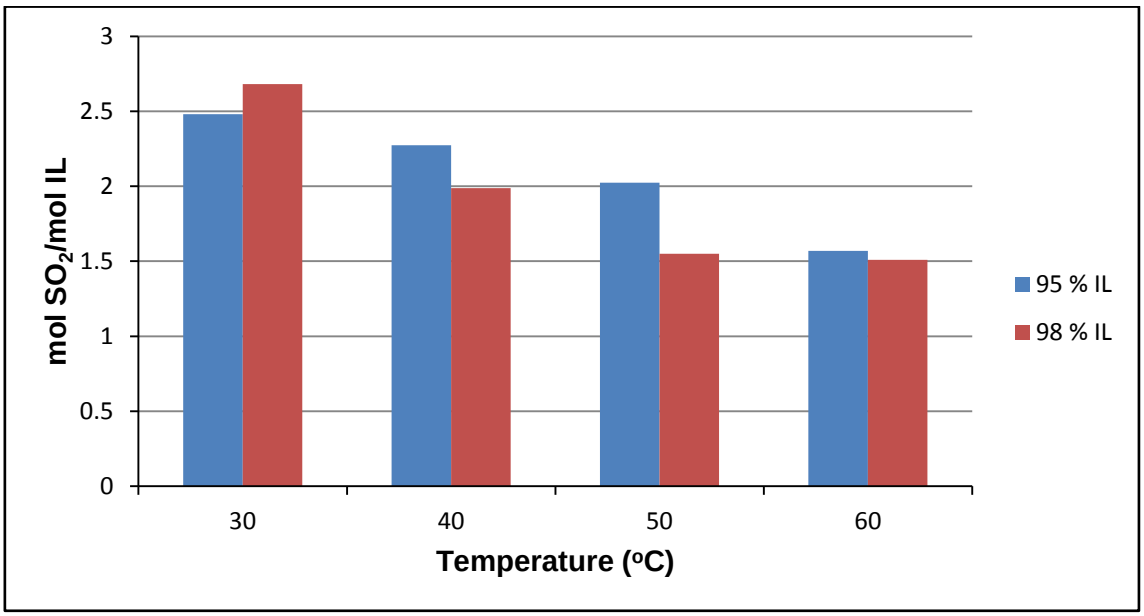


**Figure 4.9: Mol $SO_2$/mol IL with 100 mol% $SO_2$**

In Figure 4.5 to 4.9 the influence of the feed gas composition can be seen. For 0 mol% $SO_2$ (100 mol% $O_2$) in the feed stream the 95% pure ionic liquid absorbed 0.080 mol $O_2$/mol IL at 30°C and 0.047 mol $O_2$/mol IL at 40°C while the amount absorbed by the 98% pure ionic liquid was below the detection ability of the apparatus. This low $O_2$ absorption is confirmed in Chapter 5 with the pressure experiments and from literature, namely that ionic liquids absorb only very small amounts of $O_2$ (Kumełan *et al.*, 2005:595). The amount of $O_2$ absorbed is, however, very small and for the rest of the experiments it was assumed that all the absorbed gas is $SO_2$. In Figure 4.5 to 4.9 it can be seen that as the percentage $SO_2$ in the feed increases, the amount of $SO_2$ absorbed per mole of ionic liquid also increases at all

temperatures. This is to be expected, because for a higher percentage $SO_2$, the partial pressure of $SO_2$ is higher, therefore there is more $SO_2$ and less $O_2$ to absorb and therefore, the absorption is higher.

In Figure 4.5 to 4.9 it can also be seen that the temperature of the ionic liquid has a large influence on the maximum absorption of the ionic liquid. For each of the compositions the highest amount of $SO_2$ absorbed is at 30°C and the lowest at 60°C, which is consistent with results obtained by Lee *et al.* (2008:6035) and Anderson *et al.* (2006:15059). At 30°C and with the feed gas stream at 100 mol% $SO_2$ the ionic liquid absorbed 2.48 mol $SO_2$/mol IL for the 95% pure ionic liquid and 2.68 mol $SO_2$/mol IL for the 98% pure ionic liquid. This is much more than the 1.38 mol $SO_2$/mol IL that Lee *et al*. (2008:6035) observed with the same ionic liquid with a purity of 99% at 35°C and with 100 mol% $SO_2$ gas.

Figure 4.5 to 4.9 also indicate that the 95% pure ionic liquid (blue bars) achieved better absorption than the 98% pure ionic liquid (red bars), except on two occasions. Table 4.1 shows the percentage difference for the maximum absorption between the 95% and 98% pure ionic liquid for the 25, 50, 75 and 100 mol% $SO_2$ feed gas.

**Table 4.1: Percentage difference in absorption between 95% and 98% pure ionic liquid**

| Temperature (°C) | Feed gas composition (mole% $SO_2$) | Percentage difference |
|---|---|---|
| 30 | 25.0% | 21.83% |
| 40 | 25.0% | 23.17% |
| 50 | 25.0% | 30.99% |
| 60 | 25.0% | 24.52% |
| 30 | 50.0% | 11.91% |
| 40 | 50.0% | 6.01% |
| 50 | 50.0% | 12.38% |
| 60 | 50.0% | 29.14% |
| 30 | 75.0% | 23.00% |
| 40 | 75.0% | 14.86% |
| 50 | 75.0% | 9.13% |
| 60 | 75.0% | -17.09% |
| 30 | 100.0% | -8.09% |
| 40 | 100.0% | 12.57% |
| 50 | 100.0% | 23.35% |
| 60 | 100.0% | 3.83% |

In Table 4.1 it can be seen that there were only two negative percentage values that indicate the two values where the 98% pure ionic liquid had better absorption than the 95% pure ionic liquid. This data shows that for most of the experiments the 95% pure ionic liquid absorption was more than the 98% pure ionic liquid absorption. It can be seen that nearly all the experiments had a percentage difference of more than 10.55% which is the 95% confidence interval calculated in Appendix D from the reproducibility data for the temperature experiments.

From this data it is clear that the 98% pure ionic liquid does not absorb more $SO_2$ than the 95% pure ionic liquid; thus it would be better to use the 95% pure ionic liquid to absorb $SO_2$. However, from the data in Figure 4.5 it was found that the selectivity of the 95% pure ionic liquid was not as good as that of the 98% pure ionic liquid. It has to be noted however that for 30$^oC$ the 95% pure ionic liquid still absorbed about 30 times more $SO_2$ than $O_2$, which means that even if some $O_2$ was absorbed the selectivity towards $SO_2$ was still very high. It is therefore, recommended that before a final decision is made about the selectivity of the two ionic liquids further investigation is needed.

### *4.2.2* Initial absorption rate

After the establishment of the maximum absorption capacities of the ionic liquids, the next important property to be determined is the rate at which the $SO_2$ is absorbed. In this section the absorption rate of the $SO_2$ into the ionic liquid will be calculated for the different temperatures, feed gas compositions and ionic liquid purities.

To calculate the initial rate at which the ionic liquid absorbed the $SO_2$, the initial slope of the $SO_2$ absorbed versus time graph (Figure 4.2) was calculated. This gave a value of the initial absorption rate in g/s which was then converted to mol $SO_2$/mol IL·min.

Figure 4.10 to 4.13 show the absorption rate versus the temperature of the absorption chamber at 25, 50, 75 and 100 mol% $SO_2$ for the feed gas. For the feed gas at 0 mol% $SO_2$ (100 mol% $O_2$) there is basically no absorption thus the absorption rate is zero.

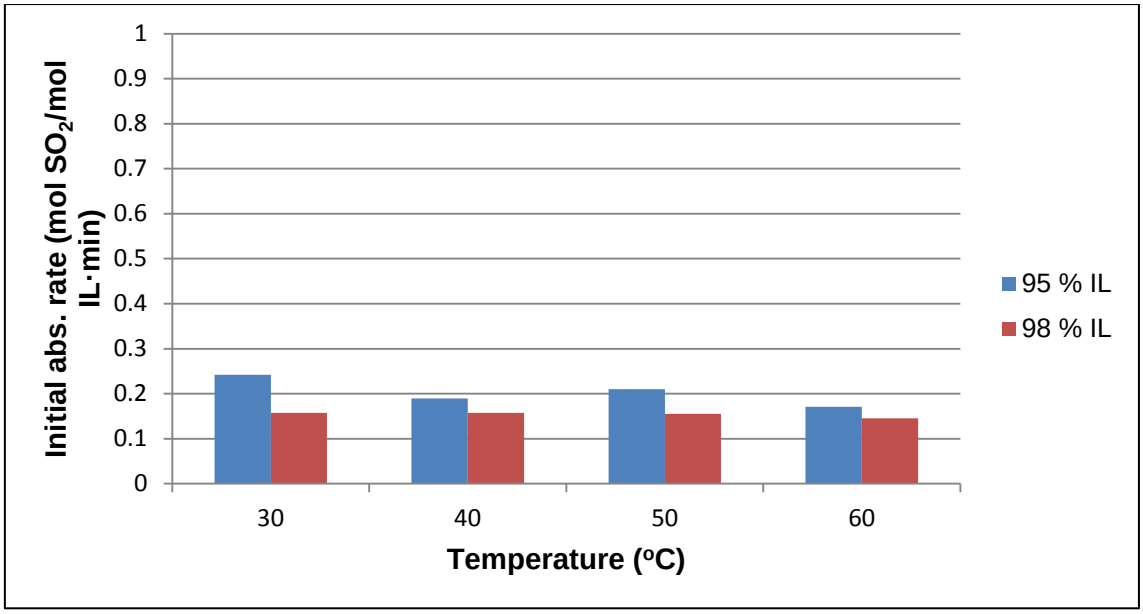


**Figure 4.10: Initial absorption rate with 25 mol% $SO_2$**

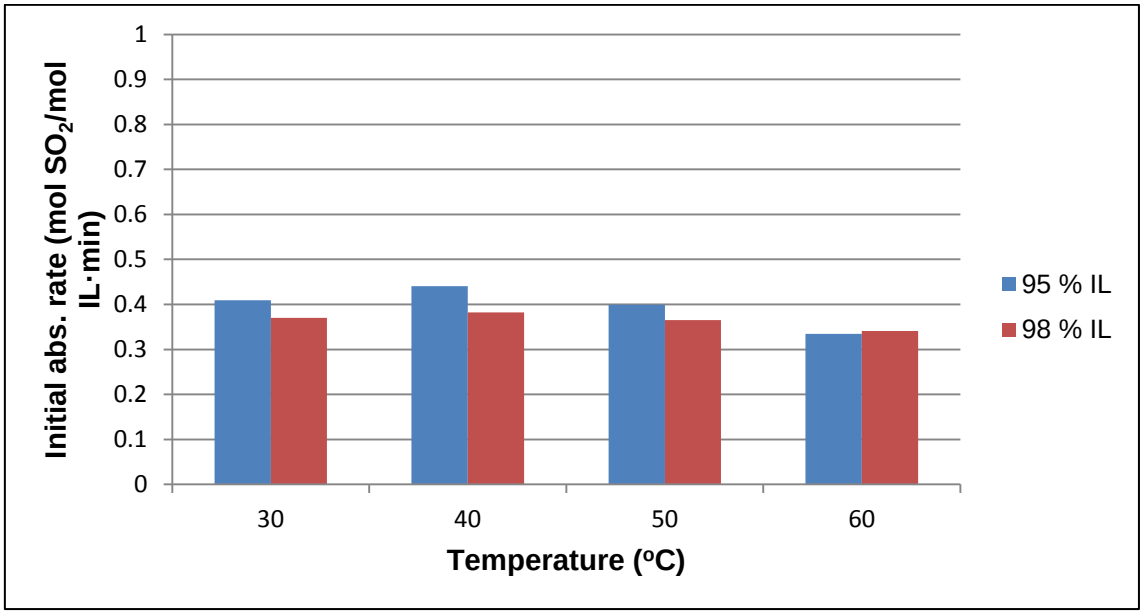


**Figure 4.11: Initial absorption rate with 50 mol% $SO_2$**

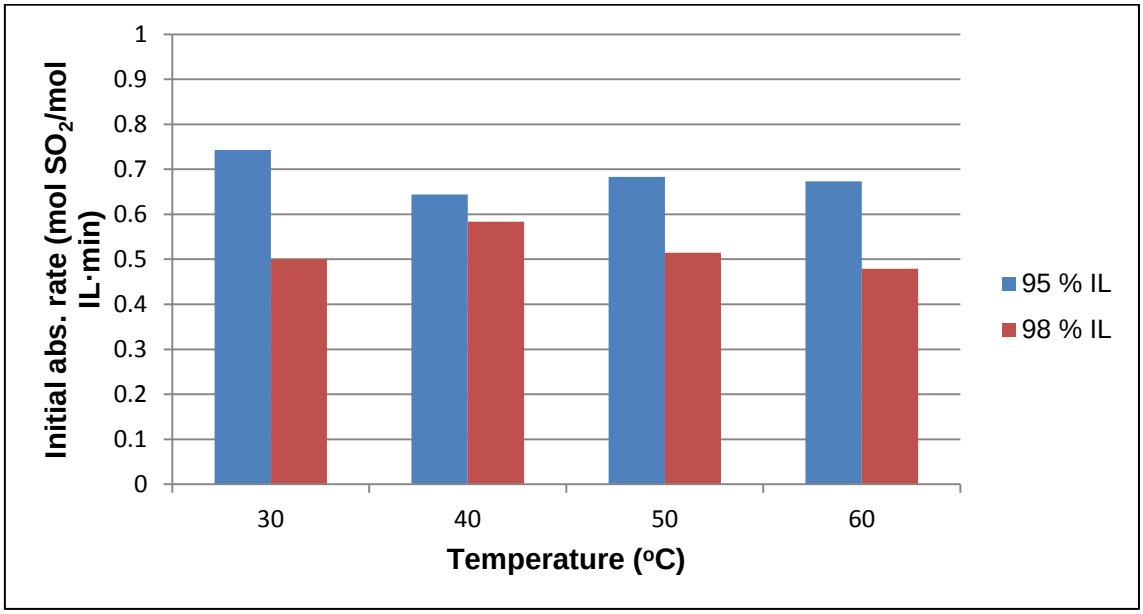


**Figure 4.12: Initial absorption rate with 75 mol% $SO_2$**

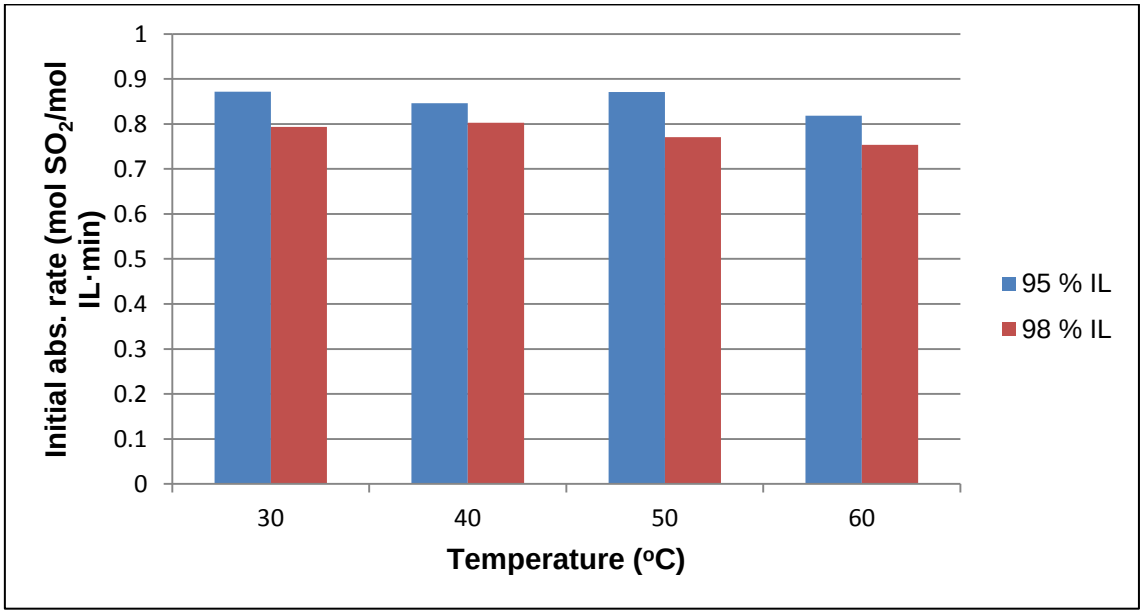


**Figure 4.13: Initial absorption rate with 100 mol% $SO_2$**

In the Figure 4.10 to Figure 4.13 it can be seen that the composition of the feed gas stream, which is a function of the partial pressure of the gas, had an influence on the initial absorption rate. When all four of the figures are considered it is clear that the initial absorption rate increases as the percentage $SO_2$ increases. This is due to the fact that when the percentage $SO_2$ in the feed stream increases the amount of $SO_2$ that is available to absorb also increases and therefore, the ionic liquid can absorb the $SO_2$ faster. The temperature of the absorption chamber did not have an influence on the initial absorption

rate. For each of the feed compositions the initial absorption rate remained almost constant across all of the temperatures, this was contrary to the maximum absorption data. When the absorption rates of all of the experiments are considered, it can be seen that the 95% pure ionic liquid consistently has a higher initial absorption rate than the 98% pure ionic liquid. This means that it will be better to use the cheaper 95% pure ionic liquid rather than the 98% pure ionic liquid.

Lee *et al.* (2008:6031.) found a maximum initial absorption rate of 0.06 mol $SO_2$/mol IL·min at 50$^o$C with a $SO_2$ feed composition of 66.6 mol% with a 99% pure ionic liquid, while the above data show an absorption rate of 0.40 mol $SO_2$/mol IL·min for a 50 mol% $SO_2$ feed at 50$^o$C with the 95% pure ionic liquid. The 98% pure ionic liquid had an absorption rate of 0.36 mol $SO_2$/mol IL·min at the same conditions. Thus the results from this study show higher initial absorption rates than obtained by Lee *et al.* (2008:6031) with the same ionic liquid at different ionic liquid purities.

### 4.2.3 Desorption rate

After the ionic liquid was saturated with $SO_2$ the temperature of the absorption chamber was increased to 125$^o$C to desorb the $SO_2$. The desorption rate was calculated in a similar way as the absorption rate in Section 4.2.2. The initial slope of the $SO_2$ absorbed versus time graph (Figure 4.2) was calculated for the section after 2000 seconds when the $SO_2$ was desorbed. From this slope the initial desorption rate in g/s was obtained and then converted to mol $SO_2$/mol IL·min.

Figure 4.14 to Figure 4.17 show the initial desorption rate versus the feed composition at 30, 40, 50 and 60$^o$C. Because no $SO_2$ was absorbed at 0 mol% $SO_2$ the desorption rate was zero in each of the graphs.

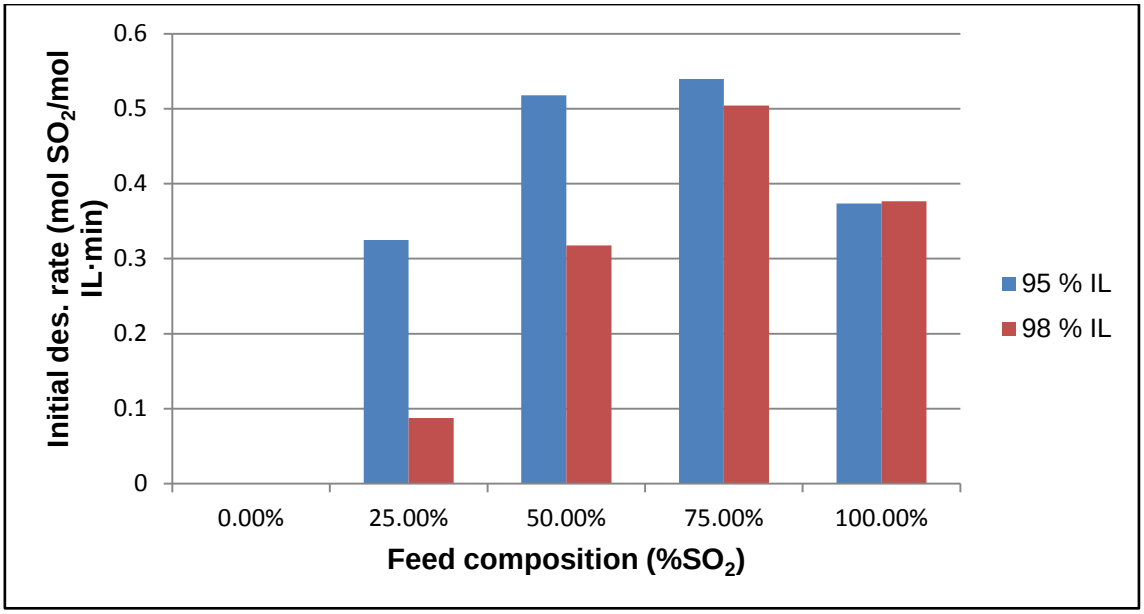


**Figure 4.14: Initial desorption rate versus composition at 30°C**

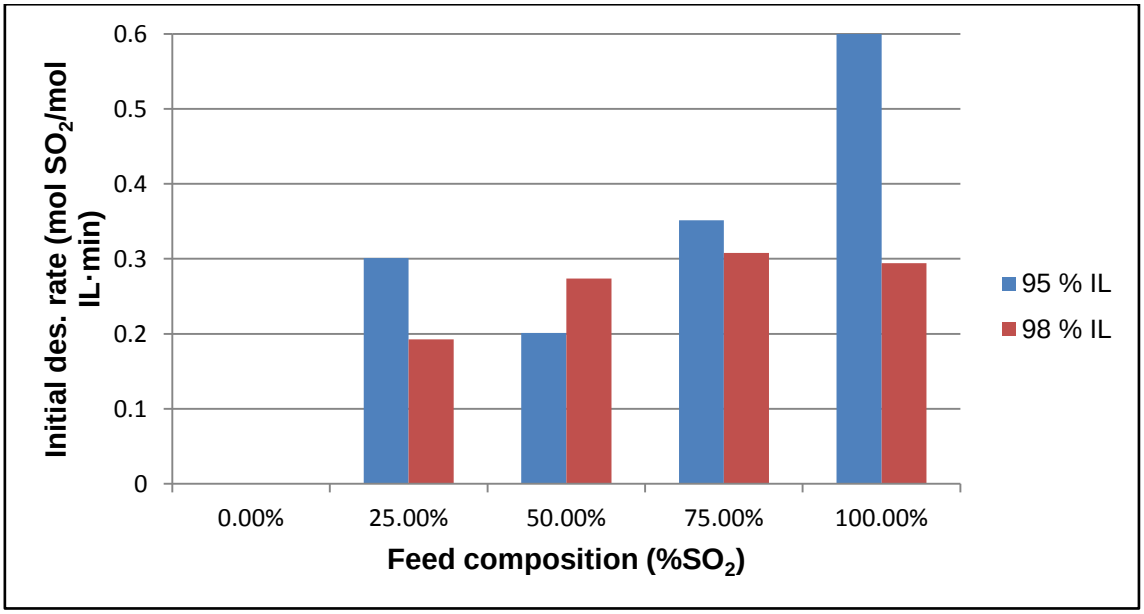


**Figure 4.15: Initial desorption rate versus composition at 40°C**

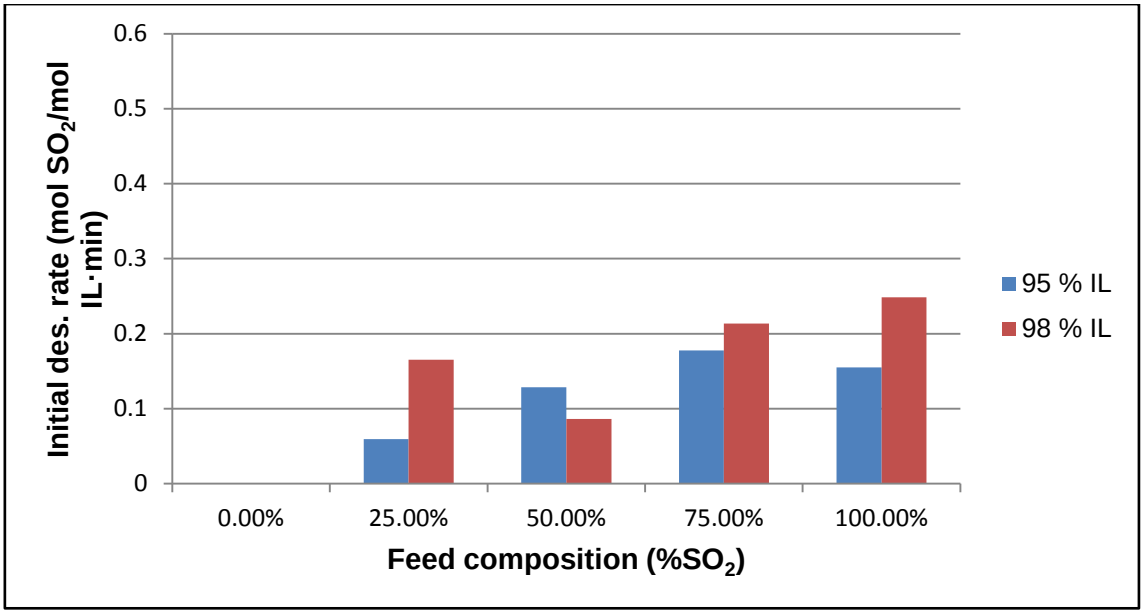


**Figure 4.16: Initial desorption rate versus composition at 50°C**

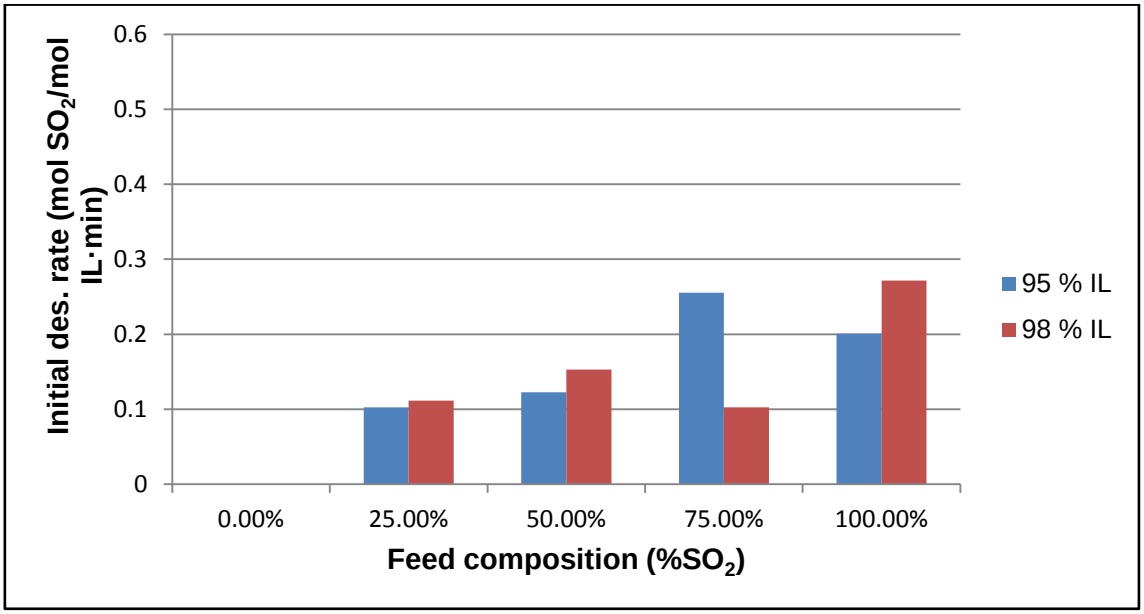


**Figure 4.17: Initial desorption rate versus composition at 60°C**

Figure 4.14 to Figure 4.17 show that there was no clear correlation between the desorption rate and the feed composition. However it may be seen that the desorption rates at 50°C and 60°C were lower than the rates at 30°C and 40°C. This can be explained by the fact that the desorption times for all of the experiments were in the same range and will be illustrated in Table 4.2, hence if more $SO_2$ was absorbed the desorption rate will be higher. There was also no clear difference between the desorption rates of the 95% and 98% pure ionic liquid.

The desorption time was calculated by taking the average value of the data points from the 2 500 second mark until the end of the experiment. This gave the value where the mass of

$SO_2$ stabilised after desorption, which was always close to zero. The desorption time was calculated as the time from when the temperature was increased until the data points reached the average value. Table 4.2 shows the desorption times of the 95% and 98% pure ionic liquids.

**Table 4.2: Desorption times of the 95% and 98% pure ionic liquids**

| Feed composition (% $SO_2$) | Temperature ($^oC$) | Desorption Time (s) | |
|---|---|---|---|
| | | 95% IL | 98% IL |
| 0.0% | 30 | 0 | 0 |
| 0.0% | 40 | 0 | 0 |
| 0.0% | 50 | 0 | 0 |
| 0.0% | 60 | 0 | 0 |
| 25.0% | 30 | 480 | 780 |
| 25.0% | 40 | 700 | 400 |
| 25.0% | 50 | 860 | 620 |
| 25.0% | 60 | 440 | 620 |
| 50.0% | 30 | 620 | 680 |
| 50.0% | 40 | 600 | 740 |
| 50.0% | 50 | 580 | 400 |
| 50.0% | 60 | 540 | 260 |
| 75.0% | 30 | 620 | 780 |
| 75.0% | 40 | 460 | 460 |
| 75.0% | 50 | 600 | 620 |
| 75.0% | 60 | 640 | 620 |
| 100.0% | 30 | 560 | 740 |
| 100.0% | 40 | 700 | 540 |
| 100.0% | 50 | 800 | 560 |
| 100.0% | 60 | 880 | 620 |

In Table 4.2 it can be seen that the desorption times for all of the experiments were in the range of about 400 – 800 seconds. Therefore, irrespective of the amount of $SO_2$ absorbed ,it always took roughly the same amount of time to desorb all the $SO_2$. This can be explained by looking at Figure 2.5. Lee *et al.* (2008:6031) also desorbed $SO_2$ from the [BMIm][$MeSO_4$] ionic liquid, but at different temperatures. It can be seen that, as the desorption temperature increased, desorption time decreased. The desorption time decreased from almost 3 600 seconds at 70$^o$C to about 600 seconds at 130$^o$C. The value of 600 seconds at 130$^o$C is very

similar to the desorption times achieved in Table 4.2 above (Lee *et al.*, 2008:6031). Thus, it can be concluded that desorption time is mostly influenced by the desorption temperature and because desorption temperature was kept constant for all the temperature experiments, desorption time was always in the same range.

### 4.3 Data modelling

During the experiments one of the most important results obtained was the maximum absorption of the ionic liquid as reported in Section 4.2.1. In Section 2.1.3.3, three absorption isotherms were evaluated. It was decided to use the Langmuir isotherm to model the data because:

- The Freundlich isotherm assumes that the amount of $SO_2$ absorbed does not have a limit. However from Figure 4.4 it may be seen that the amount of $SO_2$ absorbed reaches a maximum and does not increase any further. This is the same with all of the experiments where a limit is reached after a certain time. The limits that is reached is the maximum amount of $SO_2$ that the ionic liquid can absorb that was calculated in Section 4.2.1.
- According to Seader & Henley (2006:145) Henry's law may not be applicable to gasses with high solubility, even at low partial pressures. Consider the fact that $O_2$ has a solubility of 0.080 mol $O_2$/mol IL (Figure 4.5), $H_2$ a solubility of $2.148\times10^{-3}$ mol $H_2$/mol IL and CO a solubility of $4.458\times10^{-3}$ mol CO/mol IL in the ionic liquid [BMIm][$MeSO_4$] (Kumełan *et al.*, 2007:5). Then it can be assumed that a solubility of around 2.50 mol $SO_2$/mol IL is a high solubility. Also Henry's Law is not applicable when the graph of $SO_2$ absorbed versus the partial pressure of $SO_2$ is not a straight line. This can be seen in Figure 4.18 and Figure 4.19 where the absorption data is plotted versus the partial pressure of the $SO_2$. In Figure 4.18 and Figure 4.19 linear trend lines were also plotted together with error bars that indicate the 10.55% confidence interval. From these figures it may be seen that there are some points that do not fall within the linear band indicated by the trend line, also the general shape of the data is not 100% linear.

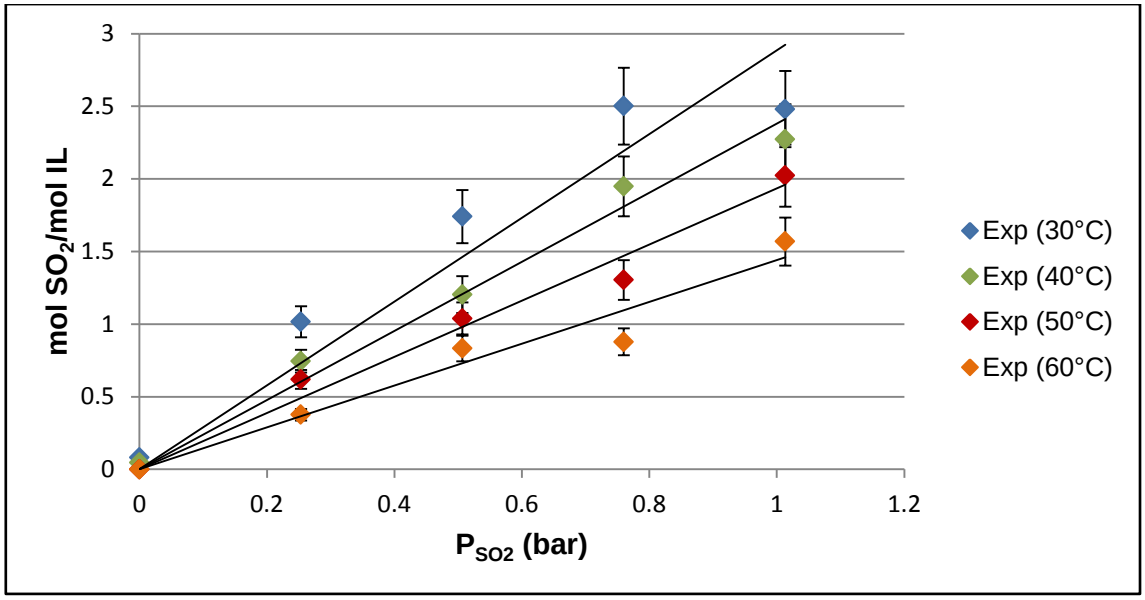


**Figure 4.18: Absorption data for the 95% pure ionic liquid**

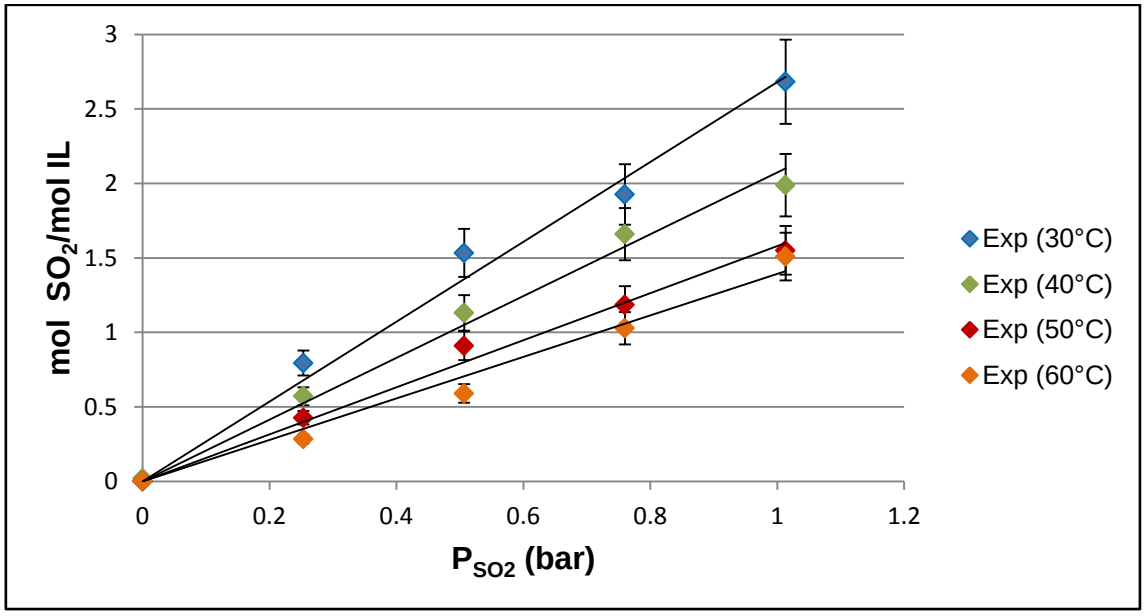


**Figure 4.19: Absorption data for the 95% pure ionic liquid**

In Section 4.3.1 to 4.3.3, the Langmuir isotherm will be fitted to the maximum absorption data. After which the model will be evaluated to see how well it fits the data. The data will also be evaluated using the Clausius-Clapeyron equation in order to calculate the heat of desorption as a function of $SO_2$ absorbed. The heat of desorption can then be used to determine if the desorption process and then the absorption process was exothermic or endothermic.

### 4.3.1 Fitted model

It was decided to model the maximum mole amount of $SO_2$ absorbed into the ionic liquid at different temperatures. Table 4.3 shows the absorption temperature, amount of $SO_2$ absorbed in the ionic liquid and partial pressure of $SO_2$.

**Table 4.3: Mole $SO_2$ absorbed per mole ionic liquid**

| 95% IL | | | 98% IL | | |
|---|---|---|---|---|---|
| **Temperature ($^oC$)** | **mol SO2/ mol IL** | **$P_{SO2}$ (bar)** | **Temperature ($^oC$)** | **mol SO2/ mol IL** | **$P_{SO2}$ (bar)** |
| 30 | 0.08 | 0.000 | 30 | 0.00 | 0.000 |
| 30 | 1.02 | 0.253 | 30 | 0.79 | 0.253 |
| 30 | 1.74 | 0.507 | 30 | 1.53 | 0.507 |
| 30 | 2.50 | 0.760 | 30 | 1.93 | 0.760 |
| 30 | 2.48 | 1.013 | 30 | 2.68 | 1.013 |
| 40 | 0.05 | 0.000 | 40 | 0.02 | 0.000 |
| 40 | 0.74 | 0.253 | 40 | 0.57 | 0.253 |
| 40 | 1.20 | 0.507 | 40 | 1.13 | 0.507 |
| 40 | 1.95 | 0.760 | 40 | 1.66 | 0.760 |
| 40 | 2.27 | 1.013 | 40 | 1.99 | 1.013 |
| 50 | 0.00 | 0.000 | 50 | 0.00 | 0.000 |
| 50 | 0.62 | 0.253 | 50 | 0.43 | 0.253 |
| 50 | 1.04 | 0.507 | 50 | 0.91 | 0.507 |
| 50 | 1.30 | 0.760 | 50 | 1.18 | 0.760 |
| 50 | 2.02 | 1.013 | 50 | 1.55 | 1.013 |
| 60 | 0.00 | 0.000 | 60 | 0.00 | 0.000 |
| 60 | 0.38 | 0.253 | 60 | 0.28 | 0.253 |
| 60 | 0.83 | 0.507 | 60 | 0.59 | 0.507 |
| 60 | 0.88 | 0.760 | 60 | 1.03 | 0.760 |
| 60 | 1.57 | 1.013 | 60 | 1.51 | 1.013 |

The above data was used to plot the mole $SO_2$ absorbed versus the partial pressure of $SO_2$ for each of the temperatures. The Langmuir equation was then used to calculate values for the mole $SO_2$ absorbed. The method of least squares was used to calculate the fitted values for k and $x_{max}$. For each of the temperatures these values of k and $x_{max}$ are shown in Table 4.4.

**Table 4.4: Values calculated for k and $x_{max}$ at each temperature**

| | k (1/bar) | | $x_{max}$ (mol $SO_2$/ mol IL) | |
|---|---|---|---|---|
| **Temperature (°C)** | **98% IL** | **95% IL** | **98% IL** | **95% IL** |
| **30** | 0.92 | 1.11 | 4.91 | 4.94 |
| **40** | 0.70 | 0.90 | 4.60 | 4.54 |
| **50** | 0.49 | 0.69 | 4.49 | 4.23 |
| **60** | 0.46 | 0.48 | 4.05 | 4.08 |

Figure 4.20 and Figure 4.21 show the experimental data together with the model data for the 95% and 98% pure ionic liquids.

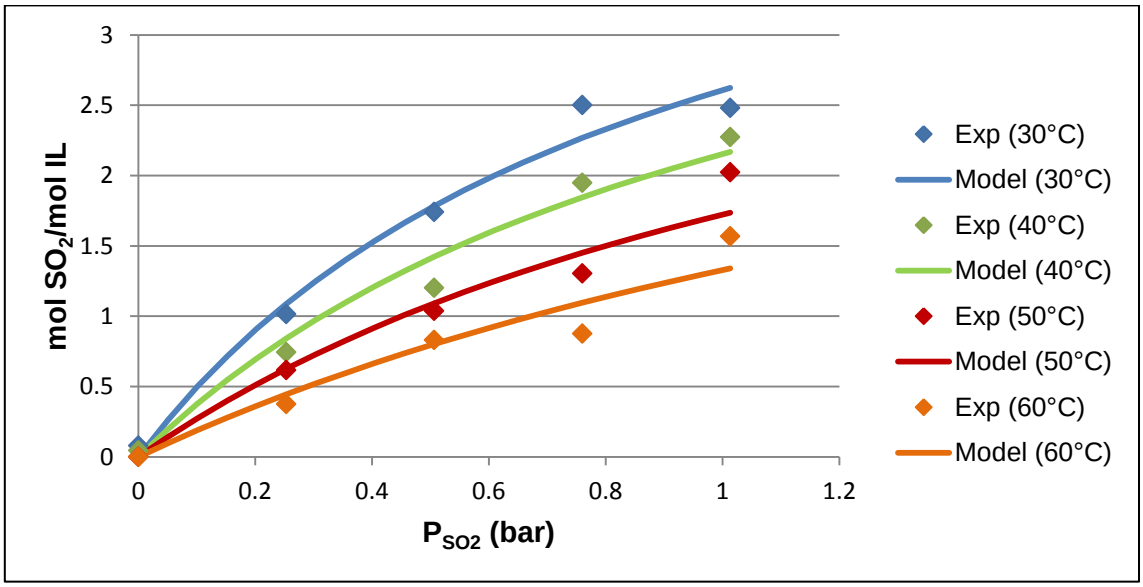


**Figure 4.20: Experimental data and model data for the 95% pure ionic liquid**

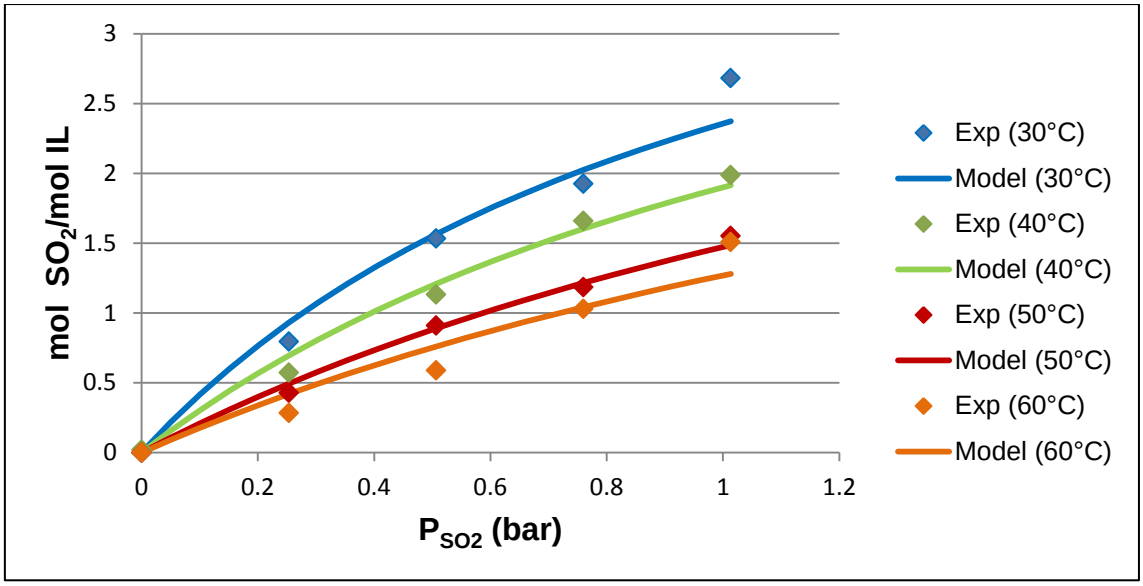


**Figure 4.21: Experimental data and model data for the 98% pure ionic liquid**

In Figure 4.20 and Figure 4.21 it can be seen that the model followed the trend of the experimental data, thus the Langmuir absorption model can be used to predict the $SO_2$ absorption into this ionic liquid. The next section will evaluate how well the model fitted the experimental data.

### 4.3.2 Model evaluation

Firstly, to evaluate how well the model fitted the data the standard deviation of the experimental values and the calculated values were calculated. The equation used to calculate the standard deviation was (Ochoa *et al.*, 2001:172):

$$SD = \sqrt{\frac{\sum(y_{exp} - y_{calc})^2}{N - p}} \qquad \text{Equation 4.2}$$

Where:

SD – Standard deviation

$y_{exp}$ – Experimental value

$y_{calc}$ – Value predicted by the model.

N – Number of data points.

p – Number of fitted parameters.

Table 4.5 shows the standard deviations calculated for each of the temperatures and both ionic liquids. These values show how much the model deviated from the experimental data.

**Table 4.5: Standard deviation in percentages**

| | SD (%) | |
|---|---|---|
| **Temperature ($^oC$)** | **95% IL** | **98% IL** |
| **30** | 21.49% | 20.41% |
| **40** | 20.51% | 10.07% |
| **50** | 19.93% | 5.77% |
| **60** | 20.13% | 18.26% |

In Table 4.5 it can be seen that the highest standard deviation was for the 95% pure ionic liquid at 30$^o$C which had a standard deviation of 21.49%. The average standard deviation for all of the experiments was 17.07%. The second method used to evaluate how well the model fitted the experimental data was to plot the experimental data versus the calculated data from the model. If the model fitted the data perfectly all of the data points would be in a straight line through the origin of the graph with a slope of one. Figure 4.22 shows the experimental data versus the calculated data from the model for the 95% and 98% pure ionic liquid.

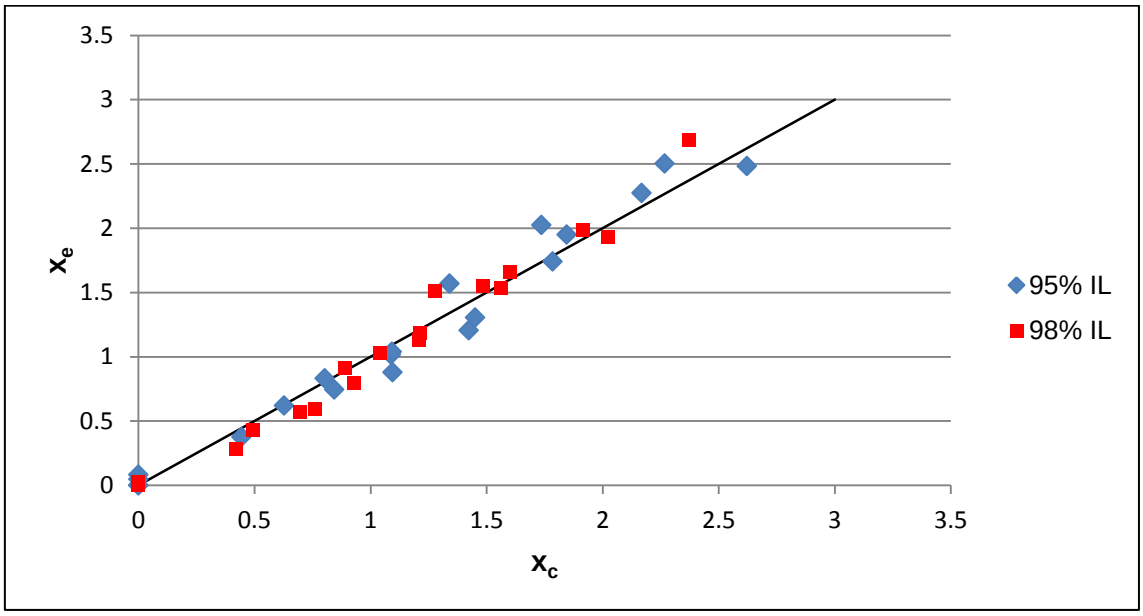


**Figure 4.22: Experimental data versus the calculated data from the model for the 95% pure ionic liquid**

The figure above shows the plot of the experimental data versus the calculated data with the black line being a straight line through the origin with a slope of one. It is clear from the figure that all the data points are close to this line, which means that the calculated model data correlated well with the experimental data.

From the standard deviation data in Table 4.5 and Figure 4.22 it can be concluded that the Langmuir absorption model fits the experimental data. This model can now be used to predict the maximum mole fraction of $SO_2$ that was absorbed into the ionic liquid at certain temperatures and pressures.

### 4.3.3 Clausius-Clapeyron

In order to determine if the absorption reaction is endothermic or exothermic the heat of desorption for the reaction has to be calculated. This can be achieved by using the Clausius-Clapeyron equation shown below (Koretsky, 2004:261):

$$\boldsymbol{d}(\ln \boldsymbol{P_{SO2}}) = -\frac{\boldsymbol{\Delta H_{des}}}{\boldsymbol{R}} \boldsymbol{d}(\frac{\mathbf{1}}{\boldsymbol{T}}) \qquad \text{Equation 4.3}$$

Where:

$P_{SO2}$ – Partial pressure of $SO_2$

$\Delta H_{des}$ – Heat of desorption

R – Gas constant (8.314 J/molK)

T – Temperature (K)

From Equation 4.3 it may be seen that a plot of $\ln(P_{SO2})$ versus 1/T would give a straight line with $-\Delta H_{abs}/R$ as the slope. Firstly the $P_{SO2}$ has to be calculated, in order to plot the graph. This was achieved by determining interpolated values for $P_{SO2}$ at three different $SO_2$ absorption amounts, namely 0.5, 1.0 and 1.5 mol $SO_2$/mol IL at each of the experimental temperatures. To determine these values Figure 4.23 and Figure 4.24 were plotted, that show the $SO_2$ absorption data versus the partial pressure of $SO_2$. The lines connecting the experimental points are not a model and only show the trend of the data. These lines will be used to read the partial pressure for each temperature at 0.5, 1.0 and 1.5 mol $SO_2$ absorbed.

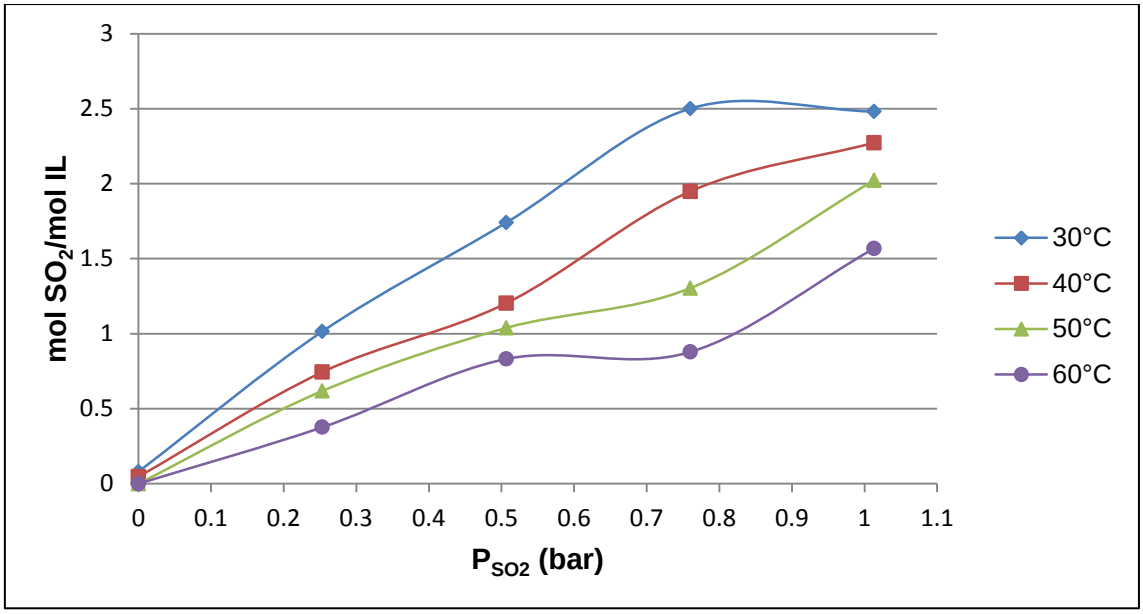


**Figure 4.23: Plot of mol $SO_2$ absorbed versus the partial pressure of $SO_2$ at 30°C, 40°C, 50°C and 60°C for 95% pure ionic liquid**

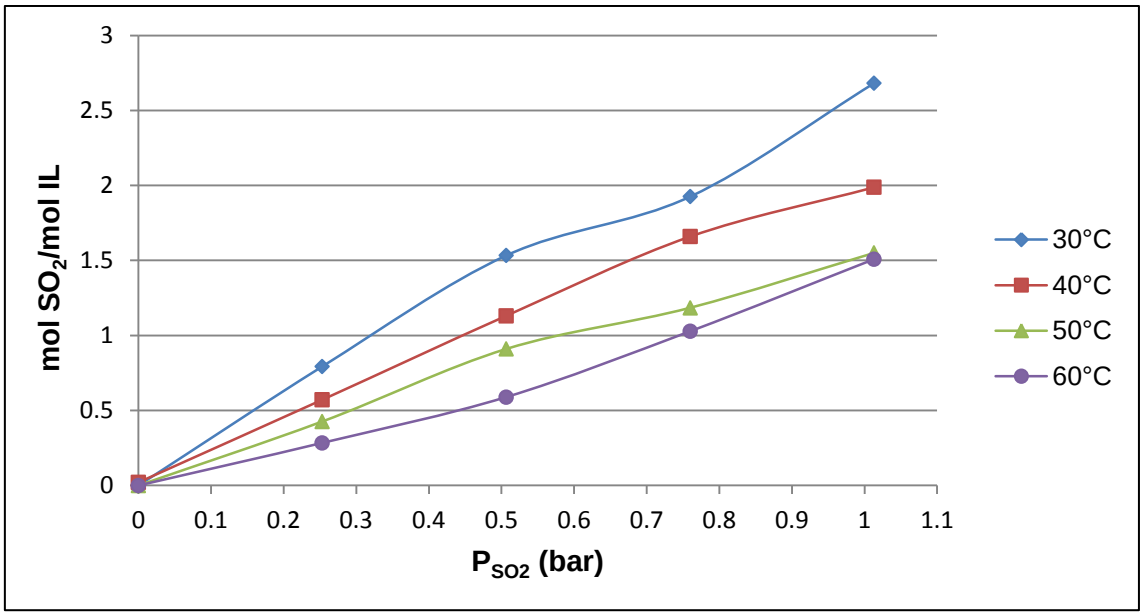


**Figure 4.24: Plot of mol $SO_2$ absorbed versus the partial pressure of $SO_2$ at 30°C, 40°C, 50°C and 60°C for 98% pure ionic liquid**

From Figure 4.23 and Figure 4.24 the $SO_2$ partial pressures for 0.5, 1.0 and 1.5 mol $SO_2$ absorbed were read from the graphs and are reported in Table 4.6.

**Table 4.6: $SO_2$ partial pressure**

| 95% Ionic liquid | | | |
|---|---|---|---|
| | $P_{SO2}$ (bar) | | |
| Temperature (°C) | 0.5 mol $SO_2$ | 1 mol $SO_2$ | 1.5 mol $SO_2$ |
| 30 | 0.11 | 0.25 | 0.42 |
| 40 | 0.16 | 0.40 | 0.61 |
| 50 | 0.20 | 0.48 | 0.84 |
| 60 | 0.32 | 0.82 | 0.99 |
| **98% Ionic liquid** | | | |
| | $P_{SO2}$ (bar) | | |
| Temperature (°C) | 0.5 mol $SO_2$ | 1 mol $SO_2$ | 1.5 mol $SO_2$ |
| 30 | 0.16 | 0.32 | 0.50 |
| 40 | 0.22 | 0.45 | 0.68 |
| 50 | 0.29 | 0.58 | 0.98 |
| 60 | 0.44 | 0.74 | 1.01 |

From the data in Table 4.6, $\ln(P_{SO2})$ versus 1/T graphs could be drawn and are shown in Figure 4.25 and Figure 4.26.

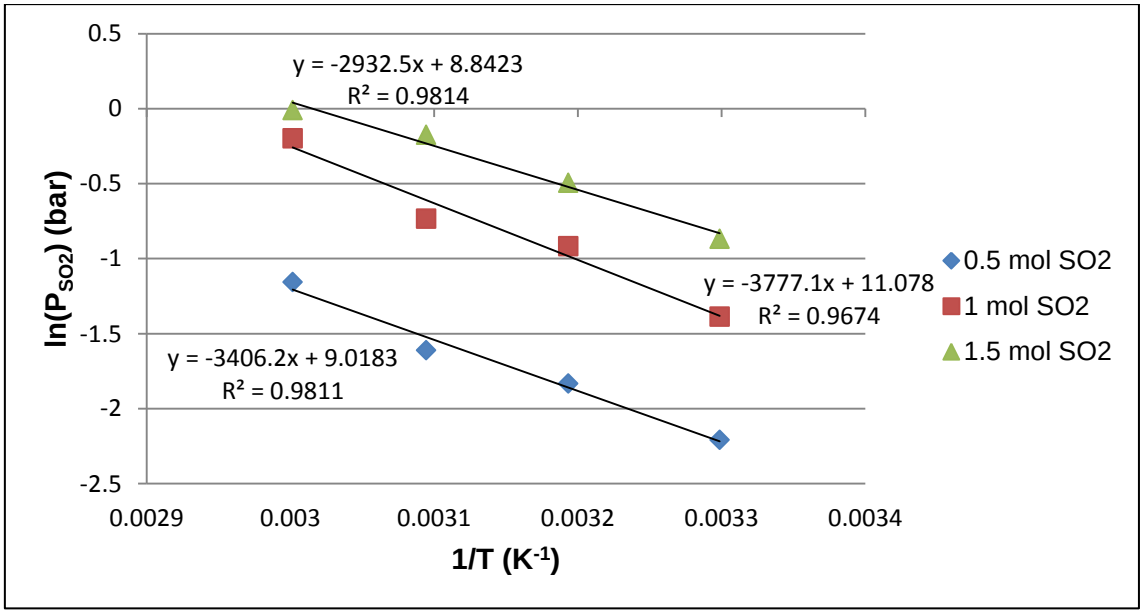


**Figure 4.25: Plot of $\ln(P_{SO2})$ versus 1/T for 95% pure ionic liquid**

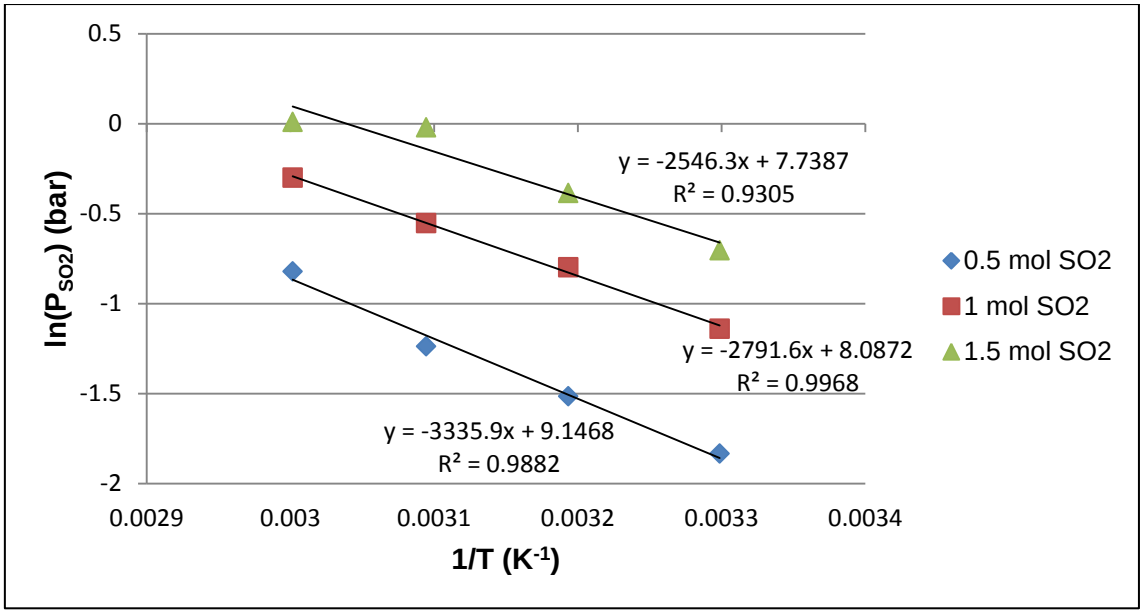


**Figure 4.26: Plot of $\ln(P_{SO2})$ versus 1/T for 98% pure ionic liquid**

By using the above figures trendlines were plotted through the data as shown above. The slopes of these trend lines were then used to calculate the heat of desorption, as shown from Equation 4.3 for each of the $SO_2$ amounts desorbed. The heat of desorption is shown in Table 4.7.

**Table 4.7: Heat of desorption**

| | $\Delta H_{abs}$ (kJ/mol) | |
|---|---|---|
| **$SO_2$ absorbed (mol $SO_2$ /mol IL)** | **95% IL** | **98% IL** |
| **0.5** | 28.32 | 27.73 |
| **1.0** | 31.40 | 23.20 |
| **1.5** | 24.38 | 21.17 |

The heat of desorption data in Table 4.7 indicate that the desorption of $SO_2$ from this ionic liquid is an endothermic reaction because the heat of desorption values are positive. The data also show a trend that the heat of desorption decreases as the amount of $SO_2$ absorbed increases. Therefore it may be concluded that the absorption reaction is exothermic if the desorption reaction is endothermic.

# Chapter 5

# Pressure experiments – Results, discussion and observations

## 5.1 Experimental results

The raw experimental data for the pressure experiments, as well as the volumes of the chambers and the constants used in the calculations, can be found in Appendix C. These results were used in the next section to plot Figure 5.1 and Figure 5.2.

## 5.2 Analysed data

Figure 5.1 shows the number of moles of gas absorbed into the ionic liquid for $O_2$ and $SO_2$ during each experimental run. For the $O_2$ experiments the pressure stabilised about five minutes after valve V-2 was opened to let the gas from E-1 into E-2. This is because the ionic liquid absorbs the $O_2$ very poorly and therefore after about five minutes the maximum amount of $O_2$ had been absorbed.

For the $SO_2$ experiments the pressure did not stabilise after five minutes as with the $O_2$, but changed for an extended period of time. During the experiment the absorption takes place very rapidly for the first ten minutes then it starts to slow down as the concentration of the $SO_2$ in the chambers decreases. The reason the concentration has an influence on the rate of absorption is because the absorption is a function of diffusion, which is a function of concentration. Thus, as the concentration of the $SO_2$ decreases the diffusion rate will decrease and therefore, the rate of absorption will also decrease. It should also be noted that the rate of diffusion is influenced by both temperature and viscosity through the diffusion coefficient (Miller, 1924:724). The influence of the concentration as well as the temperature and viscosity is discussed in Equation 5.1and 5.2. Hence the reason the pressure keeps on changing is because the ionic liquid has a very high selectivity towards $SO_2$ and the rate of

the pressure drop will diminish until all the $SO_2$ has been absorbed. Because, theoretically, all the $SO_2$ will never be completely absorbed, it was decided to let the system equalise for ten minutes before the pressure readings were taken.

The experimental errors calculated were very small and will therefore not be shown on Figure 5.1 and Figure 5.2. The errors calculated for the $O_2$ experiments with the 98% pure ionic liquid were on average 0.1% and it was less than 0.01% for all the other experiments. Figure 5.1 shows the moles of $SO_2$ and $O_2$ that were absorbed per mole of ionic liquid versus the initial feed pressure in the 95% and 98% pure ionic liquid.

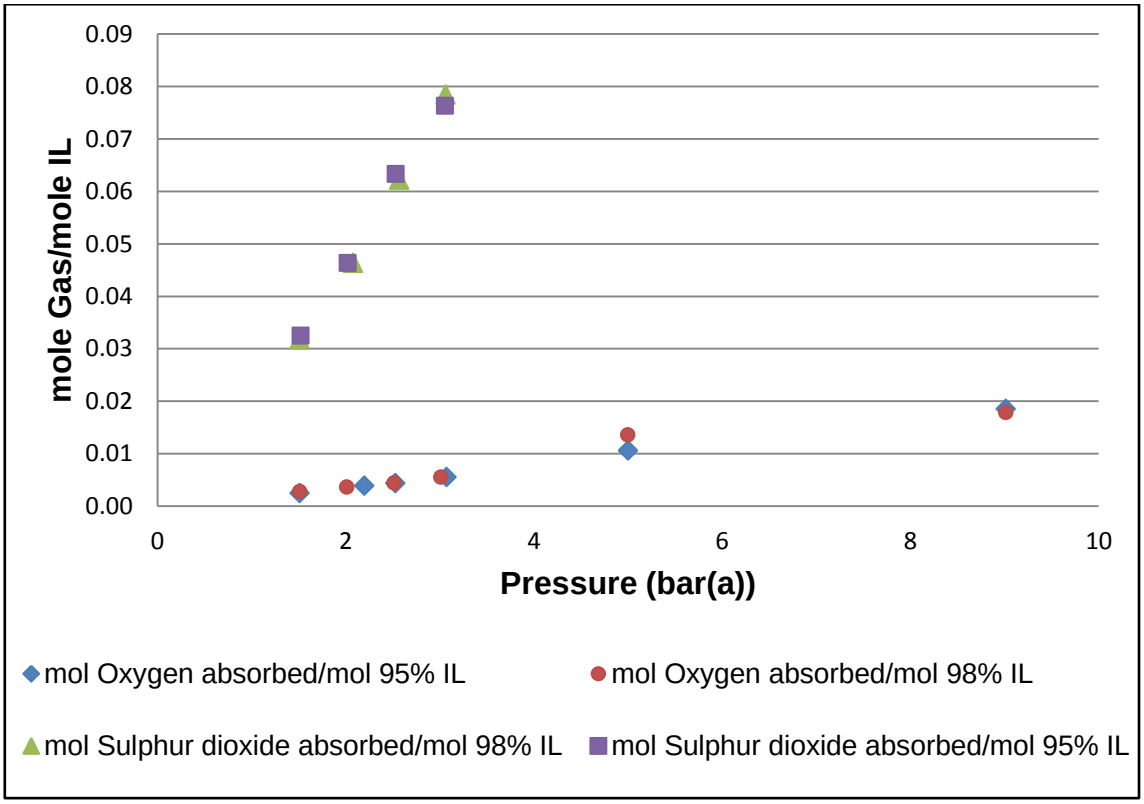


**Figure 5.1: Mole gas absorbed per mole of ionic liquid at different initial feed pressures for $SO_2$ and $O_2$ in 95% and 98% pure ionic liquid.**

In Figure 5.1 it can be seen that the number of moles of $SO_2$ that was absorbed per mole of ionic liquid was about fifteen times more than the number of moles of $O_2$ absorbed. The results in Figure 4.5 also illustrated the low $O_2$ absorption of the ionic liquid. From this it can be concluded that the ionic liquid has a high selectivity towards $SO_2$. During experiments conducted by Lee *et al.* (2008:6033) it was found that the anion in the ionic liquid had a very large effect on the absorption capacity of a specific gas. In other words, the reason that [BMIm][$MeSO_4$] has such a good selectivity towards $SO_2$ can be ascribed to the presence of the [$MeSO_4$] anion in the ionic liquid.

The data also indicated that at higher feed pressures, more $SO_2$ and $O_2$ were absorbed. However, Figure 5.1 alone cannot be used to make this assumption, because a closed system was being used with a constant volume and if the initial feed pressure in the system was increased, the number of moles of gas in the system also increased. Therefore, the fact that the absorption according to Figure 5.1 increases when the feed pressure is increased is attributed to an increase in gas molecules at higher pressures.

To overcome this problem the mole% of the gas that had been absorbed into the ionic liquid in chamber E-2 was calculated. Figure 5.2 shows the mole% of the feed gas absorbed by the ionic liquid at each of the feed pressures for the 95 and 98% pure ionic liquid.

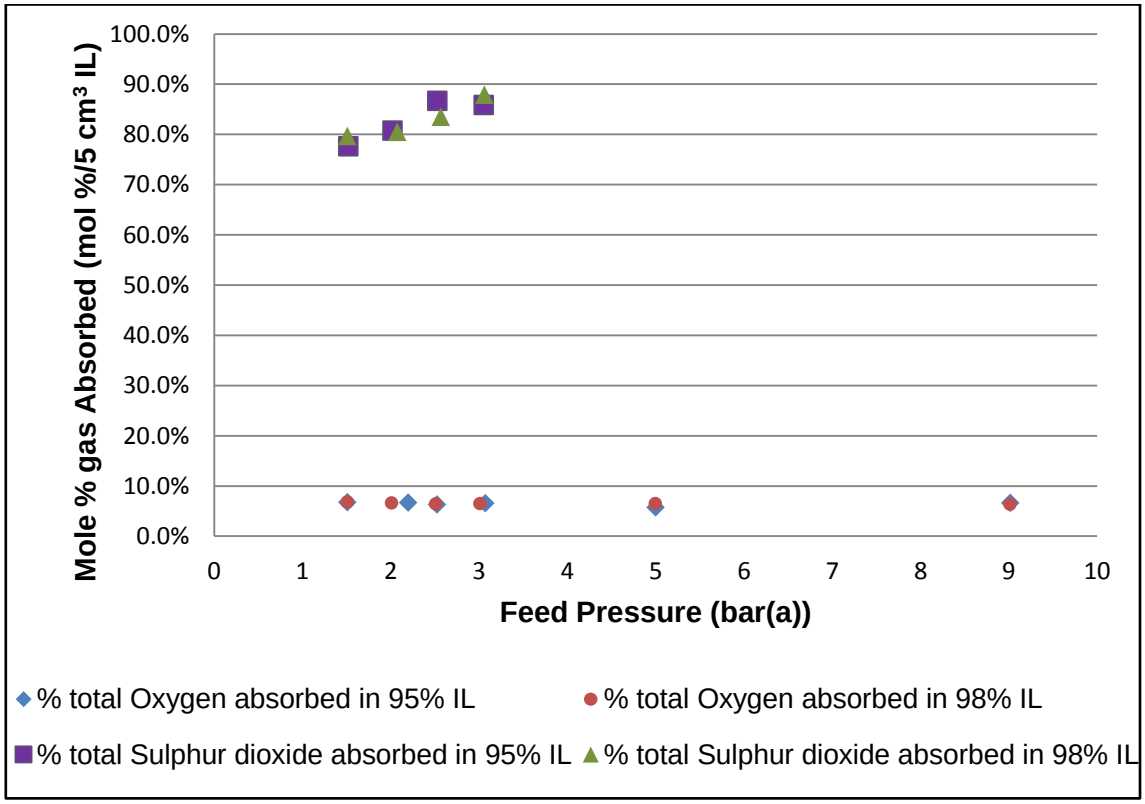


**Figure 5.2: Mole% gas fed to the system absorbed by the ionic liquid for $SO_2$ and $O_2$ at different feed pressures for 95 and 98% pure ionic liquid.**

In Figure 5.2 it can be seen that the percentage of $O_2$ absorbed into the ionic liquid remained constant at between 6 and 7 mol%. Therefore, it can be concluded that the mole percentage of $O_2$ absorbed by the ionic liquid is independent of the feed pressure. On the other hand, the data for the $SO_2$ show a clear trend for both the 95% and 98% pure ionic liquids. For the 95% pure ionic liquid the mole percentage gas absorbed into the ionic liquid increased from 77.6 mol% absorbed at 1.5 bar(a) to 85.8 mol% at 3.0 bar(a) and for the 98% pure ionic

liquid the trend increased from 79.7 mol% absorbed at 1.5 bar(a) to 87.9 mol% at 3.0 bar(a). These absorption results were obtained after the setup was allowed 10 minutes to reach equilibrium. When no mechanical stirring is possible in the sample (like the above experiments) equilibrium is reached only by diffusion of the gas into the sample (Anderson, 2008:56). Therefore trends observed in Figure 5.2 can be explained by Fick's law of diffusion, which is shown in Equation 5.1 (Seader & Henley, 2006:8):

$$\boldsymbol{J_{A_z} = -D_{AB}\frac{dc_A}{dz}} \qquad \text{Equation 5.1}$$

Where:

$J_{Az}$ – Is the molar flux of A by ordinary diffusion in the positive z direction.

$D_{AB}$ – Diffusion coefficient

$C_A$ – Molar concentration of A

$\frac{dc_A}{dz}$ – Concentration gradient of A, which is negative in the direction of ordinary diffusion.

Equation 5.1 shows that the molar flux and thus the rate of mass transfer of A is influenced by the concentration gradient of A. Because it is a closed system the concentration of the gas will increase when the feed pressure is increased. Therefore, the results in Figure 5.2 can be explained by the fact that as the feed pressure is increased the concentration, and naturally the concentration gradient, of the $SO_2$ is also increased. Fick's law shows that if the concentration gradient is increased the rate of mass transfer will increase and because the system was only allowed ten minutes to reach equilibrium the $SO_2$ absorption will also increase, as seen from the results in Figure 5.2. For pressures above 3 bar(a) it is unknown what the absorption trend will be, and further testing is required to determine how the absorption will be affected by these higher pressures. Equation 5.1 also holds true for the $O_2$ absorption, however because of the [$MeSO_4$] anion in the ionic liquid that has a good selectivity towards $SO_2$ the percentage of $O_2$ that is absorbed does not increase in Figure 5.2.

Additionally the rate of mass transfer is also influenced by both the temperature and the viscosity of the ionic liquid through the diffusion coefficient and should not be ignored. This influence can be expressed with the Stokes-Einstein equation shown below. (Miller, 1924:724):

$$\boldsymbol{D_{AB} = \frac{RT}{N_A}\cdot\frac{1}{6\pi\eta r}} \qquad \text{Equation 5.2}$$

Where:

$D_{AB}$ – Diffusion coefficient

R – Gas constant (R = 8.314 J/mol·K)

T – Absolute temperature (K)

$N_A$ – Avogadro's number (N = 6.0221415 × $10^{23}$)

η – Viscosity

r – Radius of a diffusing particle

This equation however is only valid under the following conditions:

- The particles move independently of each other.
- The particles have the same average kinetic energy as gas molecules at the same temperature.
- The equation describes spherical particles moving in a solvent of proportionately small molecules.

The final condition is not met in the case of $SO_2$ moving in an ionic liquid. Hence the Sutherland equation can be used in this case (Miller, 1924:743):

$$\boldsymbol{D_{AB}} = \frac{\boldsymbol{RT}}{\boldsymbol{N}} \cdot \frac{\mathbf{1}}{\boldsymbol{4\pi\eta r}} \qquad \text{Equation 5.3}$$

Or simplified to (Vorotyntsev *et al.*, 2010:5065):

$$\boldsymbol{D_{AB}} = \frac{\boldsymbol{k_b T}}{\boldsymbol{4\pi\eta r}} \qquad \text{Equation 5.4}$$

Where:

$k_b$ - Boltzmann constant (1.3806503 × $10^{-23}$ $m^2$ kg $s^{-2}K^{-1}$)

This equation is exactly the same as the Stokes-Einstein equation except for the denominator 4 instead of 6.

Equation 5.4 shows the relation between the diffusion coefficient (that influences the rate of mass transfer in Equation 5.1), temperature and the viscosity of the ionic liquid. From Equation 5.4 it may be seen that when the temperature of the ionic liquid increases or the viscosity decreases the diffusion coefficient will increase. When this happens the rate of mass transfer in Equation 5.1 will also increase.

The decrease of the ionic liquid viscosity during the $SO_2$ absorption process will be discussed in section 5.3.1. According to Equation 5.4 this would mean that the rate of absorption should increase as more $SO_2$ was absorbed, however as stated at the beginning of Section 5.2 the absorption rate decreased over time. Hence it can be concluded that the effect of the viscosity on the rate of absorption was smaller than that of the $SO_2$ concentration.

## 5.3 Additional results and observations

This section will describe some of the changes to the ionic liquids that were observed during the course of the pressure experiments. Experiments were also carried out to determine the change of ionic liquid volume during absorption. This section will discuss the results obtained from the volume experiments, as well as some conclusions and interesting observations about the ionic liquid observed during the experiments.

### 5.3.1 Physical changes to the ionic liquid

During the experiments the following changes were observed:

- The colour of the ionic liquid changed when it was used repeatedly. The 95% pure ionic liquid changed from light yellow to yellow and the 98% pure ionic liquid changed from colourless to yellow. After the change in colour the performance of the ionic liquids was not affected and the absorption capacity remained the same. Similar results were obtained by BASF in their pilot plant where the ionic liquid was used for three months and turned black, but it did not affect the ionic liquid performance. The colorant responsible for the change in colour has not been isolated yet because the quantities are very low; however, it is assumed that oligomers of the imidazole or even radical ions might be responsible for the change in colour (BASF, 2011). Therefore, if the colour of the ionic liquid changed during the experiments or in the HyS processes its performance would not be affected.
- The viscosity of both the 95% and 98% pure ionic liquid changed during the experiments. At the start of the experiments the ionic liquid was more viscous than water, almost like cooking oil, but when the $SO_2$ was absorbed into the ionic liquid the viscosity decreased noticeably. After the $SO_2$ had been desorbed from the ionic liquid and the liquid had cooled to room temperature the viscosity returned back to normal. As discussed in Section 2.2.1.4 a lower viscosity is advantageous for pressure drop, heat transfer and mass transfer.

### 5.3.2 Changes in ionic liquid volume

It was expected that the volume of the ionic liquid would change when $SO_2$ was absorbed. From the results in Figure 5.2 it is known that at higher pressures more $SO_2$ would be absorbed into the ionic liquid. Hence, if the volume of the ionic liquid increased when the pressure is increased it could be concluded that the increase in volume of the ionic liquid

would give an indication of the amount of $SO_2$ absorbed. To test this theory the change in volume of the ionic liquid before and after $SO_2$ absorption would be determined. To do this the 95% pure ionic liquid was saturated with $SO_2$ for twelve hours under constant $SO_2$ feed pressures of 1.5 and 2.0 bar(a), respectively. The results obtained from these two experiments are as follows:

- For the 1.5 bar(a) feed pressure the volume of the ionic liquid expanded from 5.00 $cm^3$ to 7.78 $cm^3$. This is an expansion of 55.50%.
- For the 2.0 bar(a) feed pressure the volume of the ionic liquid expanded from 5.00 $cm^3$ to 9.19 $cm^3$ . This is an expansion of 83.73%.

From these results it can be seen that the volume of the ionic liquid increased dramatically when large amounts of $SO_2$ was absorbed. It also confirms the theory that the volume increase is larger when more $SO_2$ is absorbed. This result is of crucial importance in a setup like the present, where the volume of the chambers is an important parameter. Thus, large volume changes as reported above would greatly affect the calculations made in Section 5.2. However, because chamber E-1 had such a small volume the amount of $SO_2$ available for absorption in each of the pressure experiments was very small and the volume of the ionic liquid in chamber E-2 was not altered dramatically. This lead to the following conclusions:

- The absorption results shown in Figure 5.1 and Figure 5.2 show only a small fraction of what the ionic liquid can absorb, because only a small amount of $SO_2$ was available in the setup.
- The volume change of ionic liquids as a result of absorption is an important aspect of ionic liquids that needs to be investigated further in order to design future equipment and process units to be able to handle the volume increase.

During these experiments some interesting observations were made:

- When the ionic liquid was almost completely saturated with $SO_2$ even a slight disturbance to the liquid would result in some of the $SO_2$ to desorb. For example, when the chamber was opened and the pressure allowed to equalise to atmospheric pressure some of the $SO_2$ desorbed from the ionic liquid. This also happened when the ionic liquid was stirred. At the end of the experiment an attempt was made to remove the ionic liquid from the pressure chamber using a syringe. However, when an attempt was made to transfer the liquid from the chamber to the syringe, only $SO_2$ was transferred. This happened because the change in pressure inside the syringe caused the $SO_2$ to desorb out of the liquid. (A video is available on the included CD as Appendix F).

- When the ionic liquid was placed in a heated oil bath to desorb the $SO_2$, the liquid started to bubble. This bubbling continued for about ten to twelve minutes before slowing and then stopping completely.

## 5.4 Summary

In short the following conclusions can be made from the above results:

1. At the higher $SO_2$ partial pressure more $SO_2$ is absorbed into the ionic liquid.
2. Temperature desorption works very fast and effectively. This was observed during the experiments, when the absorbed $SO_2$ desorbed very fast out of the ionic liquid for each experiment.
3. The ionic liquid was largely saturated with $SO_2$ when the volume changes were determined.
4. The ionic liquid can be desorbed by using pressure swing desorption.
5. When the ionic liquid is saturated with $SO_2$ it is very difficult to handle.
6. Both the 95 and 98% pure ionic liquids absorbed similar amounts of $SO_2$.

# Chapter 6

# Conclusions and recommendations

## 6.1 Introduction

Chapter 6 will consist of the main conclusions made from the results of Chapter 4 and Chapter 5, as well as some recommendations. The first section will revisit the objectives and hypotheses indicated at the beginning of the study and address each of them, after which Section 6.3 will present recommendations for future research and the implementation of the ionic liquids in the HyS process.

## 6.2 Conclusions

### 6.2.1 Temperature

The absorption of $SO_2$, as well as the rate of absorption changed dramatically when the ionic liquid temperature was changed. For all of the feed stream compositions the $SO_2$ absorption increased when the temperature was decreased. For the 100 mol% $SO_2$ feed stream the 98% pure ionic liquid absorbed 1.51 mol $SO_2$/mol IL at 60$^o$C and 2.68 mol $SO_2$/mol IL at 30$^o$C while the 95% pure ionic liquid absorbed 1.57 mol $SO_2$/mol IL at 60$^o$C and 2.48 $SO_2$/mol IL at 30$^o$C. Conversely, the temperatures of the absorption chamber did not have an influence on the initial absorption rate of $SO_2$. This result disproves the hypotheses in Section 2.5, which states that the absorption rate will increase with an increase in temperature.

### 6.2.2 Feed stream composition

The percentage $SO_2$ in the feed stream was changed to see how the ratio of $SO_2$ in the feed stream influenced the absorption rate. From the results it is seen that the absorption rate increased when the composition of $SO_2$ was increased. The absorption rate increased from 0.15 mol $SO_2$/mol IL·min for the 98% pure ionic liquid at 60$^o$C with 25 mol% $SO_2$ to 0.75 mol

$SO_2$/mol IL·min at 60°C with 100 mol% $SO_2$. Similarly the 95% pure ionic liquid increased from 0.17 mol $SO_2$/mol IL·min at 60°C with 25 mol% $SO_2$ to 0.82 mol $SO_2$/mol IL·min at 60°C with 100 mol% $SO_2$. This happened due to an increase in the amount of $SO_2$ that is available for absorption. For the results in Section 4.2.2 the 95% pure ionic liquid consistently had a higher initial absorption rate than the 98% pure ionic liquid.

### 6.2.3 Absorption of $O_2$

$O_2$ absorption obtained during the pressure experiments was about fifteen times lower than that of $SO_2$, without the ionic liquid having been saturated with $SO_2$. During the temperature experiments the 95% pure ionic liquid absorbed very small amounts of $O_2$ at 30 and 40°C while the 98% pure ionic liquid absorbed almost no $O_2$. Therefore these results from both Chapter 4 and Chapter 5 indicate that this ionic liquid only absorbs very small amounts of $O_2$. These amounts were about thirty times smaller than the amounts of $SO_2$ that was absorbed. Thus, it can be concluded that the amount of $O_2$ absorbed by the ionic liquid is negligibly small, because the electrolyser will not be negatively influenced by $O_2$ at such low quantities.

### 6.2.4 Feed pressure

This objective was to determine what the effects of the feed pressure of both $SO_2$ and $O_2$ have on the absorption capabilities of the ionic liquid. From the $O_2$ data it can be seen that the mole percentage of $O_2$ absorbed into the ionic liquid remained constant at between 6 and 7% for all feed pressures. Therefore, it can be concluded that the mole percentage of $O_2$ absorbed and the feed gas pressure are independent of one another. The $SO_2$ data on the other hand show a clear correlation between the mole percentage of $SO_2$ absorbed and the feed pressure of the gas. For the 95% pure ionic liquid the mole percentage absorbed into the ionic liquid increased from 77.6 mol% at 1.5 bar(a) to 85.9 mol% at 3.0 bar(a). The 98% pure ionic liquid shows similar results, namely 79.7 mol% absorbed at 1.5 bar(a) increasing to 87.9 mol% at 3.0 bar(a). It can be concluded that the feed pressure has an influence on the amount of $SO_2$ absorbed, but not on the $O_2$; hence when the feed pressure of $SO_2$ is increased the amount of $SO_2$ absorbed also increases. This trend was explained in Section 5.2 by means of Fick's law.

### 6.2.5 Desorption

After the absorption step the ionic liquid was heated to 125$^{o}$C to desorb the $SO_2$. Desorption was rapid and effective, with initial desorption rates calculated in Section 4.2.3. The desorption data showed that there was no clear correlation between the desorption rate and the feed composition, However it was found that the desorption rates of 50$^{o}$C and 60$^{o}$C were lower than the rates at 30$^{o}$C and 40$^{o}$C. This can be explained by the fact that the desorption times for all of the experiments were around 400 to 800 seconds, hence if more $SO_2$ was absorbed the desorption rate would be higher as was the case for the lower temperatures. Therefore the hypothesis that $SO_2$ is desorbed from the ionic liquid at temperatures higher than 120$^{o}$C was correct; this also explains the fact that as the temperature of the ionic liquid increases less $SO_2$ is absorbed.

### 6.2.6 Ionic liquid purity

The main objective of this study was to determine whether the purity of the ionic liquid had a significant influence on the $SO_2$ absorption capacity of the ionic liquid. The experimental data for the pressure experiments showed that the 95% and 98% pure ionic liquids absorbed similar amounts of $SO_2$. For the temperature experiments the 95% pure ionic liquid absorbed more $SO_2$ over the entire experimental range, bar two tests. The 95% pure ionic liquid however also absorbed a small amount of $O_2$ at 30$^{o}$C and 40$^{o}$C which means that the selectivity of the 95% pure ionic liquid was lower than the 98% pure ionic liquid.

These results disprove the hypothesis stated in Section 2.5, namely that a more pure ionic liquid would absorb greater amounts of $SO_2$. However it showed that the more pure ionic liquid has a better selectivity towards $SO_2$. Hence, it can be concluded that even with the $O_2$ that was absorbed it would be economically more advantageous to use the less expensive 95% pure ionic liquid rather than the expensive 98% pure liquid, because the $O_2$ would not influence the performance of the process negatively in such low quantities. Gorensek *et al.* (2009:44) also had very small amounts of $O_2$ in the feed stream to the electrolyser, indicating that a 100% pure $SO_2$ stream is not required. This finding contributes towards the commercialisation of the HyS process. Because of the expensive nature of ionic liquids, an economically more viable option was shown to be similar in efficiency. 95% pure ionic liquid has a cost of R1056.00/100g (Sigma-Aldrich, 2011) whereas 98% pure ionic liquid was quoted to be R2142.00/100g (Merck, 2011). Just by using the 95% pure ionic liquid instead of the 98% pure ionic liquid the cost of the ionic liquid can almost be halved.

### 6.2.7 Data modelling

The Langmuir absorption model was fitted to the $SO_2$ absorption data for the temperature experiments. The model followed the trend of the data well with an average standard deviation of 17.07% over all the experiments.

The Clausius-Clapeyron equation was used to determine if the desorption reaction was endothermic or exothermic by calculating the heat of desorption. The heat of desorption data in Table 4.7 indicate that the desorption of $SO_2$ from this ionic liquid is an endothermic reaction because the heat of desorption values are positive. This data also showed a trend that the heat of desorption decreased as the amount of $SO_2$ absorbed increased. Therefore if the desorption reaction was endothermic the absorption reaction was exothermic.

## 6.3 Recommendations

### 6.3.1 Future research

The following recommendations are proposed for future studies on the subject of $SO_2$ and $O_2$ separation with ionic liquids:

- Improve the pressure measurements in the pressure experiments by using pressure gauges that can log the pressure readings as a function of time. This would allow the pressure change to be presented dynamically.
- Study the effect of feed pressures greater than 3 bar(a) on the ability of the ionic liquid to absorb $SO_2$. This will help to determine what the trend of $SO_2$ absorption into the ionic liquid is at higher pressures.
- Investigate how well the ionic liquid absorbs $SO_2$ when the composition of $SO_2$ in the feed stream is very low. It is important to know if the ionic liquid can absorb the $SO_2$ from a stream containing only 1-10 mol% $SO_2$.
- Investigate the possibility to alter the current experimental setup to reduce the amount of scatter of the data during the desorption step. This has to reduce the effect of the air flow from the heater on the balance. A possibility is to increase the distance between the balance and the heater, or to use a different type of balance.
- Test other ionic liquids, as well to confirm that the [BMIm][$MeSO_4$] ionic liquid is the most suitable for the separation of $SO_2$ and $O_2$. It will be important to look at some task-specific ionic liquids that were designed specifically to absorb $SO_2$ (Jin *et al.*, 2011:6585).

- Investigate how ionic liquid purities lower than 95% will influence the absorption capabilities of the ionic liquid. Establish whether there is a minimum purity when the ability of the ionic liquid to absorb $SO_2$ starts to decline.
- Investigate how the lower selectivity of the 95% pure ionic liquid will affect the performance of the electrolyser in the HyS process if some $O_2$ enters the electrolyser, and investigate the cost of using multiple absorbers in series with the 95% pure ionic liquid versus just one absorber with the 98% pure ionic liquid.
- Investigate how the ionic liquid performs over extended periods of time in order to determine how long it can be used in the HyS process before it needs to be replaced.
- This study showed that ionic liquids have great potential to be used in the HyS process to separate $SO_2$ and $O_2$ and it showed how conditions such as temperature and pressure influence the performance of the ionic liquids. However, further research is needed to determine the parameters of the absorption and stripping columns that can be used in the HyS process. Some of these parameters include the liquid and gas flow rates, size of the columns and types of columns to use.

### 6.3.2 Implementation in the HyS process

This section will give some recommendations on how to implement the ionic liquids into the HyS process:

- During this study the single factor that had the largest influence on the performance of the ionic liquid was the temperature at which the absorption took place. The results showed that at lower temperatures the ionic liquid absorbed more $SO_2$. Therefore, in the HyS process the section where the $SO_2$ is absorbed into the ionic liquid should be operated at temperatures of 25-35$^{o}$C to insure optimal absorption.
- Temperature swing absorption can be implemented in the HyS process to absorb and desorb the $SO_2$ from the ionic liquid. Pressure swing absorption is also an option but requires compressors to increase the pressure of the gas and vacuum pumps to desorb the $SO_2$ from the ionic liquid. This equipment is expensive and a complete cost analysis has to be done to determine the best option for the HyS process.

# References

ADAM. 2011. Balances and scales. http://www.adamequipment.com/am Date of access: 5 Jul. 2011.

AIR LIQUIDE. 2009. Gas encyclopaedia. http://encyclopedia.airliquide.com/Encyclopedia.asp?GasID=27 Date of access: 30 Jun. 2011.

AKI, S.N.V.K., MELLEIN, B.R., SAURER, E.M. & BRENNECKE, J.F. 2004. High-pressure phase behavior of carbon dioxide with imidazolium-based ionic liquids. *The journal of physical chemistry B,* 108(52):20355-20365.

ANDERSON, J.L. 2008. Tunable ionic liquids for gas separation: Solubility studies for thermodynamic analysis. Dissertation-Ph.D. ed. Notre Dame: University of Notre Dame.

ANDERSON, T.W. & FINN, J.D. 1996. The new statistical analysis of data. New York: Springer. 712p.

ANDERSON, J.L., DIXON, J.K., MAGINN, E.J. & BRENNECKE, J.F. 2006. Measurement of SO2 solubility in ionic liquids. *Journal of physical chemistry B,* 110(31):15059-15062.

ANTHONY, J.L., MAGINN, E.J. & BRENNECKE, J.F. 2002. Solubilities and thermodynamic properties of gases in the ionic liquid 1-n-butyl-3-methylimidazolium hexafluorophosphate. *The journal of physical chemistry B,* 106(29):7315-7320.

BASF. 2011. Frequently asked questions. http://www.intermediates.basf.com/chemicals/ionic-liquids/faq#2 Date of access: 20 Jul. 2011.

BRECHER, L.E., SPEWOCK, S. & WARDE, C.J. 1977. The westinghouse sulfur cycle for the thermochemical decomposition of water. *International journal of hydrogen energy,* 2(1):7-15.

BROWN, L.C., BESENBRUCH, G.E., LENTSCH, R.D., SCHULTZ, K.R., FUNK, J.F., PICKARD, P.S., MARSHALL, A.C. and SHOWALTER, S.K., 2003. *High Efficiency Generation Of Hydrogen Fuels Using Nuclear Power.* GA–A24285 Rev. 1. U.S. Department of Energy.

CAMPER, D.E.I. 2006. Gas solubility and diffusion in room temperature ionic liquids with an emphasis on gas separations. Dissertation-Ph.D. ed. Boulder: University of Colorado.

DONG, W. & LONG, Y. 2004. Preparation and characterization of preferentially oriented continuous MFI-type zeolite membranes from porous glass. *Microporous and mesoporous materials,* 76(1-3):9-15.

FELDER, R.M. & ROUSSEAU, R.W. 2000. Elementary principles of chemical processes. 3rd ed. United States of America: John Wiley & Sons, Inc. 675p.

GARCÍA-ZUBIRI, I.X., GONZÁLEZ-GAITANO, G. & ISASI, J.R. 2009. Sorption models in cyclodextrin polymers: Langmuir, Freundlich, and a dual-mode approach. *Journal of colloid and interface science,* 337(1):11-18.

GARDAS, R.L., FREIRE, M.G., CARVALHO, P.J., MARRUCHO, I.M., FONSECA, I.M.A., FERREIRA, A.G.M. & COUTINHO, J.A.P. 2007. High-pressure densities and derived thermodynamic properties of imidazolium-based ionic liquids. *Journal of chemical & engineering data,* 52(1):80-88.

GORENSEK, M.B., SUMMERS, W.A., BOLTHRUNIS, C.O., LAHODA, E.J., ALLEN, D.T. and GREYVENSTEIN, R., 2009. *Hybrid sulfur process reference design and cost analysis.* Aiken: Savannah River National Laboratory.

HUANG, J., RIISAGER, A., WASSERSCHEID, P. & FEHRMANN, R. 2006a. Reversible physical absorption of SO2 by ionic liquids. *Chemical communications,* (38):4027-4029.

HUANG, J., RIISAGER, A., WASSERSCHEID, P. & FEHRMANN, R. 2006b. Reversible physical absorption of SO2 by ionic liquids. *Chemical communications,* (38):4027-4029.

HUDDLESTON, J.G., VISSER, A.E., MATTHEW REICHERT, W., WILLAUER, H.D., BROKER, G.A. & ROGERS, R.D. 2001. Characterization and comparison of hydrophilic and hydrophobic room temperature ionic liquids incorporating the imidazolium cation. *Green chemistry,* 3(1):156-164.

JIN, M., HOU, Y., WU, W., REN, S., TIAN, S., XIAO, L. & LEI, Z. 2011. Solubilities and thermodynamic properties of SO2 in ionic liquids. *The journal of physical chemistry B,* 115(20):6585-6591.

JOHNSTON, B., MAYO, M.C. & KHARE, A. 2005. Hydrogen: The energy source for the 21st century. *Technovation,* 25(6):569-585.

JONKER, A. 2009. Techno-economic evaluation of different technologies for the separation of sulphur dioxide and oxygen applicable to the hybrid sulphur (hys) process. Master of Engineering ed. Potchefstroom: NWU. 43-186.

KIM, C.S., LEE, K.Y., GONG, G.T., KIM, H., LEE, B.G. & JUNG, G.D. 2008. Sulfur dioxide separation and recovery with ionic liquid absorbents. http://www.nt.ntnu.no/users/skoge/prost/proceedings/aiche-008/data/papers/p124708.pdf. Date of access: July 14. 2010.

KIM, C.S., LEE, K.Y., SONG, K.H., GONG, G.T., YOO, K.S., KIM, H., LEE, B.G., AHN, B.S. & JUNG, K.D. 2007. Novel separation process of gaseous mixture of SO2 and O2 with ionic liquid for hydrogen production in thermochemical sulfur-iodine water splitting cycle. (In Anon. 2007.

KIM, D.J. 2004. Adsorption isotherms of 2,2,4-trimethylpentane and toluene vapors on hydrocarbon adsorber and light-off catalyst. *Journal of colloid and interface science,* 269(2):290-295.

KORETSKY, M.D. 2004. Engineering and chemical thermodynamics. United States of America: Wiley & Sons, Inc. 553p.

KUMEŁAN, J., KAMPS, Á.P., URUKOVA, I., TUMA, D. & MAURER, G. 2005. Solubility of oxygen in the ionic liquid [bmim][PF6]: Experimental and molecular simulation results. *The journal of chemical thermodynamics,* 37(6):595-602.

KUMEŁAN, J., PÉREZ-SALADO KAMPS, Á., TUMA, D. & MAURER, G. 2007. Solubility of the single gases H2 and CO in the ionic liquid [bmim][CH3SO4]. *Fluid phase equilibria,* 260(1):3-8.

LATTIN, W.C. & UTGIKAR, V.P. 2007. Transition to hydrogen economy in the united states: A 2006 status report. *International journal of hydrogen energy,* 32(15):3230-3237.

LE ROUX, M. and HATTINGH, B.B., 2010. *HyS Hydrogen Production Process Development Special Studies: Section 4: Separation.* Potchefstroom: .

LEE, K.Y., GONG, G.T., SONG, K.H., KIM, H., JUNG, K. & KIM, C.S. 2008. Use of ionic liquids as absorbents to separate SO2 in SO2/O2 in thermochemical processes to produce hydrogen. *International journal of hydrogen energy,* 33(21):6031-6036.

LEYBROS, J., SATURNIN, A., MANSILLA, C., GILARDI, T. & CARLES, P. 2010. Plant sizing and evaluation of hydrogen production costs from advanced processes coupled to a nuclear heat source: Part II: Hybrid-sulphur cycle. *International journal of hydrogen energy,* 35(3):1019-1028.

LOCATI, C., LAFONT, U., PETERS, C.J. & KELDER, E.M. 2009. Interaction between carbon dioxide and ionic liquids: Novel electrolyte candidates for safer li-ion batteries. *Journal of power sources,* 189(1):454-457.

MANAN, N.A., HARDACRE, C., JACQUEMIN, J., ROONEY, D.W. & YOUNGS, T.G.A. 2009. Evaluation of gas solubility prediction in ionic liquids using COSMOthermX. *Journal of chemical & engineering data,* 54(7):2005-2022.

MERCK. 2011. 1-butyl-3-methylimidazolium methylsulfate. http://www.merck-chemicals.com/africa/1-butyl-3-methylimidazolium-methylsulfate/MDA_CHEM-490063/p_uuid?WT_oss=490063&WT_oss_r=1 Date of access: 19 Feb. 2011.

MILLER, C.C. 1924. The stokes-einstein law for diffusion in solution. *Proceedings of the royal society of london.series A, containing papers of a mathematical and physical character,* 106(740):pp. 724-749.

MULDER, M. 1998. Basic principles of membrane technology. 2nd ed. ed. Dordrecht: Kluwer Academic Publishers. 568p.

OCHOA, J., CASSANELLO, M.C., BONELLI, P.R. & CUKIERMAN, A.L. 2001. CO2 gasification of argentinean coal chars: A kinetic characterization. *Fuel processing technology,* 74(3):161-176.

ORME, C.J., KLAEHN, J.R. & STEWART, F.F. 2009. Membrane separation processes for the benefit of the sulfur–iodine and hybrid sulfur thermochemical cycles. *International journal of hydrogen energy,* 34(9):4088-4096.

PEREIRO, A.B., VERDÃA, P., TOJO, E. & RODRÃGUEZ, A. 2007. Physical properties of 1-butyl-3-methylimidazolium methyl sulfate as a function of temperature. *Journal of chemical & engineering data,* 52(2):377-380.

PERRY, R.H. & GREEN, D.W. 1997. Perry's chemical engineers' handbook. 7th ed. ed. New York: McGraw-Hill. 30-36p.

PLECHKOVA, N.V. & SEDDON, K.R. 2008. Applications of ionic liquids in the chemical industry. *The royal society of chemistry,* 37(1):123-150.

REN, W. 2009. High-pressure phase equilibria of ionic liquids and compressed gases for applications in reactions and absorption refrigeration. Doctor of Philosophy ed. University of Kansas.

REN, S., HOU, Y., WN, W., LIU, Q., XIAO, Y. & CHEN, X. 2010. Properties of ionic liquids absorbing so2 and the mechanism of the absorption. *Journal of physical chemistry B,* 114(6):2175-2179.

SEADER, J.D. & HENLEY, E.J. 2006. Separation process principles. 2nd ed. John wiley & Sons inc. 756p.

SEO, Y., KIM, S. & HONG, S.U. 2006. Highly selective polymeric membranes for gas separation. *Polymer,* 47(13):4501-4504.

SHAFIEE, S. & TOPAL, E. 2009. When will fossil fuel reserves be diminished? *Energy policy,* 37(1):181-189.

SHIFLETT, M.B. & YOKOZEKI, A. 2010. Chemical absorption of sulfur dioxide in room-temperature ionic liquids. *Industrial and engineering chemistry research,* 49(3):1370-1377.

SIGMA-ALDRICH. 2011. 1-butyl-3-methylimidazolium methyl sulfate. http://www.sigmaaldrich.com/catalog Date of access: 23 Jun. 2011.

SORIANO, A.N., DOMA JR., B.T. & LI, M. 2008. Solubility of carbon dioxide in 1-ethyl-3-methylimidazolium 2-(2-methoxyethoxy) ethylsulfate. *The journal of chemical thermodynamics,* 40(12):1654-1660.

SUMMERS, W.A., GORENSEK, M.B. and BUCKNER, M.R., 2005. *The hybrid sulfur cycle for nuclear hydrogen production.* Aiken: Savannah River National Laboratory.

TONDEUR, D. & TENG, F. 2008. Chapter 18 - carbon capture and storage for greenhouse effect mitigation. (In Trevor M. Letcher, ed. Future energy. Oxford: Elsevier. p. 303-331.).

VOROTYNTSEV, M.A., ZINOVYEVA, V.A. & PICQUET, M. 2010. Diffusional transport in ionic liquids: Stokes–Einstein relation or "sliding sphere" model? ferrocene (fc) in imidazolium liquids. *Electrochimica acta,* 55(18):5063-5070.

WONG, D.S.H., CHEN, J.P., CHANG, J.M. & CHOU, C.H. 2002. Phase equilibria of water and ionic liquids [emim][PF6] and [bmim][PF6]. *Fluid phase equilibria,* 194-1971089-1095.

# Appendix A

# Calibration data

**Mass flow controller calibration**

As stated in Section 3.3.3 the mass flow controllers had to be calibrated before use. This was done by plotting the controller setting versus the flow rate for each of the gasses. Firstly the pressure regulators of the $SO_2$ and $O_2$ were set at 1.5 and 5 bar respectively. Then the controller value was set to a specific setting and the flow rate of the gas through the controller was measured with a bubble flow meter. The flow rate was calculated by measuring the time it took the gas to fill 10 $cm^3$ of the flow meter, this time was then converted to a flow rate in $cm^3/s$. Each reading was repeated three times and then an average value used. After this the controller setting was changed and the readings taken again. Table A.1 and Table A.2 show the data that was used to calculate the calibration curves.

**Table A.1: Calibration data for $O_2$**

| Controller setting (%) | Time 1 | Time 2 | Time 3 | Time (avg.) | Flow rate ($cm^3/s$) |
|---|---|---|---|---|---|
| **0** | - | - | - | - | 0 |
| **3** | 15.24 | 15.68 | 15.75 | 15.56 | 0.64 |
| **5** | 9.31 | 9.18 | 9.3 | 9.26 | 1.08 |
| **10.1** | 4.62 | 4.62 | 4.62 | 4.62 | 2.16 |
| **15.2** | 3.06 | 3.05 | 3.05 | 3.05 | 3.28 |
| **20.1** | 2.31 | 2.37 | 2.31 | 2.33 | 4.29 |

**Table A.2: Calibration data for $SO_2$**

| Controller setting (%) | Time 1 | Time 2 | Time 3 | Time (avg.) | Flow rate ($cm^3/s$) |
|---|---|---|---|---|---|
| **0** | - | - | - | - | 0 |
| **3** | 18.74 | 18.74 | 18.7 | 18.73 | 0.53 |
| **5** | 11.93 | 11.87 | 11.83 | 11.88 | 0.84 |
| **10** | 6.25 | 6.25 | 6.25 | 6.25 | 1.6 |
| **15** | 4.19 | 4.25 | 4.25 | 4.23 | 2.36 |
| **20.1** | 3.27 | 3.24 | 3.31 | 3.27 | 3.05 |

**Gas chromatograph calibration**

Table A.3 shows the raw data obtained during the calibration of the GC it shows the composition of the feed stream followed by the area of the $SO_2$ and $O_2$ peaks and their ratios that was repeated once and finally it shows the average ratio of the areas and the feed ratio.

**Table A.3: Calibration data for GC**

| Feed ratio ($SO_2/O_2$) | Area 1 $SO_2$ | Area 1 $O_2$ | Ratio | Area 2 $SO_2$ | Area 2 $O_2$ | Ratio | Average ratio |
|---|---|---|---|---|---|---|---|
| **9** | 72803.8 | 4672.9 | 15.58 | 72607.9 | 4352.19 | 16.68 | 16.13 |
| **4** | 64361.5 | 8732.2 | 7.37 | 64189.4 | 8639.22 | 7.43 | 7.40 |
| **2.3** | 56234.4 | 12732 | 4.41 | 56343.7 | 12606.9 | 4.47 | 4.44 |
| **1.5** | 48095.8 | 16731 | 2.87 | 47986.8 | 16700.1 | 2.87 | 2.87 |
| **1** | 40090 | 20453.5 | 1.96 | 40175.5 | 20504.3 | 1.96 | 1.96 |
| **0.67** | 32256 | 24029.1 | 1.34 | 32156.8 | 23987.8 | 1.34 | 1.34146 |
| **0.43** | 24172.5 | 27486.2 | 0.88 | 24185.6 | 27441.7 | 0.88 | 0.88 |
| **0.25** | 16488.3 | 30738.4 | 0.54 | 16432.2 | 30764 | 0.53 | 0.54 |
| **0.11** | 8561.934 | 34028.3 | 0.25 | 8563.8 | 34135.9 | 0.25 | 0.25 |

# Appendix B

# Additional data for temperature experiments

During the temperature experiments the flow of the stream exiting the absorption chamber was also measured at certain times during the experiment. These measurements were made for all of the temperature experiments but only the data for one is shown below. The flow data in Table B.1 was from the experiment with the 95% pure ionic liquid at 30$^{o}$C and 100% $SO_2$.

**Table B.1: Flow data**

| Time (s) | Flow (s) | Flow ($cm^3$/s) |
|---|---|---|
| 15 | 0 | 0.000 |
| 45 | 13.4 | 0.746 |
| 180 | 2.76 | 3.623 |
| 360 | 2.26 | 4.425 |
| 600 | 2.18 | 4.587 |
| 900 | 2.08 | 4.808 |
| 1200 | 2.07 | 4.831 |

Figure B.1 shows the plot of the flow versus time for the same experiment.

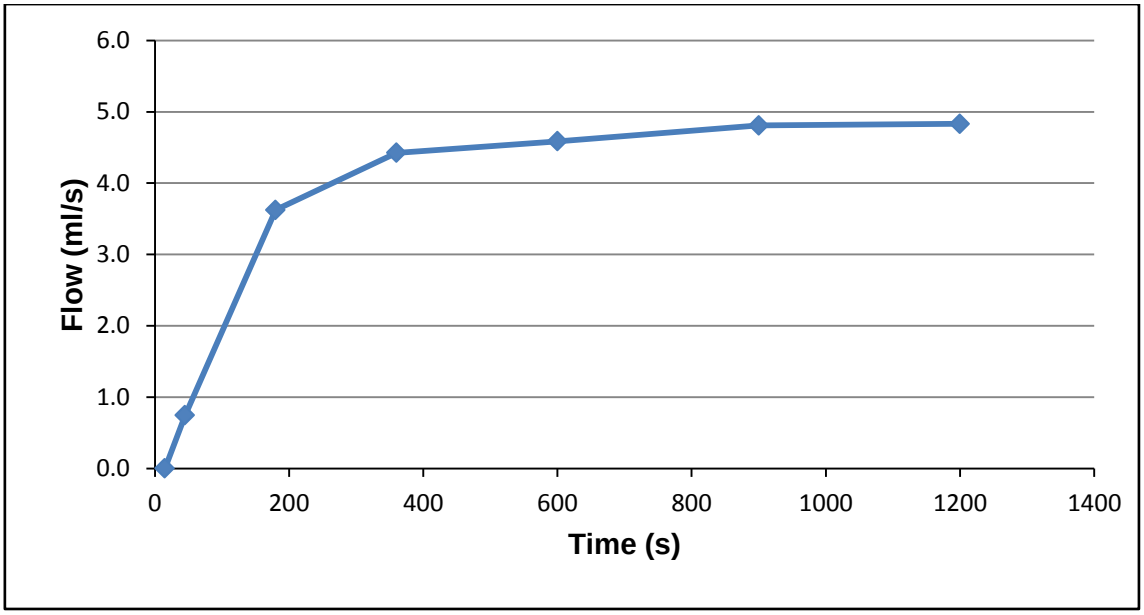


**Figure B.1: Plot of the flow data**

Table B.2 shows the data obtained from the GC when the stream exiting the absorption chamber was analysed. This table shows the experiment number, the area of the $SO_2$ and $O_2$ peaks together with their ratio, the ratio of the gas composition calculated with Equation 3.4 and the percentage compositions of $SO_2$ and $O_2$.

**Table B.2: GC data**

| Exp | Area $SO_2$ | Area $O_2$ | Area ratio | Gas composition ratio | mol%$SO_2$ | mol%$O_2$ |
|---|---|---|---|---|---|---|
| **1** | 1.00E-02 | 3.91E+04 | 2.55E-07 | 1.41E-07 | 0.00% | 100.00% |
| **2** | 1.00E-02 | 3.96E+04 | 2.52E-07 | 1.39E-07 | 0.00% | 100.00% |
| **3** | 1.00E-02 | 3.86E+04 | 2.59E-07 | 1.43E-07 | 0.00% | 100.00% |
| **4** | 1.00E-02 | 3.81E+04 | 2.62E-07 | 1.45E-07 | 0.00% | 100.00% |
| **5** | 7.26E+03 | 3.58E+04 | 2.03E-01 | 1.12E-01 | 10.06% | 89.94% |
| **6** | 1.24E+04 | 3.40E+04 | 3.64E-01 | 2.01E-01 | 16.74% | 83.26% |
| **7** | 1.19E+04 | 3.33E+04 | 3.59E-01 | 1.98E-01 | 16.53% | 83.47% |
| **8** | 1.52E+04 | 3.17E+04 | 4.80E-01 | 2.65E-01 | 20.94% | 79.06% |
| **9** | 1.93E+04 | 3.02E+04 | 6.40E-01 | 3.53E-01 | 26.09% | 73.91% |
| **10** | 2.96E+04 | 2.48E+04 | 1.20E+00 | 6.60E-01 | 39.75% | 60.25% |
| **11** | 3.13E+04 | 2.43E+04 | 1.29E+00 | 7.11E-01 | 41.54% | 58.46% |
| **12** | 3.63E+04 | 2.28E+04 | 1.59E+00 | 8.77E-01 | 46.72% | 53.28% |
| **13** | 4.60E+04 | 1.76E+04 | 2.62E+00 | 1.45E+00 | 59.11% | 40.89% |
| **14** | 5.19E+04 | 1.35E+04 | 3.83E+00 | 2.12E+00 | 67.91% | 32.09% |
| **15** | 5.49E+04 | 1.38E+04 | 3.96E+00 | 2.19E+00 | 68.62% | 31.38% |
| **16** | 5.65E+04 | 1.18E+04 | 4.77E+00 | 2.63E+00 | 72.46% | 27.54% |
| **17** | 7.51E+04 | 4.59E+01 | 1.64E+03 | 9.04E+02 | 99.89% | 0.11% |

| Exp | Area $SO_2$ | Area $O_2$ | Area ratio | Gas composition ratio | mol%$SO_2$ | mol%$O_2$ |
|---|---|---|---|---|---|---|
| **18** | 7.86E+04 | 4.32E+01 | 1.82E+03 | 1.00E+03 | 99.90% | 0.10% |
| **19** | 7.85E+04 | 3.31E+01 | 2.37E+03 | 1.31E+03 | 99.92% | 0.08% |
| **20** | 7.82E+04 | 3.12E+01 | 2.51E+03 | 1.38E+03 | 99.93% | 0.07% |
| **21** | 1.00E-02 | 3.87E+04 | 2.58E-07 | 1.42E-07 | 0.00% | 100.00% |
| **22** | 1.00E-02 | 3.76E+04 | 2.66E-07 | 1.47E-07 | 0.00% | 100.00% |
| **23** | 1.00E-02 | 3.79E+04 | 2.64E-07 | 1.46E-07 | 0.00% | 100.00% |
| **24** | 1.00E-02 | 3.75E+04 | 2.66E-07 | 1.47E-07 | 0.00% | 100.00% |
| **25** | 7.52E+03 | 3.49E+04 | 2.16E-01 | 1.19E-01 | 10.64% | 89.36% |
| **26** | 1.02E+04 | 3.29E+04 | 3.10E-01 | 1.71E-01 | 14.60% | 85.40% |
| **27** | 1.26E+04 | 3.19E+04 | 3.95E-01 | 2.18E-01 | 17.89% | 82.11% |
| **28** | 1.57E+04 | 3.10E+04 | 5.05E-01 | 2.79E-01 | 21.80% | 78.20% |
| **29** | 2.43E+04 | 2.77E+04 | 8.75E-01 | 4.83E-01 | 32.56% | 67.44% |
| **30** | 2.86E+04 | 2.49E+04 | 1.15E+00 | 6.32E-01 | 38.73% | 61.27% |
| **31** | 3.25E+04 | 2.32E+04 | 1.40E+00 | 7.74E-01 | 43.62% | 56.38% |
| **32** | 3.55E+04 | 2.20E+04 | 1.62E+00 | 8.92E-01 | 47.14% | 52.86% |
| **33** | 4.64E+04 | 1.66E+04 | 2.79E+00 | 1.54E+00 | 60.62% | 39.38% |
| **34** | 5.14E+04 | 1.35E+04 | 3.81E+00 | 2.10E+00 | 67.79% | 32.21% |
| **35** | 5.46E+04 | 1.21E+04 | 4.50E+00 | 2.48E+00 | 71.27% | 28.73% |
| **36** | 5.84E+04 | 1.22E+04 | 4.80E+00 | 2.65E+00 | 72.59% | 27.41% |
| **37** | 7.58E+04 | 5.54E+01 | 1.37E+03 | 7.55E+02 | 99.87% | 0.13% |
| **38** | 7.56E+04 | 5.01E+01 | 1.51E+03 | 8.33E+02 | 99.88% | 0.12% |
| **39** | 7.64E+04 | 7.77E+01 | 9.83E+02 | 5.43E+02 | 99.82% | 0.18% |
| **40** | 7.65E+04 | 4.57E+01 | 1.68E+03 | 9.25E+02 | 99.89% | 0.11% |

Table B.3 shows the analysed data of the temperature experiments which includes the temperature and feed stream composition for each experiment. Then it shows the maximum absorption, mole $SO_2$ absorbed per mole ionic liquid as well as the initial absorption tempo and finally it gives the desorption time as well as the initial desorption tempo for each experiment.

**Table B.3: Analysed data for temperature experiments**

| | | Absorption | | | Desorption | |
|---|---|---|---|---|---|---|
| **Temp. (°C)** | **Comp. (mole%$SO_2$)** | **Max. (g)** | **mol $SO_2$/mol IL** | **Tempo (mol $SO_2$/mol IL·min)** | **Time (s)** | **Tempo (mol $SO_2$/mol IL·min)** |
| 30 | 0.0% | 0.075 | 0.080 | 0 | 0 | 0 |
| 40 | 0.0% | 0.043 | 0.047 | 0 | 0 | 0 |
| 50 | 0.0% | 0 | 0 | 0 | 0 | 0 |
| 60 | 0.0% | 0 | 0 | 0 | 0 | 0 |
| 30 | 25.0% | 0.943 | 1.015 | 0.242 | 480 | 0.325 |
| 40 | 25.0% | 0.691 | 0.744 | 0.189 | 700 | 0.301 |
| 50 | 25.0% | 0.575 | 0.619 | 0.210 | 860 | 0.059 |
| 60 | 25.0% | 0.350 | 0.376 | 0.171 | 440 | 0.103 |
| 30 | 50.0% | 1.617 | 1.741 | 0.409 | 620 | 0.518 |
| 40 | 50.0% | 1.118 | 1.203 | 0.440 | 600 | 0.201 |
| 50 | 50.0% | 0.965 | 1.039 | 0.399 | 580 | 0.129 |
| 60 | 50.0% | 0.773 | 0.832 | 0.334 | 540 | 0.123 |
| 30 | 75.0% | 2.323 | 2.501 | 0.743 | 620 | 0.540 |
| 40 | 75.0% | 1.810 | 1.949 | 0.644 | 460 | 0.351 |
| 50 | 75.0% | 1.211 | 1.304 | 0.683 | 600 | 0.178 |
| 60 | 75.0% | 0.816 | 0.878 | 0.673 | 640 | 0.255 |
| 30 | 100.0% | 2.305 | 2.481 | 0.872 | 560 | 0.374 |
| 40 | 100.0% | 2.112 | 2.273 | 0.846 | 700 | 0.600 |
| 50 | 100.0% | 1.879 | 2.023 | 0.871 | 800 | 0.155 |
| 60 | 100.0% | 1.458 | 1.569 | 0.819 | 880 | 0.201 |
| 30 | 0.0% | 0 | 0 | 0 | 0 | 0 |
| 40 | 0.0% | 0.019 | 0.021 | 0 | 0 | 0 |
| 50 | 0.0% | 0 | 0 | 0 | 0 | 0 |
| 60 | 0.0% | 0 | 0 | 0 | 0 | 0 |
| 30 | 25.0% | 0.737 | 0.794 | 0.157 | 780 | 0.088 |
| 40 | 25.0% | 0.531 | 0.572 | 0.157 | 400 | 0.193 |
| 50 | 25.0% | 0.397 | 0.427 | 0.155 | 620 | 0.165 |
| 60 | 25.0% | 0.264 | 0.284 | 0.145 | 620 | 0.112 |
| 30 | 50.0% | 1.424 | 1.533 | 0.370 | 680 | 0.318 |
| 40 | 50.0% | 1.051 | 1.131 | 0.382 | 740 | 0.274 |
| 50 | 50.0% | 0.846 | 0.910 | 0.365 | 400 | 0.086 |
| 60 | 50.0% | 0.548 | 0.589 | 0.341 | 260 | 0.153 |
| 30 | 75.0% | 1.789 | 1.926 | 0.501 | 780 | 0.504 |
| 40 | 75.0% | 1.541 | 1.659 | 0.583 | 460 | 0.308 |
| 50 | 75.0% | 1.101 | 1.185 | 0.515 | 620 | 0.213 |
| 60 | 75.0% | 0.955 | 1.028 | 0.479 | 620 | 0.102 |
| 30 | 100.0% | 2.491 | 2.681 | 0.793 | 740 | 0.376 |
| 40 | 100.0% | 1.847 | 1.988 | 0.803 | 540 | 0.294 |
| 50 | 100.0% | 1.440 | 1.550 | 0.770 | 560 | 0.249 |
| 60 | 100.0% | 1.402 | 1.509 | 0.753 | 620 | 0.272 |

# Appendix C

# Additional data for pressure experiments

## C.1 Raw Experimental Data

**Table C.1: Volume and Constants Table**

| | | |
|---|---|---|
| **Without Ionic liquid** | | |
| **Volume chamber 1** | 18.9 | $cm^3$ |
| **Volume chamber 2** | 21.8 | $cm^3$ |
| **Total Volume** | 40.7 | $cm^3$ |
| **With Ionic liquid** | | |
| **Volume chamber 1** | 18.9 | $cm^3$ |
| **Volume chamber 2** | 16.8 | $cm^3$ |
| **Total Volume** | 35.7 | $cm^3$ |
| **Constant Table** | | |
| **Gas Constant (R)** | 8.314 | J/molK |
| **Temperature (K)** | 298 | K |
| **IL MW** | 250.32 | g/mol |
| **95% IL Density** | 1.213 | $g/cm^3$ |

**Table C.2: Pressure readings for 95% IL ($SO_2$)**

| Run no. | Vacuum (bar(g)) | | | | Run no. | E-1 Pressurized (bar(g)) | | | |
|---|---|---|---|---|---|---|---|---|---|
| | E-1 Low | E-1 high | E-2 Low | E-2 High | | E-1 Low | E-1 high | E-2 Low | E-2 High |
| **1.1** | -0.784 | -0.794 | -0.775 | -0.785 | **1.1** | 0.634 | 0.644 | -0.775 | -0.785 |
| **1.2** | -0.769 | -0.779 | -0.759 | -0.769 | **1.2** | 0.5 | 0.51 | -0.759 | -0.769 |
| **1.3** | -0.762 | -0.772 | -0.751 | -0.761 | **1.3** | 0.507 | 0.517 | -0.751 | -0.761 |
| **2.1** | -0.77 | -0.78 | -0.763 | -0.773 | **2.1** | 1.107 | 1.117 | -0.763 | -0.773 |
| **2.2** | -0.774 | -0.784 | -0.763 | -0.773 | **2.2** | 1.009 | 1.019 | -0.763 | -0.773 |
| **2.3** | -0.762 | -0.772 | -0.754 | -0.764 | **2.3** | 1.009 | 1.019 | -0.754 | -0.764 |
| **3.1** | -0.786 | -0.796 | -0.776 | -0.786 | **3.1** | 1.516 | 1.526 | -0.776 | -0.786 |
| **3.2** | -0.763 | -0.773 | -0.759 | -0.769 | **3.2** | 1.515 | 1.525 | -0.759 | -0.769 |
| **3.3** | -0.761 | -0.771 | -0.756 | -0.766 | **3.3** | 1.545 | 1.555 | -0.756 | -0.766 |
| **4.1** | -0.769 | -0.779 | -0.757 | -0.767 | **4.1** | 2.04 | 2.05 | -0.757 | -0.767 |
| **4.2** | -0.761 | -0.771 | -0.75 | -0.76 | **4.2** | 2.073 | 2.083 | -0.75 | -0.76 |
| **4.3** | -0.762 | -0.772 | -0.754 | -0.764 | **4.3** | 2.028 | 2.038 | -0.754 | -0.764 |

| Run no. | After Equalization (bar(g)) | | | |
|---|---|---|---|---|
| | E-1 Low | E-1 high | E-2 Low | E-2 High |
| **1.1** | -0.615 | -0.625 | -0.606 | -0.616 |
| **1.2** | -0.623 | -0.633 | -0.61 | -0.62 |
| **1.3** | -0.61 | -0.62 | -0.595 | -0.605 |
| **2.1** | -0.606 | -0.596 | -0.596 | -0.586 |
| **2.2** | -0.59 | -0.58 | -0.577 | -0.567 |
| **2.3** | -0.593 | -0.583 | -0.58 | -0.57 |
| **3.1** | -0.634 | -0.624 | -0.622 | -0.612 |
| **3.2** | -0.644 | -0.634 | -0.631 | -0.621 |
| **3.3** | -0.6 | -0.59 | -0.598 | -0.588 |
| **4.1** | -0.578 | -0.568 | -0.562 | -0.552 |
| **4.2** | -0.555 | -0.545 | -0.542 | -0.532 |
| **4.3** | -0.563 | -0.553 | -0.554 | -0.544 |

**Table C.3: Pressure readings for 98% IL ($SO_2$)**

| Run no. | Vacuum (bar(g)) | | | | Run no. | E-1 Pressurized (bar(g)) | | | |
|---|---|---|---|---|---|---|---|---|---|
| | E-1 Low | E-1 high | E-2 Low | E-2 High | | E-1 Low | E-1 high | E-2 Low | E-2 High |
| **1.1** | -0.766 | -0.776 | -0.757 | -0.767 | **1.1** | 0.496 | 0.506 | -0.757 | -0.767 |
| **1.2** | -0.776 | -0.786 | -0.766 | -0.776 | **1.2** | 0.501 | 0.511 | -0.766 | -0.776 |
| **1.3** | -0.782 | -0.792 | -0.767 | -0.777 | **1.3** | 0.486 | 0.496 | -0.767 | -0.777 |
| **2.1** | -0.776 | -0.786 | -0.768 | -0.778 | **2.1** | 1.066 | 1.076 | -0.768 | -0.778 |
| **2.2** | -0.77 | -0.78 | -0.762 | -0.772 | **2.2** | 0.995 | 1.005 | -0.762 | -0.772 |
| **2.3** | -0.78 | -0.79 | -0.771 | -0.781 | **2.3** | 1.064 | 1.074 | -0.771 | -0.781 |
| **3.1** | -0.778 | -0.788 | -0.77 | -0.78 | **3.1** | 1.554 | 1.564 | -0.77 | -0.78 |
| **3.2** | -0.77 | -0.78 | -0.769 | -0.779 | **3.2** | 1.574 | 1.584 | -0.759 | -0.769 |
| **3.3** | -0.775 | -0.785 | -0.65 | -0.66 | **3.3** | 1.542 | 1.552 | -0.765 | -0.775 |
| **4.1** | -0.745 | -0.755 | -0.739 | -0.749 | **4.1** | 2.049 | 2.059 | -0.737 | -0.747 |
| **4.2** | -0.761 | -0.771 | -0.754 | -0.764 | **4.2** | 2.038 | 2.048 | -0.754 | -0.764 |
| **4.3** | -0.773 | -0.783 | -0.765 | -0.775 | **4.3** | 2.072 | 2.082 | -0.765 | -0.775 |

| Run no. | After Equalization (bar(g)) | | | |
|---|---|---|---|---|
| | E-1 Low | E-1 high | E-2 Low | E-2 High |
| **1.1** | -0.609 | -0.619 | -0.598 | -0.608 |
| **1.2** | -0.642 | -0.652 | -0.63 | -0.64 |
| **1.3** | -0.644 | -0.654 | -0.63 | -0.64 |
| **2.1** | -0.597 | -0.587 | -0.584 | -0.574 |
| **2.2** | -0.584 | -0.574 | -0.57 | -0.56 |
| **2.3** | -0.617 | -0.607 | -0.608 | -0.598 |
| **3.1** | -0.638 | -0.628 | -0.624 | -0.614 |
| **3.2** | -0.556 | -0.546 | -0.544 | -0.534 |
| **3.3** | -0.581 | -0.571 | -0.572 | -0.562 |
| **4.1** | -0.615 | -0.605 | -0.6 | -0.59 |
| **4.2** | -0.575 | -0.565 | -0.564 | -0.554 |
| **4.3** | -0.602 | -0.592 | -0.59 | -0.58 |

**Table C.4: Pressure readings for 95% IL ($O_2$)**

| Run no. | Vacuum (bar(g)) | | | | Run no. | E-1 Pressurized (bar(g)) | | | |
|---|---|---|---|---|---|---|---|---|---|
| | E-1 Low | E-1 high | E-2 Low | E-2 High | | E-1 Low | E-1 high | E-2 Low | E-2 High |
| **1.1** | -0.703 | -0.713 | -0.696 | -0.706 | **1.1** | 0.496 | 0.506 | -0.696 | -0.706 |
| **1.2** | -0.708 | -0.718 | -0.692 | -0.702 | **1.2** | 0.507 | 0.517 | -0.695 | -0.705 |
| **1.3** | -0.706 | -0.716 | -0.693 | -0.703 | **1.3** | 0.498 | 0.508 | -0.692 | -0.702 |
| **2.1** | -0.706 | -0.716 | -0.691 | -0.701 | **2.1** | 1.184 | 1.194 | -0.693 | -0.703 |
| **2.2** | -0.709 | -0.719 | -0.695 | -0.705 | **2.2** | 1.217 | 1.227 | -0.694 | -0.704 |
| **2.3** | -0.692 | -0.702 | -0.683 | -0.693 | **2.3** | 1.104 | 1.114 | -0.687 | -0.697 |
| **3.1** | -0.705 | -0.715 | -0.696 | -0.706 | **3.1** | 1.513 | 1.523 | -0.693 | -0.703 |
| **3.2** | -0.705 | -0.715 | -0.692 | -0.702 | **3.2** | 1.495 | 1.505 | -0.693 | -0.703 |
| **3.3** | -0.707 | -0.717 | -0.693 | -0.703 | **3.3** | 1.528 | 1.538 | -0.695 | -0.705 |
| **4.1** | -0.699 | -0.709 | -0.687 | -0.697 | **4.1** | 2.068 | 2.078 | -0.686 | -0.696 |
| **4.2** | -0.705 | -0.715 | -0.695 | -0.705 | **4.2** | 2.058 | 2.068 | -0.686 | -0.696 |
| **4.3** | -0.708 | -0.718 | -0.692 | -0.702 | **4.3** | 1.999 | 2.009 | -0.689 | -0.699 |
| **5.1** | -0.773 | -0.783 | -0.762 | -0.772 | **5.1** | 5.008 | 5.018 | -0.761 | -0.771 |
| **5.2** | -0.776 | -0.786 | -0.765 | -0.775 | **5.2** | 4.995 | 5.005 | -0.762 | -0.772 |
| **5.3** | -0.789 | -0.799 | -0.774 | -0.784 | **5.3** | 5 | 5.01 | -0.774 | -0.784 |
| **6.1** | -0.706 | -0.716 | -0.692 | -0.702 | **6.1** | 8.002 | 8.012 | -0.692 | -0.702 |
| **6.2** | -0.706 | -0.716 | -0.694 | -0.704 | **6.2** | 8.031 | 8.041 | -0.691 | -0.701 |
| **6.3** | -0.707 | -0.717 | -0.694 | -0.704 | **6.3** | 8.003 | 8.013 | -0.694 | -0.704 |

| Run no. | After Equalization (bar(g)) | | | |
|---|---|---|---|---|
| | E-1 Low | E-1 high | E-2 Low | E-2 High |
| **1.1** | -0.11 | -0.12 | -0.099 | -0.109 |
| **1.2** | -0.098 | -0.108 | -0.081 | -0.091 |
| **1.3** | -0.106 | -0.116 | -0.094 | -0.104 |
| **2.1** | 0.221 | 0.231 | 0.234 | 0.244 |
| **2.2** | 0.244 | 0.254 | 0.256 | 0.266 |
| **2.3** | 0.187 | 0.197 | 0.199 | 0.209 |
| **3.1** | 0.398 | 0.408 | 0.412 | 0.422 |
| **3.2** | 0.382 | 0.392 | 0.393 | 0.403 |
| **3.3** | 0.388 | 0.398 | 0.408 | 0.418 |
| **4.1** | 0.678 | 0.688 | 0.692 | 0.702 |
| **4.2** | 0.658 | 0.668 | 0.674 | 0.684 |
| **4.3** | 0.622 | 0.632 | 0.64 | 0.65 |
| **5.1** | 2.087 | 2.097 | 2.104 | 2.114 |
| **5.2** | 2.1 | 2.11 | 2.114 | 2.124 |
| **5.3** | 2.108 | 2.118 | 2.12 | 2.13 |
| **6.1** | 3.577 | 3.587 | 3.589 | 3.599 |
| **6.2** | 3.608 | 3.618 | 3.624 | 3.634 |
| **6.3** | 3.593 | 3.603 | 3.608 | 3.618 |

**Table C.5 Pressure readings for 98% IL ($O_2$)**

| Run no. | Vacuum (bar(g)) | | | | Run no. | E-1 Pressurized (bar(g)) | | | |
|---|---|---|---|---|---|---|---|---|---|
| | E-1 Low | E-1 high | E-2 Low | E-2 High | | E-1 Low | E-1 high | E-2 Low | E-2 High |
| **1.1** | -0.702 | -0.712 | -0.687 | -0.697 | **1.1** | 0.495 | 0.505 | -0.689 | -0.699 |
| **1.2** | -0.705 | -0.715 | -0.692 | -0.702 | **1.2** | 0.499 | 0.509 | -0.692 | -0.702 |
| **1.3** | -0.758 | -0.768 | -0.747 | -0.757 | **1.3** | 0.496 | 0.506 | -0.746 | -0.756 |
| **2.1** | -0.705 | -0.715 | -0.69 | -0.7 | **2.1** | 0.999 | 1.009 | -0.691 | -0.701 |
| **2.2** | -0.706 | -0.716 | -0.694 | -0.704 | **2.2** | 0.992 | 1.002 | -0.692 | -0.702 |
| **2.3** | -0.795 | -0.805 | -0.783 | -0.793 | **2.3** | 0.997 | 1.007 | -0.785 | -0.795 |
| **3.1** | -0.708 | -0.718 | -0.695 | -0.705 | **3.1** | 1.498 | 1.508 | -0.694 | -0.704 |
| **3.2** | -0.703 | -0.713 | -0.691 | -0.701 | **3.2** | 1.504 | 1.514 | -0.694 | -0.704 |
| **3.3** | -0.794 | -0.804 | -0.782 | -0.792 | **3.3** | 1.499 | 1.509 | -0.778 | -0.788 |
| **4.1** | -0.706 | -0.716 | -0.696 | -0.706 | **4.1** | 1.997 | 2.007 | -0.696 | -0.706 |
| **4.2** | -0.706 | -0.716 | -0.694 | -0.704 | **4.2** | 1.996 | 2.006 | -0.692 | -0.702 |
| **4.3** | -0.795 | -0.805 | -0.78 | -0.79 | **4.3** | 2.025 | 2.035 | -0.782 | -0.792 |
| **5.1** | -0.773 | -0.783 | -0.764 | -0.774 | **5.1** | 4.984 | 4.994 | -0.764 | -0.774 |
| **5.2** | -0.792 | -0.802 | -0.781 | -0.791 | **5.2** | 4.989 | 4.999 | -0.781 | -0.791 |
| **5.3** | -0.787 | -0.797 | -0.778 | -0.788 | **5.3** | 5.018 | 5.028 | -0.777 | -0.787 |
| **6.1** | -0.79 | -0.8 | -0.777 | -0.787 | **6.1** | 8.06 | 8.07 | -0.778 | -0.788 |
| **6.2** | -0.794 | -0.804 | -0.781 | -0.791 | **6.2** | 7.996 | 8.006 | -0.781 | -0.791 |
| **6.3** | -0.8 | -0.81 | -0.785 | -0.795 | **6.3** | 8 | 8.01 | -0.784 | -0.794 |

| Run no. | After Equalization (bar(g)) | | | |
|---|---|---|---|---|
| | E-1 Low | E-1 high | E-2 Low | E-2 High |
| **1.1** | -0.114 | -0.124 | -0.098 | -0.108 |
| **1.2** | -0.102 | -0.112 | -0.098 | -0.108 |
| **1.3** | -0.134 | -0.144 | -0.121 | -0.131 |
| **2.1** | 0.134 | 0.144 | 0.152 | 0.162 |
| **2.2** | 0.13 | 0.14 | 0.14 | 0.15 |
| **2.3** | 0.081 | 0.091 | 0.096 | 0.106 |
| **3.1** | 0.389 | 0.399 | 0.404 | 0.414 |
| **3.2** | 0.379 | 0.389 | 0.395 | 0.405 |
| **3.3** | 0.336 | 0.346 | 0.353 | 0.363 |
| **4.1** | 0.632 | 0.642 | 0.647 | 0.657 |
| **4.2** | 0.623 | 0.633 | 0.641 | 0.651 |
| **4.3** | 0.595 | 0.605 | 0.609 | 0.619 |
| **5.1** | 1.982 | 1.992 | 1.996 | 2.006 |
| **5.2** | 2.061 | 2.071 | 2.075 | 2.085 |
| **5.3** | 2.083 | 2.093 | 2.097 | 2.107 |
| **6.1** | 3.601 | 3.611 | 3.62 | 3.63 |
| **6.2** | 3.537 | 3.547 | 3.554 | 3.564 |
| **6.3** | 3.556 | 3.566 | 3.577 | 3.587 |

## C.2 Processed Data

The two tables below gives the mole amounts of gas absorbed per mole of ionic liquid for the $O_2$ and the $SO_2$. The pressure is the equilibrium pressure of the two chambers after the pressure has equalised.

**Table C.6 Experimental results for $O_2$ absorption into both ionic liquids with the variances for each experimental set**

| 95% IL | | | 98% IL | | |
|---|---|---|---|---|---|
| **mole absorbed/ mole IL** | **Pressure (bar(a))** | **mole absorbed/ mole IL variance** | **mole absorbed/ mole IL** | **Pressure (bar(a))** | **mole absorbed/ mole IL variance** |
| 2.6867E-03 | 8.9736E-01 | 7.3147E-08 | 2.9564E-03 | 8.9835E-01 | 3.3359E-08 |
| 2.1794E-03 | 9.1512E-01 | | 2.6197E-03 | 8.9835E-01 | |
| 2.5957E-03 | 9.0229E-01 | | 2.6653E-03 | 8.7565E-01 | |
| 4.0965E-03 | 1.2359E+00 | 3.3239E-08 | 3.3702E-03 | 1.1549E+00 | 7.4986E-08 |
| 3.7677E-03 | 1.2576E+00 | | 3.5841E-03 | 1.1431E+00 | |
| 3.7957E-03 | 1.2013E+00 | | 3.9138E-03 | 1.0997E+00 | |
| 3.9006E-03 | 1.4115E+00 | 1.7844E-07 | 3.9173E-03 | 1.4037E+00 | 1.9673E-07 |
| 4.3694E-03 | 1.3928E+00 | | 4.6748E-03 | 1.3948E+00 | |
| 4.7437E-03 | 1.4076E+00 | | 4.6958E-03 | 1.3533E+00 | |
| 4.9186E-03 | 1.6879E+00 | 2.6937E-07 | 5.1237E-03 | 1.6435E+00 | 1.3510E-07 |
| 5.7372E-03 | 1.6701E+00 | | 5.6568E-03 | 1.6376E+00 | |
| 5.8807E-03 | 1.6366E+00 | | 5.8286E-03 | 1.6060E+00 | |
| 1.1506E-02 | 3.0814E+00 | 7.6687E-07 | 1.7037E-02 | 2.9748E+00 | 8.9334E-06 |
| 1.0379E-02 | 3.0913E+00 | | 1.2008E-02 | 3.0528E+00 | |
| 9.7813E-03 | 3.0972E+00 | | 1.1724E-02 | 3.0745E+00 | |
| 1.9230E-02 | 4.5470E+00 | 3.5914E-07 | 1.7068E-02 | 4.5776E+00 | 8.1498E-07 |
| 1.8216E-02 | 4.5815E+00 | | 1.8836E-02 | 4.5125E+00 | |
| 1.8170E-02 | 4.5658E+00 | | 1.7633E-02 | 4.5352E+00 | |

**Table C.7 Experimental results for $SO_2$ absorption into both ionic liquids with the variances for each experimental set**

| 95% IL | | | 98% IL | | |
|---|---|---|---|---|---|
| **mole absorbed/ mole IL** | **Press (bar(a))** | **mole absorbed/ mole IL variance** | **mole absorbed/ mole IL** | **Press (bar(a))** | **mole absorbed/ mole IL variance** |
| 3.4910E-02 | 3.9699E-01 | 4.35644E-06 | 3.0656E-02 | 4.0489E-01 | 9.24188E-07 |
| 3.1502E-02 | 3.9304E-01 | | 3.2496E-02 | 3.7330E-01 | |
| 3.1117E-02 | 4.0785E-01 | | 3.2058E-02 | 3.7330E-01 | |
| 4.8980E-02 | 4.1673E-01 | 5.13153E-06 | 4.6930E-02 | 4.2857E-01 | 4.2911E-06 |
| 4.4859E-02 | 4.3548E-01 | | 4.4061E-02 | 4.4239E-01 | |
| 4.5289E-02 | 4.3252E-01 | | 4.8084E-02 | 4.0489E-01 | |
| 6.3102E-02 | 3.9107E-01 | 4.55679E-07 | 6.4649E-02 | 3.8909E-01 | 4.56662E-06 |
| 6.4113E-02 | 3.8219E-01 | | 6.0766E-02 | 4.6805E-01 | |
| 6.2833E-02 | 4.1475E-01 | | 6.1161E-02 | 4.4041E-01 | |
| 7.6690E-02 | 4.5028E-01 | 3.11351E-07 | 7.9761E-02 | 4.1278E-01 | 2.59662E-06 |
| 7.6641E-02 | 4.7002E-01 | | 7.6672E-02 | 4.4831E-01 | |
| 7.5700E-02 | 4.5818E-01 | | 7.9013E-02 | 4.2265E-01 | |

**Table C.8: % mole of $O_2$ absorbed by the ionic liquid**

| 95% IL | | 98% IL | |
|---|---|---|---|
| **Feed pressure (bar(a))** | **mole% of total $O_2$ absorbed** | **Feed pressure (bar(a))** | **mole% of total $O_2$ absorbed** |
| **1.51** | 6.78% | **1.51** | 6.83% |
| **2.20** | 6.68% | **2.01** | 6.65% |
| **2.53** | 6.28% | **2.51** | 6.46% |
| **3.07** | 6.57% | **3.01** | 6.53% |
| **5.00** | 5.70% | **5.00** | 6.48% |
| **9.02** | 6.62% | **9.01** | 6.34% |

**Table C.9: % mole of $SO_2$ absorbed by the ionic liquid**

| 95% IL | | 98% IL | |
|---|---|---|---|
| **Feed pressure (bar(a))** | **mole% of total $SO_2$ absorbed** | **Feed pressure (bar(a))** | **mole% of total $SO_2$ absorbed** |
| **1.52** | 77.64% | **1.51** | 79.67% |
| **2.02** | 80.77% | **2.08** | 80.49% |
| **2.53** | 86.69% | **2.57** | 83.48% |
| **3.05** | 85.87% | **3.06** | 87.90% |

# Appendix D

# Reproducibility data

In order to determine if the results of the temperature experiments are reproducible ten of the forty experiments were carried out three times and the 95% confidence interval for each of them were calculated. This was achieved with the following equation (Anderson & Finn, 1996:354):

$$\mathbf{95\%}\ \boldsymbol{CI} = \mathbf{1.96}\frac{\boldsymbol{SD}}{\sqrt{\boldsymbol{N}}} \qquad \text{Equation D.1}$$

Where:

95% CI – 95% confidence interval

SD – Standard deviation

N – Amount of data points

For each of the experiments the above parameters as well as the average value (x) were calculated for the three sets of data. The 95% confidence interval was then calculated for each of the experiments. The confidence interval was calculated between the time 500 seconds and 2000 seconds for each of the experiments. This was chosen because that is the time at which maximum absorption is normally reached.

After the confidence intervals for each of the experiments were calculated it was converted to a percentage of the average value for each of the experiments with the following equation:

$$\mathbf{95\%}\ \boldsymbol{CI\ in\ persent} = \frac{\mathbf{95\%}\ \boldsymbol{CI}}{\boldsymbol{average\ value}} \times \mathbf{100} \qquad \text{Equation D.2}$$

Two of the experiments that were repeated were carried out at 0 mol% $SO_2$ these two were excluded from the confidence interval calculations, because the average value for these two experiments was about zero. If the average value is very small then the percent 95% confidence interval will approach infinity.

The confidence interval for the remaining eight experiments were calculated with Equation D.1 and then converted to a percentage of the average with Equation D.2. The average of those eight values were then taken and calculated as 10.55%. This means that there is a 95% probability that the parameter for the experiment will fall within either +10.55% or -

10.55% of the average of the experiment when it is repeated (Anderson & Finn, 1996:354). Table D.1 shows the confidence interval for each of the eight experiments that was calculated as well as the average value.

**Table D.1: Confidence interval calculations**

| Exp. | 95% CI/average | 95%CI (%) |
|---|---|---|
| **6** | 0.1281 | 12.81% |
| **9** | 0.0803 | 8.03% |
| **15** | 0.0432 | 4.32% |
| **18** | 0.0505 | 5.05% |
| **26** | 0.2588 | 25.88% |
| **29** | 0.1118 | 11.18% |
| **35** | 0.1078 | 10.78% |
| **38** | 0.0634 | 6.34% |
| | **Average** | **10.55%** |

Figure D.1 to Figure D.10 shows the experimental data for the experiments that was used to calculate the repeatability. Each of the figures shows the mass of the ionic liquid versus time for the three experiments that were repeated for each of the conditions.

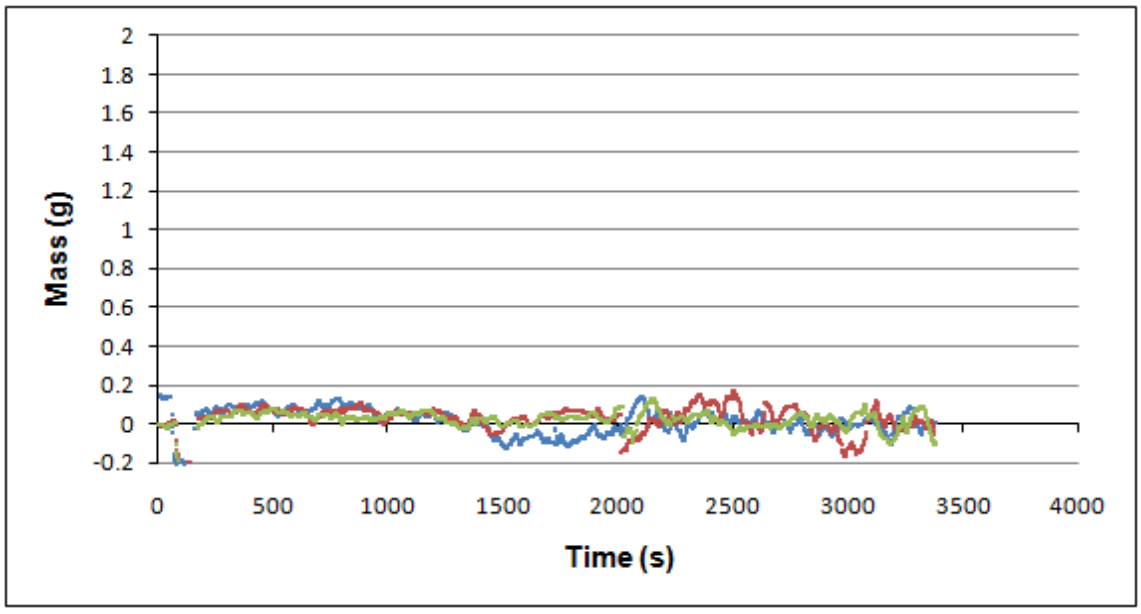


**Figure D.1: Reproducibility data for the 95% pure IL at 60°C with 0 mol% $SO_2$**

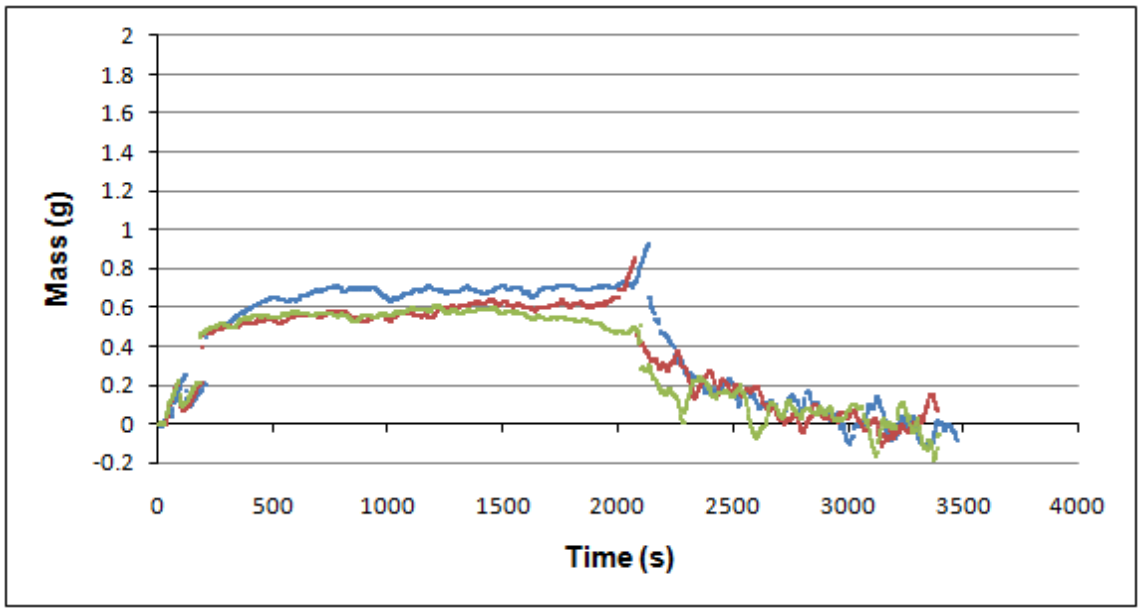


**Figure D.2: Reproducibility data for the 95% pure IL at 40°C with 25 mol% $SO_2$**

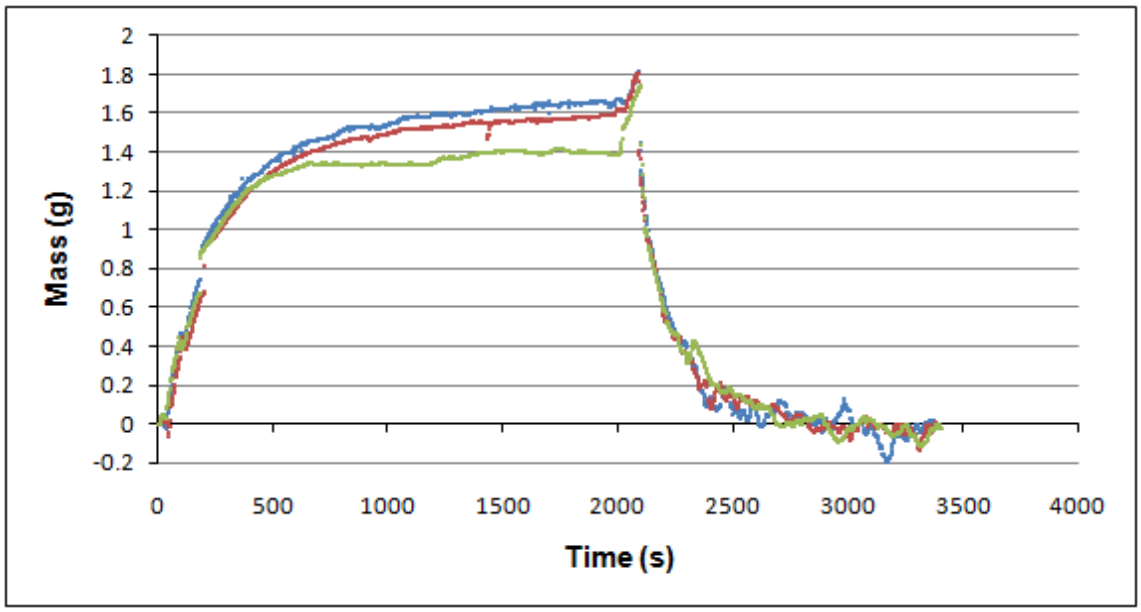


**Figure D.3: Reproducibility data for the 95% pure IL at 30°C with 50 mol% $SO_2$**

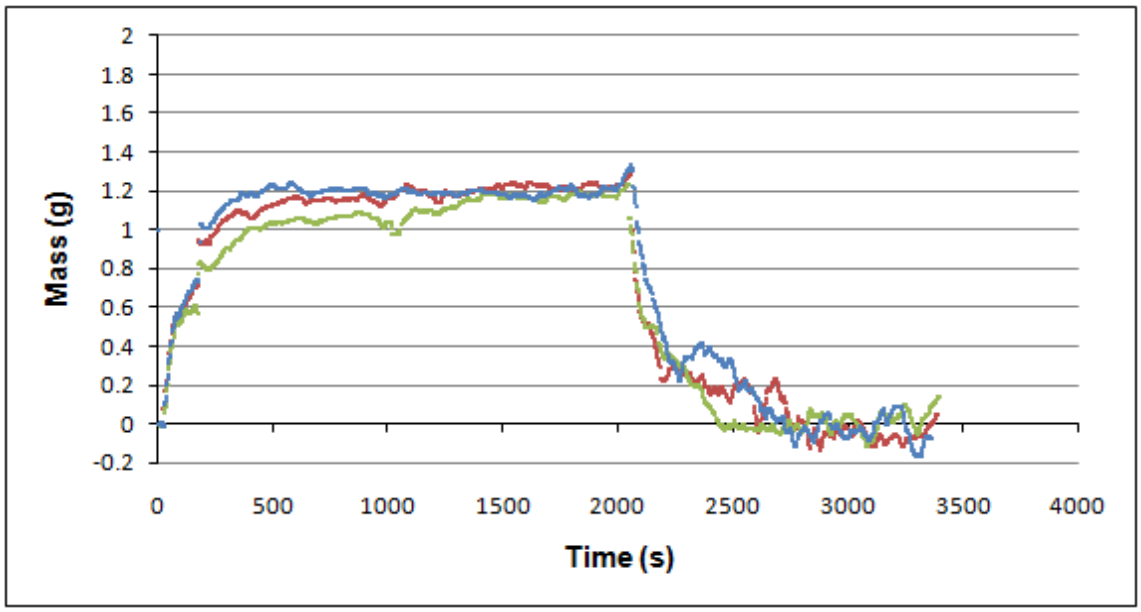


**Figure D.4: Reproducibility data for the 95% pure IL at 50°C with 75 mol% $SO_2$**

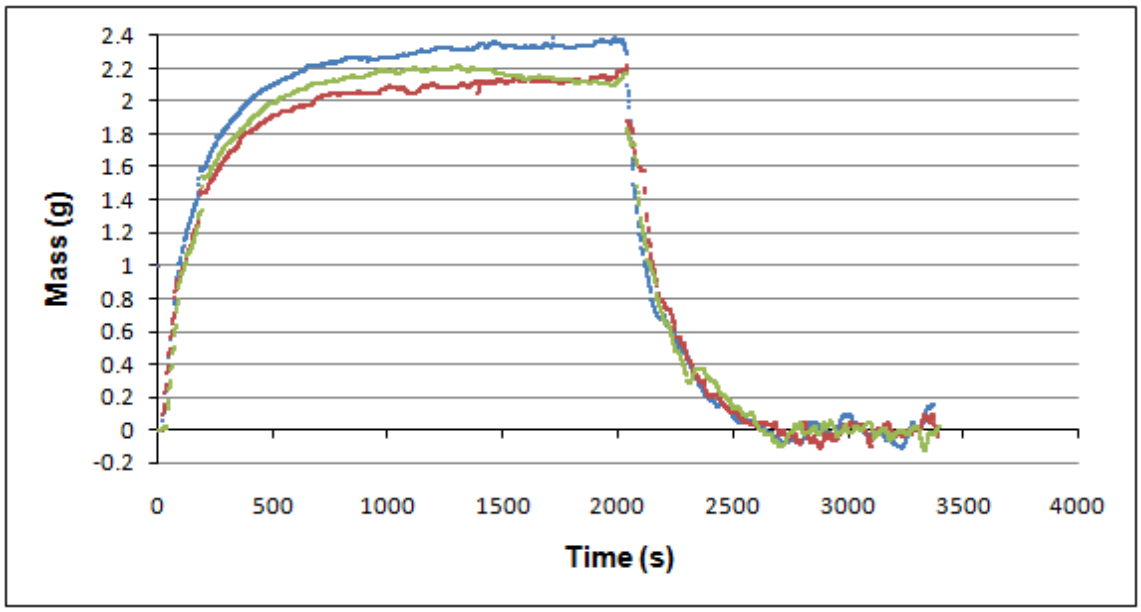


**Figure D.5: Reproducibility data for the 95% pure IL at 40°C with 100 mol% $SO_2$**

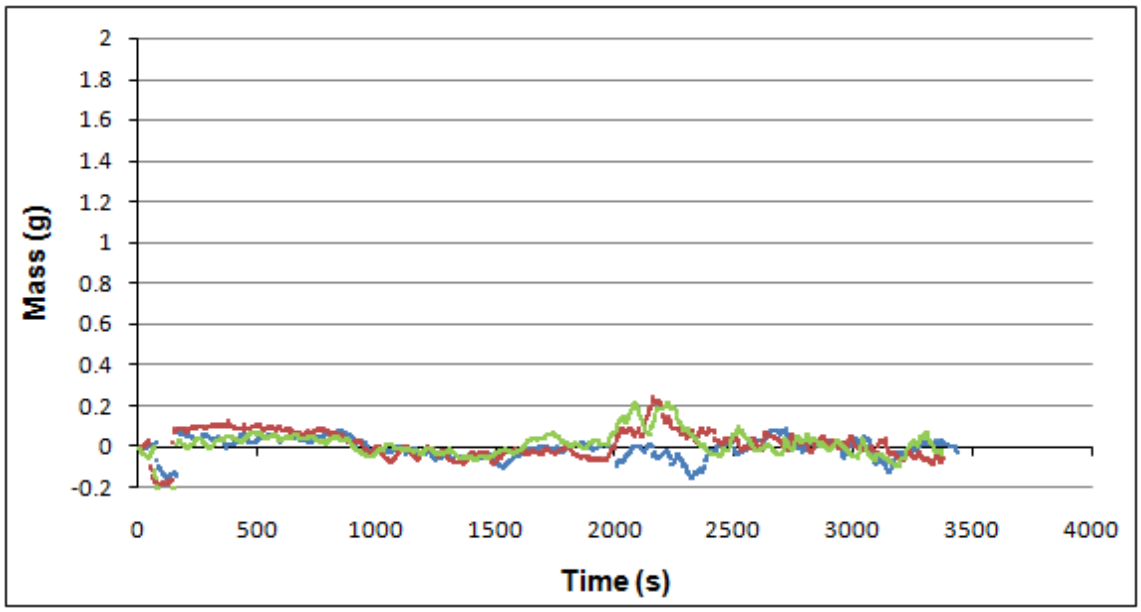


**Figure D.6: Reproducibility data for the 98% pure IL at 60°C with 0 mol% $SO_2$**

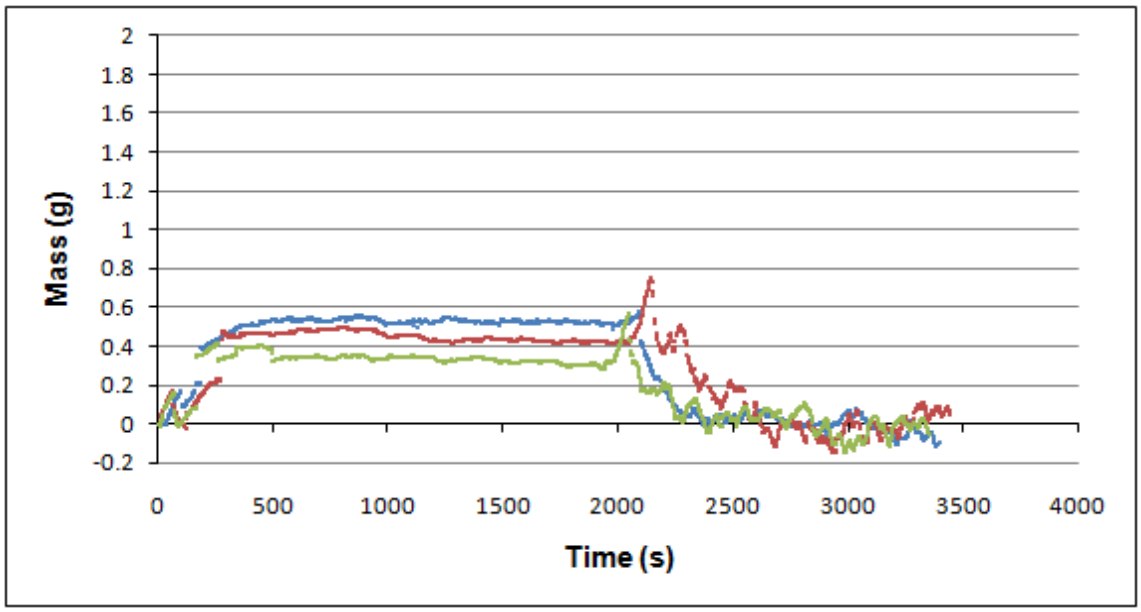


**Figure D.7: Reproducibility data for the 98% pure IL at 40°C with 25 mol% $SO_2$**

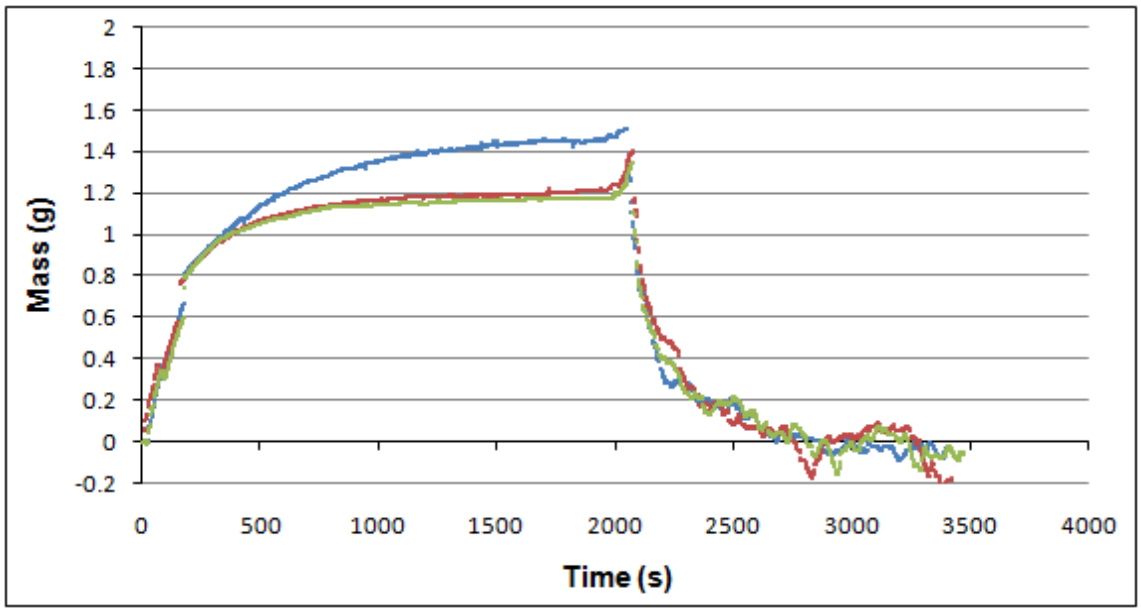


**Figure D.8: Reproducibility data for the 98% pure IL at 30°C with 50 mol% $SO_2$**

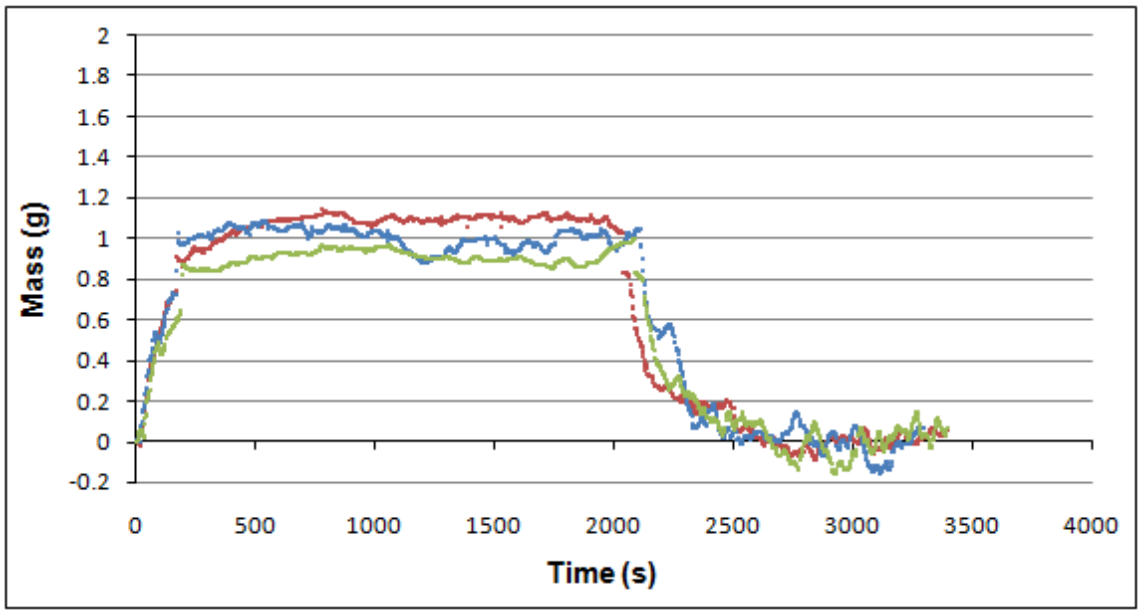


**Figure D.9: Reproducibility data for the 98% pure IL at 50°C with 75 mol% $SO_2$**

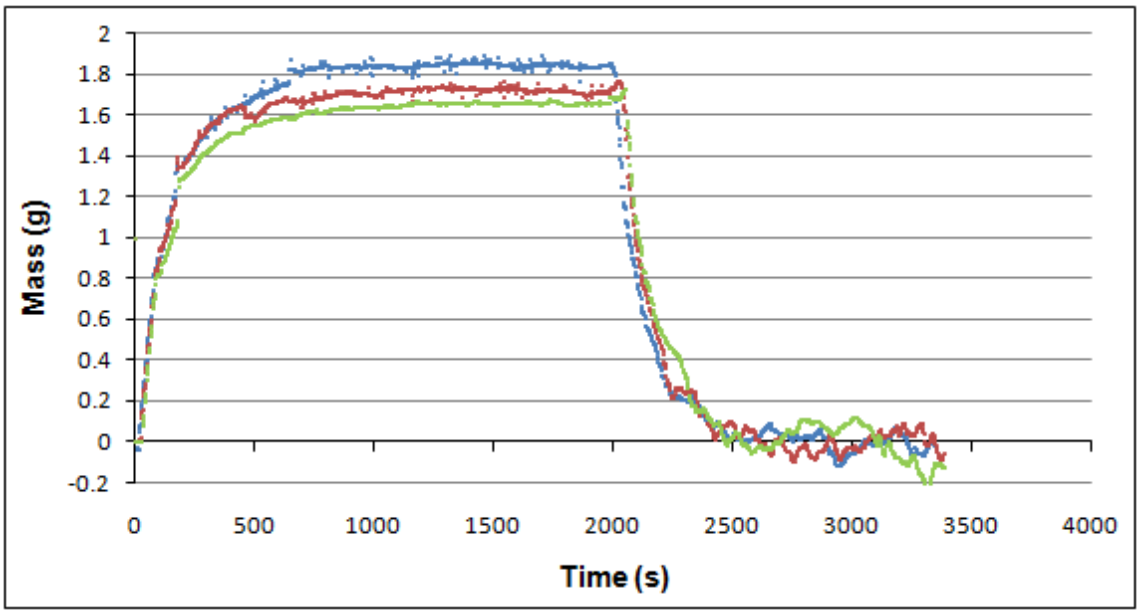


**Figure D.10: Reproducibility data for the 98% pure IL at 40°C with 100 mol% $SO_2$**

# Appendix E

# Sample calculations

## E.1 Calculations for temperature experiments

In this section all of the calculations for the temperature experiments will be illustrated. The raw data that was obtained from the balance was shown in Section 4.1 as well as how the number of data points was reduced. Figure E.1 shows the experimental data of the experiment at 40°C with 100 mol% $SO_2$ in the feed stream and the 98% pure ionic liquid.

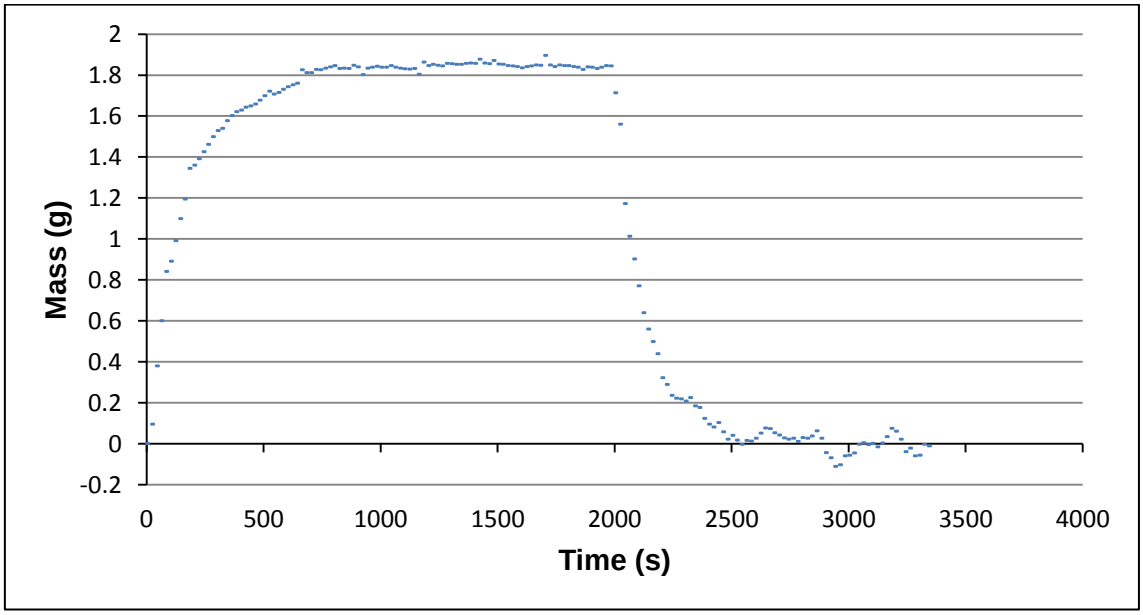


**Figure E.1: Experimental data at 40°C with 100 mol% $SO_2$ and the 98% pure ionic liquid**

The first step was to determine the maximum absorption for the experiment which was explained in Section 4.2.1. In order to determine the maximum absorption the average of the data points between time 1000 and 1900 seconds were determined:

$$Max\ SO_2\ absorbed = 1.847\ g$$

Now the amount of mole $SO_2$ that was absorbed into the ionic liquid per mole of ionic liquid was determined:

$$Mole\ SO_2\ absorbed\ per\ mole\ IL = \frac{Mole_{SO2}\ absorbed}{Mole_{\ IL}}$$

The $Mole_{SO2}$ absorbed was calculated as:

$$Mole_{SO2}\ absorbed = \frac{Max\ SO_2\ absorbed}{MW_{SO2}}$$

Where:

$MW_{SO2}$ – Molecular weight of $SO_2$ (64.066 g/mol)

The $mole_{IL}$ can be calculated as:

$$Mole_{IL} = \frac{V_{IL}\rho_{IL}}{MW_{IL}}$$

Where:

$V_{IL}$ – Volume of the ionic liquid used in the experiment (3 $cm^3$)

$\rho_{IL}$ – Density of the ionic liquid (1.21 $g/cm^3$)

$MW_{IL}$ – Molecular weight of the ionic liquid (250.32 g/mol)

Thus:

$$Mole_{IL} = \frac{(3)(1.21)}{250.32} = 0.0145\ mol$$

Now:

$$Mole_{SO2}\ absorbed = \frac{1.847}{64.066} = 0.0288\ mol$$

And:

$$Mole\ SO_2\ absorbed\ per\ mole\ IL = \frac{0.0288}{0.0145} = 1.988\ \frac{mol\ SO_2}{mol_{IL}}$$

After the mole $SO_2$ absorbed per mole ionic liquid the initial absorption rate of the $SO_2$ had to be calculated. This was done by calculating the initial slope of the $SO_2$ absorbed versus time graph (Figure E.1). In order to do this the average slope between the points from 20 seconds to 80 seconds was calculated:

$$Initial\ absorption\ rate\ = 0.012\ g/mol$$

This value is then converted to mol $SO_2$/mol IL·min:

$$Initial\ absorption\ rate\ = 0.803\ \frac{mol\ SO_2}{mol\ IL \cdot min}$$

Secondly the initial desorption rate was calculated as described in Section 4.2.3. This is similar to the way the initial absorption rate was calculated in this case the initial slope of the $SO_2$ absorbed versus time graph (Figure E.1) was calculated for the section after 2000 seconds when the $SO_2$ was desorbed. This was done by calculating the average slope between the points from 2100 seconds to 2160 seconds:

$$Initial\ desorption\ rate\ = 0.0046\ g/mol$$

This value is then converted to mol $SO_2$/mol IL·min:

$$Initial\ desorption\ rate\ = 0.294\ \frac{mol\ SO_2}{mol\ IL \cdot min}$$

Then the desorption time was calculated as described in Section 4.2.3. This is similar to the way the absorption time was calculated in this case the average value of the data points from time 2500 seconds to the end of the experiment was calculated. After which the time at which the data points reached the average value was determined, then the time from when the temperature was increased to when the data points reached the average value was calculated and this was the desorption time.

$$Desorption\ time = 540s$$

After this the maximum absorption data was modelled with the Langmuir absorption model which was discussed in Section 4.3.1. The mole amount of $SO_2$ that was absorbed by the ionic liquid was plotted versus partial pressure of $SO_2$ for each of the temperatures. The Langmuir equation was then used to calculate values for the mole $SO_2$ absorbed after which the method of least squares was used to calculate the fitted values for k and $x_{max}$. For the 98% pure ionic liquid at 40$^o$C the value of k = 0.7 1/bar and the $x_{max}$ value was 4.60 mol $SO_2$/ mol IL. After this the evaluation of the model was done in Section 4.3.2.

Finally the heat of desorption for the desorption reaction was calculated by using the Clausius-Clapeyron equation (Equation 4.3). Firstly $P_{SO2}$ was calculated by determining interpolated values for $P_{SO2}$ at three different $SO_2$ absorption amounts, namely 0.5, 1.0 and 1.5 mol $SO_2$/mol IL at each of the experimental temperatures. To determine these values Figure 4.23 and Figure 4.24 were plotted, that show the $SO_2$ absorption data versus the partial pressure of $SO_2$. The $SO_2$ partial pressures of the 98% pure ionic liquid at 40$^o$C for 0.5, 1.0 and 1.5 mol $SO_2$/mol IL was 0.22, 0.45 and 0.68 bar respectively. From this data the ln($P_{SO2}$) versus 1/T graphs were drawn. The slopes of the data in these graphs were then used to calculate the heat of desorption at each amount of $SO_2$ absorbed which is shown in Table 4.7.

## E.2 Calculations for pressure experiments

This section will show all of the calculations that were made for the pressure experiments. The raw data for one of the experiments will be taken and then all of the calculations that were made in order to calculate the percent of the gas that was absorbed into the ionic liquid

will be shown. The first step was to obtain the raw data, for this section the data from the experiment with the 95% pure ionic liquid at 3 bar(a) feed pressure with $SO_2$ was used. Table E.1 shows an example of data obtained from the pressure experiments.

**Table E.1: Example of raw data for pressure experiment**

| | **E-1 (bar(g))** | **E-2 (bar(g))** | **E-1 (Pa(a))** | **E-2 (Pa(a))** |
|---|---|---|---|---|
| **Vacuum** | -0.772 | -0.764 | 24125 | 24925 |
| **E-1 Pressurised** | 2.038 | -0.764 | 305125 | 24925 |
| **Equalised pressure** | -0.553 | -0.544 | 46025 | 46925 |

Table E.1 shows the pressure in both chamber E-1 and E-2 when the setup was under vacuum, when chamber E-1 was pressurised and after the pressure had been equalised, these pressures were obtained in bar(g) and then they were converted to Pa(a). The next step was to calculate the delta pressure between the vacuum and E-1 pressurised in order to calculate the amount of mole gas that was in E-1 before the gas was absorbed into the ionic liquid. This was done as follows:

$$Delta\ P = 305125\ \text{Pa} - 24125\ \text{Pa} = 281000\ \text{Pa}$$

After which the amount of mole in chamber E-1 was calculated with the ideal gas law:

$$Mole = \frac{\Delta \text{PV}}{\text{RT}}$$

Where :

Mole – Amount of mole in chamber E-1 before the gas is absorbed into the ionic liquid.

∆P – 281000 Pa

V – Volume of chamber E-1 ($18.9\times10^{-6}$ $m^3$)

R – Gas constant (8.314 J/molK)

T – Temperature (298 K)

$$Mole\ E-1\ before\ equalisation = \frac{(281000)(18.9\times10^{-6})}{(8.314)(298)} = 2.144\times10^{-3}\ mol$$

Then valve V-2 was opened and the gas was allowed to absorb into the ionic liquid after the pressure equalised the mole amount of gas was determined for both chamber E-1 and E-2

by again using the ideal gas law. Firstly the delta pressure between the pressurised E-1 and the equalised pressure was calculated for both E-1 and E-2:

$$\Delta P\ E-1 = 305125\ Pa - 46025\ Pa = 259100\ Pa$$

$$\Delta P\ E-2 = 24925\ Pa - 46925\ Pa = 22000\ Pa$$

Now the amount of mole in both E-1 and E-2 was calculated with the ideal gas law, where the temperature, gas constant and volume of E-1 remained the same as in the calculation above and the volume of E-2 is equal to $16.8\times10^{-6}$ $m^3$:

$$Mole\ E-1 = \frac{(259100)(18.9\times10^{-6})}{(8.314)(298)} = 1.671\times10^{-4}\ mol$$

$$Mole\ E-2 = \frac{(22000)(16.8\times10^{-6})}{(8.314)(298)} = 1.492\times10^{-4}\ mol$$

Hence the mole amount of gas that was absorbed by the ionic liquid can now be calculated:

$$Mole\ absorbed = Mole\ in\ E-1\ before\ eqialisation - (Mole\ E-1 + Mole\ E-2)$$

$$Mole\ absorbed = \ 2.144\times10^{-3} - \ (1.671\times10^{-4} + \ 1.492\times10^{-4}) = 1.827\times10^{-3}$$

In Chapter 5 the mole amount of gas that was absorbed into the ionic liquid per mole of ionic liquid was also calculated:

$$Mole\ absorbed\ per\ mole\ IL = \frac{Mole\ absorbed}{Mole\ IL}$$

$$Mole\ IL = \frac{V_{IL}\rho_{IL}}{MW_{IL}}$$

Where:

$V_{IL}$ – Volume of ionic liquid used (5 $cm^3$)

$\rho_{IL}$ – Density of ionic liquid (1.21 $g/cm^3$)

$MW_{IL}$ – Molecular weight of ionic liquid (250.32 g/mol)

$$Mole\ IL = \frac{(5)(1.213)}{250.32} = 2.423\times10^{-2}\ mol$$

Then:

$$Mole\ absorbed\ per\ mole\ IL = \frac{1.827 \times 10^{-3}}{2.423 \times 10^{-2}} = 7.542 \times 10^{-2}\ mol$$

This was done three times and the average value of the three experiments was taken as the mole value of gas absorbed per mole ionic liquid. The mole percent of the gas that was fed to the ionic liquid that was actually absorbed was also calculated:

$$Percent\ mole\ absorbed = \frac{Mole\ absorbed}{Mole\ E-1\ before\ equalisation} \times 100$$

$$Percent\ mole\ absorbed = \frac{1.827 \times 10^{-3}}{2.144 \times 10^{-3}} \times 100\ = 85.2\ mol\%$$

The percent value was also calculated for all three experiments and the average value taken as the final mole percent gas absorbed.

# Appendix F

# CD

The data on the CD will include:

- The desorption video discussed in Section 5.3.2.
- MSDS for [BMIm][$MeSO_4$].
- MSDS for Oxygen.
- MSDS for Sulphur dioxide.
- Digital copy of the dissertation.

# Safety Data Sheet

According to EC Directive 91/155/EEC

Date of issue: 08.05.2007
Supersedes edition of 22.09.2004

## 1. Identification of the substance/preparation and of the company/undertaking

*Identification of the product*

Catalogue No.: 490063

Product name: 1-Butyl-3-methylimidazolium methylsulfate for synthesis

*Use of the substance/preparation*

Solvent
Chemical for synthesis

*Company/undertaking identification*

Company: Merck KGaA * 64271 Darmstadt * Germany * Phone: +49 6151 72-0

Emergency telephone No.: Please contact the regional Merck representation in your country.

## 2. Composition/information on ingredients

CAS-No.: 401788-98-5

*M:* 250.32 g/mol

Formula Hill: $C_9H_{18}N_2O_4S$

## 3. Hazards identification

Causes burns.

Caution! Substance not yet fully tested.

The test results available so far do not permit a complete evaluation. Further risks cannot be excluded if the product is handled inappropriately.

## 4. First aid measures

After inhalation: fresh air. Call in physician.
After skin contact: wash off with plenty of water. Dab with polyethylene glycol 400. Immediately remove contaminated clothing.
After eye contact: rinse out with plenty of water with the eyelid held wide open. Immediately call in ophtalmologist.
After swallowing: make victim drink plenty of water, avoid vomiting (risk of perforation!). Immediately call in physician. Do not attempt to neutralize.

## 5. Fire-fighting measures

Suitable extinguishing media:
Water, $CO_2$, foam, powder.

Special risks:
Combustible. Development of hazardous combustion gases or vapours possible in the event of fire. The following may develop in event of fire: nitrogen oxides, sulfur oxides.

Special protective equipment for fire fighting:
Do not stay in dangerous zone without self-contained breathing apparatus. In order to avoid contact with skin, keep a safety distance and wear suitable protective clothing.

Other information:
Contain escaping vapours with water. Prevent fire-fighting water from entering surface water or groundwater.

## 6. Accidental release measures

Person-related precautionary measures:
Avoid substance contact. Do not inhale vapours/aerosols. Ensure supply of fresh air in enclosed rooms.

Environmental-protection measures:
Do not allow to enter sewerage system.

Procedures for cleaning / absorption:
Take up with liquid-absorbent material (e.g. Chemizorb® ). Forward for disposal. Clean up affected area.

## 7. Handling and storage

*Handling:*

No further requirements.

*Storage:*

Tightly closed. At +15˚C to +25˚C.

## 8. Exposure controls/personal protection

*Personal protective equipment:*

Protective clothing should be selected specifically for the working place, depending on concentration and quantity of the hazardous substances handled. The resistance of the protective clothing to chemicals should be ascertained with the respective supplier.

Respiratory protection: required when vapours/aerosols are generated.

Eye protection: required

Hand protection:

In full contact:

| | |
|---|---|
| Glove material: | nitrile rubber |
| Layer thickness: | 0.11 mm |
| Breakthrough time: | > 480 Min. |

In splash contact:

| | |
|---|---|
| Glove material: | nitrile rubber |
| Layer thickness: | 0.11 mm |
| Breakthrough time: | > 480 Min. |

The protective gloves to be used must comply with the specifications of EC directive 89/686/EEC and the resultant standard EN374, for example KCL 741 Dermatril® L (full contact), 741 Dermatril® L (splash contact).
This recommendation applies only to the product stated in the safety data sheet and supplied by us as well as to the purpose specified by us. When dissolving in or mixing with other substances and under conditions deviating from those stated in EN374 please contact the supplier of CE-approved gloves (e.g. KCL GmbH, D-36124 Eichenzell, Internet: www.kcl.de).

Other protective equipment: Suitable protective clothing.

Industrial hygiene:
Immediately change contaminated clothing. Apply skin- protective barrier cream. Wash hands and face after working with substance.

## 9. Physical and chemical properties

| | | | |
|---|---|---|---|
| Form: | | liquid | |
| Colour: | | brownish to brown | |
| Odour: | | | |
| pH value | | | not available |
| Melting point | | | not available |
| Boiling point | | | not available |
| Ignition temperature | | | not available |
| Flash point | | | not available |
| Explosion limits | lower | | not available |
| | upper | | not available |
| Density | | (20 ˚C) | 1.21 g/cm$^3$ |
| Solubility in Water | | | not available |

## 10. Stability and reactivity

*Conditions to be avoided*

Strong heating.

*Substances to be avoided*

Violent reactions possible with: strong oxidizing agents.

*Hazardous decomposition products*
in the event of fire: See chapter 5.

## 11. Toxicological information

*Acute toxicity*

Quantitative data on the toxicity of this product are not available.

*Further toxicological information*

After inhalation: Irritations of the mucous membranes, coughing, and dyspnoea.
After skin contact: burns.
After eye contact: burns.
After swallowing: burns in mouth, throat, oesophagus and gastrointestinal tract. Risk of perforation in the oesophagus and stomach.

*Further data*

Further hazardous properties cannot be excluded.
The product should be handled with the care usual when dealing with chemicals.

## 12. Ecological information

Ecotoxic effects:
Quantitative data on the ecological effect of this product are not available.

Further ecologic data:
Do not allow to enter waters, waste water, or soil!

## 13. Disposal considerations

*Product:*

Chemicals must be disposed of in compliance with the respective national regulations. Under www.retrologistik.de you will find country- and substance-specific information as well as contact partners.

*Packaging:*

Merck product packaging must be disposed of in compliance with the country-specific regulations or must be passed to a packaging return system. Under www.retrologistik.de you will find special information on the respective national conditions as well as contact partners.

## 14. Transport information

Road & Rail ADR, RID
UN 3265 AETZENDER SAURER ORGANISCHER FLUESSIGER STOFF, N.A.G.
(1-BUTYL-3-METHYL-IMIDAZOLIUMMETHYLSULFAT), 8, III

Inland waterway ADN, ADNR not tested

Sea IMDG-Code
UN 3265 CORROSIVE LIQUID, ACIDIC, ORGANIC, N.O.S.
(1-BUTYL-3-METHYL-IMIDAZOLIUM METHYL SULFATE), 8, III
Ems F-A S-B

Air CAO, PAX
UN 3265 CORROSIVE LIQUID, ACIDIC, ORGANIC, N.O.S.
(1-BUTYL-3-METHYL-IMIDAZOLIUM METHYL SULFATE), 8, III

The transport regulations are cited according to international regulations and in the form applicable in Germany . Possible national deviations in other countries are not considered.

## 15. Regulatory information

*Labelling according to EC Directives*

| | | |
|---|---|---|
| Symbol: | C | Corrosive |
| R-phrases: | 34 | Causes burns. |
| S-phrases: | 26-36/37/39-45 | In case of contact with eyes, rinse immediately with plenty of water and seek medical advice. Wear suitable protective clothing, gloves and eye/face protection. In case of accident or if you feel unwell, seek medical advice immediately (show the label where possible). |
| Additional labelling | Caution! Substance not yet fully tested. | |

## 16. Other information

*Reason for alteration*

General update.

*Regional representation:*

This information is given on the authorised Safety Data Sheet for your country.

*The information contained herein is based on the present state of our knowledge. It characterizes the product with regard to the appropriate safety precautions. It does not represent a guarantee of the properties of the product.*

# Material Safety Data Sheet

Oxygen

## Section 1. Chemical product and company identification

**Product name** : Oxygen

**Supplier** : AIRGAS INC., on behalf of its subsidiaries
259 North Radnor-Chester Road
Suite 100
Radnor, PA 19087-5283
1-610-687-5253

**Product use** : Synthetic/Analytical chemistry.

**Synonym** : Molecular oxygen; Oxygen molecule; Pure oxygen; O2; Liquid-oxygen-; UN 1072; UN 1073; Dioxygen; Oxygen USP, Aviator's Breathing Oxygen (ABO)

**MSDS #** : 001043

**Date of Preparation/Revision** : **6/16/2011.**

**In case of emergency** : 1-866-734-3438

## Section 2. Hazards identification

**Physical state** : Gas.

**Emergency overview** : DANGER!

GAS:
OXIDIZER.
CONTACT WITH COMBUSTIBLE MATERIAL MAY CAUSE FIRE.
CONTENTS UNDER PRESURE.
Do not puncture or incinerate container.
May cause severe frostbite.
LIQUID:
OXIDIZER.
CONTACT WITH COMBUSTIBLE MATERIAL MAY CAUSE FIRE.
Extremely cold liquid and gas under pressure.
May cause severe frostbite.

Do not puncture or incinerate container. Store in tightly-closed container. Avoid contact with combustible materials.

Contact with rapidly expanding gases or liquids can cause frostbite.

**Routes of entry** : Inhalation

**Potential acute health effects**

**Eyes** : May cause eye irritation. Contact with rapidly expanding gas may cause burns or frostbite. Contact with cryogenic liquid can cause frostbite and cryogenic burns.

**Skin** : May cause skin irritation. Contact with rapidly expanding gas may cause burns or frostbite. Contact with cryogenic liquid can cause frostbite and cryogenic burns.

**Inhalation** : Respiratory system irritation after overexposure to high oxygen concentrations.

**Ingestion** : Ingestion is not a normal route of exposure for gases. Contact with cryogenic liquid can cause frostbite and cryogenic burns.

**Medical conditions aggravated by over-exposure** : Acute or chronic respiratory conditions may be aggravated by overexposure to this gas.

**See toxicological information (Section 11)**

## Section 3. Composition, Information on Ingredients

| Name | CAS number | % Volume | Exposure limits |
|---|---|---|---|
| Oxygen | 7782-44-7 | 100 | |

## Section 4. First aid measures

No action shall be taken involving any personal risk or without suitable training.If it is suspected that fumes are still present, the rescuer should wear an appropriate mask or self-contained breathing apparatus.It may be dangerous to the person providing aid to give mouth-to-mouth resuscitation.

**Eye contact** : Check for and remove any contact lenses. Immediately flush eyes with plenty of water for at least 15 minutes, occasionally lifting the upper and lower eyelids. Get medical attention immediately.

**Skin contact** : None expected.

**Frostbite** : Try to warm up the frozen tissues and seek medical attention.

**Inhalation** : If inhaled, remove to fresh air. If not breathing, give artificial respiration. Get medical attention.

**Ingestion** : As this product is a gas, refer to the inhalation section.

## Section 5. Fire-fighting measures

**Flammability of the product** : Non-flammable.

**Products of combustion** : No specific data.

**Fire hazards in the presence of various substances** : Extremely flammable in the presence of the following materials or conditions: reducing materials, combustible materials and organic materials.

**Fire-fighting media and instructions** : Use an extinguishing agent suitable for the surrounding fire.

Apply water from a safe distance to cool container and protect surrounding area. If involved in fire, shut off flow immediately if it can be done without risk.

Contains gas under pressure. Contact with combustible material may cause fire. This material increases the risk of fire and may aid combustion. In a fire or if heated, a pressure increase will occur and the container may burst or explode.

**Special protective equipment for fire-fighters** : Fire-fighters should wear appropriate protective equipment and self-contained breathing apparatus (SCBA) with a full face-piece operated in positive pressure mode.

## Section 6. Accidental release measures

**Personal precautions** : Immediately contact emergency personnel. Keep unnecessary personnel away. Use suitable protective equipment (section 8). Eliminate all ignition sources if safe to do so. Do not touch or walk through spilled material. Shut off gas supply if this can be done safely. Isolate area until gas has dispersed.

**Environmental precautions** : Avoid dispersal of spilled material and runoff and contact with soil, waterways, drains and sewers.

**Methods for cleaning up** : Immediately contact emergency personnel. Stop leak if without risk. Use spark-proof tools and explosion-proof equipment. Note: see section 1 for emergency contact information and section 13 for waste disposal.

## Section 7. Handling and storage

**Handling** : High pressure gas. Do not puncture or incinerate container. Use equipment rated for cylinder pressure. Close valve after each use and when empty. Store in tightly-closed container. Avoid contact with combustible materials. Protect cylinders from physical damage; do not drag, roll, slide, or drop. Use a suitable hand truck for cylinder movement.

Never allow any unprotected part of the body to touch uninsulated pipes or vessels that contain cryogenic liquids. Prevent entrapment of liquid in closed systems or piping without pressure relief devices. Some materials may become brittle at low temperatures and will easily fracture.

**Storage** : Keep container tightly closed. Keep container in a cool, well-ventilated area. Separate from acids, alkalies, reducing agents and combustibles. Cylinders should be stored upright, with valve protection cap in place, and firmly secured to prevent falling or being knocked over. Cylinder temperatures should not exceed 52 °C (125 °F).
For additional information concerning storage and handling refer to Compressed Gas Association pamphlets P-1 Safe Handling of Compressed Gases in Containers and P-12 Safe Handling of Cryogenic Liquids available from the Compressed Gas Association, Inc.

## Section 8. Exposure controls/personal protection

**Engineering controls** : Use only with adequate ventilation. Use process enclosures, local exhaust ventilation or other engineering controls to keep worker exposure to airborne contaminants below any recommended or statutory limits.

**Personal protection**

**Eyes** : Safety eyewear complying with an approved standard should be used when a risk assessment indicates this is necessary to avoid exposure to liquid splashes, mists or dusts.

When working with cryogenic liquids, wear a full face shield.

**Skin** : Personal protective equipment for the body should be selected based on the task being performed and the risks involved and should be approved by a specialist before handling this product.

**Respiratory** : Use a properly fitted, air-purifying or air-fed respirator complying with an approved standard if a risk assessment indicates this is necessary. Respirator selection must be based on known or anticipated exposure levels, the hazards of the product and the safe working limits of the selected respirator.

The applicable standards are (US) 29 CFR 1910.134 and (Canada) Z94.4-93

**Hands** : Chemical-resistant, impervious gloves complying with an approved standard should be worn at all times when handling chemical products if a risk assessment indicates this is necessary.

Insulated gloves suitable for low temperatures

**Personal protection in case of a large spill** : Self-contained breathing apparatus (SCBA) should be used to avoid inhalation of the product.

**Product name**

Oxygen

**Consult local authorities for acceptable exposure limits.**

## Section 9. Physical and chemical properties

**Molecular weight** : 32 g/mole

**Molecular formula** : O2

**Boiling/condensation point** : -183°C (-297.4°F)

**Melting/freezing point** : -218.4°C (-361.1°F)

**Critical temperature** : -118.6°C (-181.5°F)

**Vapor density** : 1.105 (Air = 1) Liquid Density@BP: 71.23 lb/ft3 (1141 kg/m3)

**Specific Volume ($ft^3$/lb)** : 12.0482

**Gas Density (lb/$ft^3$)** : 0.083

## Section 10. Stability and reactivity

**Stability and reactivity** : The product is stable.

**Incompatibility with various substances** : Extremely reactive or incompatible with the following materials: oxidizing materials, reducing materials and combustible materials.

**Hazardous decomposition products** : Under normal conditions of storage and use, hazardous decomposition products should not be produced.

**Hazardous polymerization** : Under normal conditions of storage and use, hazardous polymerization will not occur.

## Section 11. Toxicological information

**Toxicity data**

**Other toxic effects on humans** : No specific information is available in our database regarding the other toxic effects of this material to humans.

**Specific effects**

**Carcinogenic effects** : No known significant effects or critical hazards.

**Mutagenic effects** : No known significant effects or critical hazards.

**Reproduction toxicity** : No known significant effects or critical hazards.

## Section 12. Ecological information

**Aquatic ecotoxicity**

Not available.

**Environmental fate** : Not available.

**Environmental hazards** : This product shows a low bioaccumulation potential.

**Toxicity to the environment** : Not available.

## Section 13. Disposal considerations

**Product removed from the cylinder must be disposed of in accordance with appropriate Federal, State, local regulation.Return cylinders with residual product to Airgas, Inc.Do not dispose of locally.**

## Section 14. Transport information

| Regulatory information | UN number | Proper shipping name | Class | Packing group | Label | Additional information |
|---|---|---|---|---|---|---|
| **DOT Classification** | UN1072<br><br>UN1073 | OXYGEN, COMPRESSED<br><br>Oxygen, refrigerated liquid | 2.2 | Not applicable (gas). |  <br>  | **Limited quantity**<br>Yes.<br><br>**Packaging instruction**<br>**Passenger aircraft**<br>Quantity limitation:<br>75 kg<br><br>**Cargo aircraft**<br>Quantity limitation:<br>150 kg<br><br>**Special provisions**<br>A52 |
| **TDG Classification** | UN1072<br><br>UN1073 | OXYGEN, COMPRESSED<br><br>Oxygen, refrigerated liquid | 2.2 | Not applicable (gas). |  <br>  | **Explosive Limit and Limited Quantity Index**<br>0.125<br><br>**ERAP Index**<br>3000<br><br>**Passenger Carrying Ship** |

| | | | | | | |
|---|---|---|---|---|---|---|
| | | | | | | Index<br>50<br><br>**Passenger Carrying Road or Rail Index**<br>75<br><br>**Special provisions**<br>42 |
| **Mexico Classification** | UN1072<br><br>UN1073 | OXYGEN, COMPRESSED<br><br>Oxygen, refrigerated liquid | 2.2 | Not applicable (gas). |  | - |

**"Refer to CFR 49 (or authority having jurisdiction) to determine the information required for shipment of the product."**

# Section 15. Regulatory information

## United States

**U.S. Federal regulations** :

**TSCA 8(a) IUR**: Partial exemption
**United States inventory (TSCA 8b)**: This material is listed or exempted.

**SARA 302/304/311/312 extremely hazardous substances**: No products were found.
**SARA 302/304 emergency planning and notification**: No products were found.
**SARA 302/304/311/312 hazardous chemicals**: Oxygen
**SARA 311/312 MSDS distribution - chemical inventory - hazard identification**: Oxygen: Fire hazard, Sudden release of pressure, Delayed (chronic) health hazard

**State regulations** :

**Connecticut Carcinogen Reporting**: This material is not listed.
**Connecticut Hazardous Material Survey**: This material is not listed.
**Florida substances**: This material is not listed.
**Illinois Chemical Safety Act**: This material is not listed.
**Illinois Toxic Substances Disclosure to Employee Act**: This material is not listed.
**Louisiana Reporting**: This material is not listed.
**Louisiana Spill**: This material is not listed.
**Massachusetts Spill**: This material is not listed.
**Massachusetts Substances**: This material is listed.
**Michigan Critical Material**: This material is not listed.
**Minnesota Hazardous Substances**: This material is not listed.
**New Jersey Hazardous Substances**: This material is listed.
**New Jersey Spill**: This material is not listed.
**New Jersey Toxic Catastrophe Prevention Act**: This material is not listed.
**New York Acutely Hazardous Substances**: This material is not listed.
**New York Toxic Chemical Release Reporting**: This material is not listed.
**Pennsylvania RTK Hazardous Substances**: This material is listed.
**Rhode Island Hazardous Substances**: This material is not listed.

## Canada

**WHMIS (Canada)** :

Class A: Compressed gas.
Class C: Oxidizing material.

**CEPA Toxic substances**: This material is not listed.
**Canadian ARET**: This material is not listed.
**Canadian NPRI**: This material is not listed.
**Alberta Designated Substances**: This material is not listed.
**Ontario Designated Substances**: This material is not listed.
**Quebec Designated Substances**: This material is not listed.

## Section 16. Other information

**United States**

**Label requirements** : GAS:
OXIDIZER.
CONTACT WITH COMBUSTIBLE MATERIAL MAY CAUSE FIRE.
CONTENTS UNDER PRESURE.
Do not puncture or incinerate container.
May cause severe frostbite.
LIQUID:
OXIDIZER.
CONTACT WITH COMBUSTIBLE MATERIAL MAY CAUSE FIRE.
Extremely cold liquid and gas under pressure.
May cause severe frostbite.

**Canada**

**Label requirements** : Class A: Compressed gas.
Class C: Oxidizing material.

**Hazardous Material Information System (U.S.A.)** :

| | |
|---|---|
| Health | 0 |
| Flammability | 0 |
| Physical hazards | 0 |

**liquid:**

| | |
|---|---|
| Health | 3 |
| Fire hazard | 0 |
| Reactivity | 0 |
| Personal protection | |

**National Fire Protection Association (U.S.A.)** :

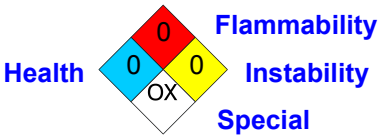


**liquid:**

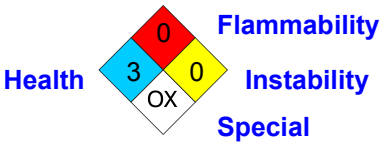


**Notice to reader**

**To the best of our knowledge, the information contained herein is accurate. However, neither the above-named supplier, nor any of its subsidiaries, assumes any liability whatsoever for the accuracy or completeness of the information contained herein.**
**Final determination of suitability of any material is the sole responsibility of the user. All materials may present unknown hazards and should be used with caution. Although certain hazards are described herein, we cannot guarantee that these are the only hazards that exist.**

# MATERIAL SAFETY DATA SHEET (MSDS)
# SULPHUR DIOXIDE



DATE: May 2010 Version 2

Ref. No.: MS 026

## 1 PRODUCT AND COMPANY IDENTIFICATION

| | |
|---|---|
| **Product Names** | SULPHUR DIOXIDE |
| **Synonym** | Sulfurous Acid Anhydride |
| **Chemical Formula** | $SO_2$ |
| **Trade Name** | Sulphur Dioxide |
| **Colour coding** | Brunswick green (H.O7) body with a Golden yellow (B49) shoulder Valve CGA 240 – Steel 3/8 inch 18 NGT right hand female |
| **Company Identification** | African Oxygen Limited<br>23 Webber Street<br>Johannesburg, 2001<br>Tel. No: (011) 490-0400<br>Fax No: (011) 490-0506 |
| **Emergency Number** | **086 011 1185 or**<br>**(011) 873 4382 [24 hours]** |

## 2 COMPOSITION/INFORMATION ON INGREDIENTS

| | |
|---|---|
| **Chemical Name** | Sulphur Dioxide |
| **Chemical Family** | Inorganic, acidic gas |
| **CAS No.** | 7446-09-5 |
| **UN No.** | 1079 |
| **ERG No**. | 125 |
| **Hazchem Warning** | Toxic and corrosive gas |

## 3 HAZARDS IDENTIFICATION

**Main Hazards**
All cylinders are portable gas containers, and must be regarded as pressure vessels at all times. Sulphur dioxide is a highly irritating gas; it readily elicits respiratory reflexes. It is intensely irritating to the eyes, throat, and respiratory tract.

**Adverse Health effects**
Inhalation of this gas in concentrations of 8-12ppm in air causes throat irritation, coughing, constriction of the chest, lachrimation, and smarting of the eyes. A concentration of 150 ppm can be endured only a few minutes, because of eye irritation and the effect on the membranes of the nose, throat and lungs. Exposure to a concentration of 500 ppm by volume in air for a few minutes is very dangerous.

**Chemical hazards**
Sulphur dioxide dissolves in water forming sulphurous acid, which is unstable toward heat. In many of its reactions, sulphur dioxide behaves as a reducing agent.

**Biological Hazards**
Liquid Sulphur dioxide may cause skin and eye burns upon contact with these tissues, which results from the freezing effect of the liquid on the skin or eyes. Low (1%) concentrations of the vapour are irritating to moist skin within a period of 3 minutes.

**Vapour Inhalation**
Acute exposure through inhalation may result in dryness and irritation of the nose and throat, choking, sneezing, coughing, and bronchospasm. Severe overexposure may cause death through systemic acidosis, from pulmonary oedema, or from respiratory arrest.

**Eye Contact**
Corneal burns, opacification of the cornea, and blindness may result if liquid Sulphur dioxide is splashed in the eyes. Sulphur dioxide can penetrate the intact cornea and cause iritis.

**Skin Contact**
Liquid sulphur dioxide can cause frostbite and skin burns, and it converts to sulphurous acid in moist environments, which may cause skin irritation.

**Ingestion**
Severe burns to the mouth, throat, and gastrointestinal system may occur.

## 4 FIRST AID MEASURES

Move victims of sulphur dioxide inhalation to fresh air. If breathing has ceased, begin artificial respiration immediately. Administer oxygen if exposure has been severe and breathing is difficult. Skin exposure first aid treatment includes flushing the contaminated skin with copious amounts of water, and continuing as required in order to control burning sensation. Medical attention should be sought if irritation persists, or if skin is broken or blistered. In the event of eye contact, flush eyes immediately with copious amounts of water for at least 15 minutes. Eyelids should be held apart to ensure complete irrigation. Seek medical attention immediately.

## 5 FIRE FIGHTING MEASURES

**Extinguishing Media**
As sulphur dioxide is non-flammable, the correct extinguishing media should be used for the surrounding fire.

**Specific Hazards**
Water should never be sprayed at or into a tank or system which is leaking sulphur dioxide. The presence of water causes sulphur dioxide to be very corrosive, and water directed into a tank would also increase the venting rate.

**Emergency Actions**
A sulphur dioxide container exposed to a fire should be removed. If for any reason it cannot be removed, the container should be kept cool with a water spray until well after the fire is out. Fire fighting personnel should be equipped with protective clothing and respiratory equipment. CONTACT THE NEAREST AFROX BRANCH.

**Protective Clothing**
Exposed fire fighters should wear approved self- contained breathing apparatus with full face mask.

**Environmental Precautions**
When sulphur dioxide is released to the environment, the appropriate regulatory agency should be notified. In the event of a release however, provincial, municipal, and/or local reporting regulations must be complied with. It is most important that the response groups in the area affected be notified as quickly as possible.

## 6 ACCIDENTAL RELEASE MEASURES

**Personal Precautions**
It is essential that every facility handling sulphur dioxide has an emergency plan outlining the actions that employees should take in case of specific emergencies. These actions should include alerting fellow employees and area emergency control groups of the nature and extent of the emergency. The plan should also include co-ordination procedures with area emergency control groups in the event of a major release. If, despite all precautions, persons should become trapped in a sulphur dioxide atmosphere, they should breathe as little as possible and open their eyes only when necessary. Partial protection may be gained by holding a wet cloth over the nose and mouth.

**Environmental Precautions**
Only personnel trained for and designated to handle emergencies should attempt to stop a leak. Respiratory equipment of a type suitable for sulphur dioxide must be worn. All persons not so equipped must leave the affected area until the leak has been stopped.

**Small spills**
If sulphur dioxide is released, the irritating effect of the vapour will force personnel to leave the area long before they have been exposed to dangerous concentrations. Sulphur dioxide is fairly soluble in cool water and therefore the vapour concentration can be reduced by the use of spray or fog nozzles. If disposal of sulphur dioxide becomes necessary, such as from a leaking container or vessel, it can be vented into a lime or caustic soda solution. The resulting salt solution should be taken to a plant treating unit for neutralisation and disposal.

**Large spills**
See "Personal Precautions" above.

## 6 HANDLING AND STORAGE

Sulphur dioxide should be handled only in a well-ventilated area, preferably a hood with forced ventilation. Personnel handling sulphur dioxide should wear chemical safety goggles and/or plastic face shields, approved safety shoes, and rubber gloves. Additional gas masks, air-line gas masks, and self-contained breathing apparatus should be conveniently located for use in emergencies. Instant-acting safety showers should be available in convenient locations. Cylinders should always be transported in the upright position, with the valve uppermost, and be firmly secured. Use the "first in - first out" inventory system to prevent full cylinders from being stored for excessive periods of time. Compliance with all relevant legislation is essential. Keep away from children.

## 8 EXPOSURE CONTROLS/PERSONAL PROTECTION

**Occupational exposure hazards**
Prolonged or repeated exposure may cause impaired lung function, bronchitis, hacking cough, nasal irritation and discharge, increased fatigue, alteration in the sense of taste and smell, and longer duration of common colds.

| | |
|---|---|
| TLV | 2 ppm |
| STEL | (15 minutes) 5 ppm |
| IDLH | 100 ppm |

**Engineering control measures**
Engineering control measures are preferred to reduce exposures. General methods include mechanical ventilation, process or personal enclosure, and control of process conditions. Administrative controls and personal protective equipment may also be required
.

**Personal protection**
Use an approved gas mask or self contained breathing apparatus when entering a sulphur dioxide contaminated area.

**Eyes**
Wear a chemical safety goggle or full face shield when handling cylinders.

**Hands**
Wear suitable protective gloves when handling cylinders.

**Feet**
Wear protective foot wear when working with cylinders.

**Skin**
Wear suitable protective clothing to prevent the gas from coming into direct contact with skin.

## 9 PHYSICAL AND CHEMICAL PROPERTIES

**PHYSICAL DATA**

| | |
|---|---|
| Chemical Symbol | $SO_2$ |
| Molecular Weight | 64,063 |
| Specific volume | @ 20°C & 101,325 kPa 366.9 ml/g |
| Relative density of gas | @ 101,325 kPa (Air = 1) 2,263 |
| Boiling point | @ 101,325 kPa - 10°C |
| Colour | None |
| Taste | Acidic |
| | Odour Pungent, Sulphurous |

## 10 STABILITY AND REACTIVITY

**Conditions to avoid**
Overheating of cylinders. Never use cylinders as rollers or supports; or for any other purpose than the storage of sulphur dioxide.

**Incompatible Material**
Moist sulphur dioxide is corrosive to carbon steel; therefore, other materials of construction have to be considered in this case.

**Hazardous Decomposition Products**
Sulphur dioxide is not flammable, or explosive, in either the gaseous or liquid state. It is a relatively stable chemical. Temperatures above 2000ºC are required to bring about detectable decomposition of sulphur dioxide.

## 11 TOXICOLOGICAL INFORMATION

**Acute Toxicity**
In extreme cases, dental cavities, loss of fillings, gum disorders, and the rapid and painless destruction of teeth may result from repeated overexposure. See section 3.

**Skin & eye contact**
See Section 3

**Chronic Toxicity**
See Section 3

**Carcinogenicity**
No known effect

**Mutagenicity**
No known effect

**Reproductive Hazards**
No known effect

## 12 ECOLOGICAL INFORMATION

**Environment**
Poses a severe hazard to the ecology in the form of "acid rain".

## 13 DISPOSAL CONSIDERATIONS

**Disposal Methods**
Due to the complexity and scope of sulphur dioxide disposal procedures, care must be taken to ensure that all existing regulations are complied with. For more detailed information or guidance. CONTACT THE NEAREST AFROX BRANCH.

## 14 TRANSPORT INFORMATION

**ROAD TRANSPORTATION**

| | |
|---|---|
| UN No. | 1079 |
| Class | 2.3 |
| Subsidiary risk | Toxic and corrosive gas |
| ERG No | 125 |
| Hazchem warning | Toxic and corrosive gas |

**SEA TRANSPORTATION**
IMDG 1079
Class 2.3
Label Toxic gas

**AIR TRANSPORTATION**

| | |
|---|---|
| ICAO/IATA Code | 1079 |
| Class | 2.3 |
| Subsidiary risk | Toxic and corrosive gas |

**Packaging instructions**
- Cargo 200
- Passenger Forbidden

Maximum quantity allowed
- Cargo 25 kg
- Passengers forbidden

## 15 REGULATORY INFORMATION

EEC Hazard class Toxic, Corrosive gas.

| | | |
|---|---|---|
| **Risk phrases** | R23 | Toxic By Inhalation |
| | R34 | Causes burns |
| | | |
| **Safety phrases** | S(1/2) | Keep locked up and out of reach of children |
| | S9 | Keep container in a well-ventilated place |
| | S26 | In case of contact with eyes, rinse immediately with plenty of water and seek medical advice |
| | S29 | Do not empty in drains |
| | S(36/37/39) | Wear suitable protective clothing, gloves and eye/face protection |
| | S45 | In case of accident or if you feel unwell, seek medical advice immediately and show label were possible |
| | S51 | Use only in well ventilated areas |
| | S57 | Use appropriate containment to avoid environmental contamination |

National legislation None
Refer to SANS 10265 for explanation of the above.

## 16 OTHER INFORMATION

Ensure all national/local regulations are observed. Ensure operators understand the toxicity hazard. Users of breathing apparatus must be trained. Ensure operators understand the toxicity hazard. Before using this product in any new process or experiment, a through material compatibility and safety study should be carried out.

**Bibliography**

Bibliography
Compressed Gas Association, Arlington, Virginia
Handbook of Compressed Gases - 3rd Edition
Matheson Gas Data Book - 6th Edition
SANS 11014 - Safety data sheet for chemical products: Content and order of sections
SANS 10265 – Classification and Labelling of Dangerous Substances

## 17 EXCLUSION OF LIABILITY

Information contained in this publication is accurate at the date of publication. Whilst AFROX made best endeavour to ensure that the information contained in this publication is accurate at the date of publication, AFROX does not accept liability for an inaccuracy or liability arising from the use of this information, or the use, application, adaptation or process of any products described here

# Appendix G

## Article

This section contains the article that was submitted to the International Journal of Hydrogen Energy:

# The effect of ionic liquid purity on the separation of $SO_2$ and $O_2$ in the HyS process

**[a]SL Rabie & [a*]M le Roux**

**Corresponding author: marco.leroux@nwu.ac.za Tel: +27 18 299 1990 Fax: +27 18 299 1535*

*[a]School of Chemical and Minerals Engineering*

*North-West University, Potchefstroom campus*

*Private Bag X6001*

*Potchefstroom*

*South Africa, 2522*

**Abstract**

In the HyS process sulphuric acid is decomposed to form $SO_2$ and $O_2$. After the decomposition step, it is necessary to purify the $SO_2$ before sending it to an electrolyser wherein $SO_2$-depolarised electrolysis of water occurs. Past success in using ionic liquids to act as an $SO_2$ solvent for the separation of $SO_2$ from $O_2$ is well documented. Most of these studies make use of high purity ionic liquids that is very expensive. This study was conducted to determine the use of a lesser pure ionic liquid for the separation of $SO_2$ from $O_2$. The amount of $SO_2$ that was absorbed as well as the absorption rate of $SO_2$ were determined at different feed pressures, absorption temperatures and feed gas compositions. In order to determine the effect of ionic liquid purity on the absorption process all of the experiments were carried out using both 95% and 98% pure 1-Butyl-3-Methylimidazolium methyl sulphate. Results obtained confirmed previous findings in terms of temperature, gas composition and feed pressure dependence of $SO_2$ absorption. It did however also confirm that the 95% pure ionic liquid performed similar or even better than the 98% pure ionic liquid. It can therefore be concluded that a less expensive option for use in thermo-chemical cycles is viable.

**Keywords:** Sulphur dioxide ($SO_2$), Oxygen ($O_2$), separation, Hybrid sulphur process, ionic liquid purity

## 1. Introduction

Fossil fuels currently meet most of the world's energy requirements; examples of these include burning coal to generate electricity, using oil to manufacture petroleum products,

which in turn is used to power vehicles, and using gas to heat homes. It is well documented that the burning of fossil fuels contributes towards atmospheric pollution. Apart from this negativity, fossil fuels are also a non-renewable energy source that is heading to depletion at a fast rate. For these reasons, it is important to explore alternative energy sources for future use. Hydrogen provides an excellent option as an energy carrier, which can be implemented in several sectors ranging from automotive to hardcore industrial manufacturing. The main advantages provided by hydrogen is, firstly, its abundance (it is one of the most abundant elements in the universe) and, secondly, the fact that it is a clean fuel (when hydrogen is combusted the only by-product is water vapour). Therefore, hydrogen is a very attractive option as alternative fuel source for the future [1].

One of the ways to manufacture hydrogen is by using a thermochemical cycle like the Hybrid Sulphur (HyS) cycle. In 2002, the HyS cycle was identified as the leading contender from 115 thermochemical hydrogen production cycles to produce hydrogen commercially [2]. The HyS cycle is one of the simplest thermochemical cycles due to the fact that it only has liquid reagents and consists of just two reaction steps. These two reactions are the decomposition of sulphuric acid at 800$^{o}$C [3]:

$$H_2SO_4 \rightarrow H_2O + SO_2 + \frac{1}{2}O_2 \quad (1)$$

and the $SO_2$-depolarised electrolysis of water [3]:

$$SO_2 + 2H_2O \rightarrow H_2 + H_2SO_4 \quad (2)$$

The first step in the HyS process is the decomposition of sulphuric acid at high temperatures, which is common to all sulphur cycles. According to reaction 1, it produces three products namely $H_2O$, $SO_2$ and $O_2$. From this product mixture, $O_2$ is removed while make-up water is added to the remaining $SO_2$ and $H_2O$. This mixture e is then fed to the anode side of the electrolyser where electrolysis takes place [3]. $H_2$ is produced at the cathode while $H_2SO_4$ is formed at the anode. $H_2SO_4$ is then recycled back to step one and the $H_2$ is removed as the main product [4].

In the original design of the HyS cycle, the removal of $O_2$ was achieved by a series of six knock-out drums followed by an absorption tower [2]. Although this design proved successful in separating $O_2$ from the mixture, it is rather capital and energy intensive. Kim et al. [5] proposed a separation technique for $SO_2$ and $O_2$ that was very similar to the Linde Solinox process. This technique consists of a separation and regeneration cycle for the separation of $SO_2$ and $O_2$ using temperature swing ionic liquid absorption. This technique was designed specifically for thermochemical cycles. Lee et al. [6] demonstrated the validity of using 99%

pure [BMIm][$MeSO_4$] (1-Butyl-3-Methylimidazolium methyl sulphate) for the separation of $SO_2$ and $O_2$. The results showed favourable absorption of $SO_2$ into the ionic liquid as well as almost perfect recovery of $SO_2$ from the ionic liquid at elevated temperatures above 110°C.

Huang et al. [7] studied the effect of temperature on the absorption amount of $SO_2$ into the ionic liquid, as well as the regeneration capabilities of the ionic liquid. Anderson et al. [8] also investigated the effect of temperature on the absorption capabilities of $SO_2$ into ionic liquids. Their study further included the effect of changes in the partial pressure of the $SO_2$ in the feed, from which Henry constants at three pressures were determined from the solubility data (although it was found that absorption happened outside the Henry regime, it was used for comparison with other systems). Finally, Lee et al. [6] studied the effect that different $SO_2$ compositions in the feed gas stream had at different temperatures on the amount of $SO_2$ absorbed. They also calculated the Henry constants for the different temperatures. Huang et al., Anderson et al. and Lee et al. concluded that [6-8]:

- The amount of $SO_2$ absorbed by the ionic liquid increased at lower absorption temperatures.
- $SO_2$ absorption increased at a higher $SO_2$ partial pressure in the feed stream.
- The absorption capability of the ionic liquid did not change after repeated use.
- The Henry constants of the ionic liquids decreased when the temperature was reduced, which also indicated that the absorption capability increased with decreasing temperature.

## 2. Experimental material and methods

### 2.1 Materials

Ultra high purity (UHP) $O_2$ with a purity of 99.995% and liquid $SO_2$ with a purity of 99.9% were purchased form Afrox in South Africa and used as received. The ionic liquid [BMIm][$MeSO_4$] with purities of 95% (Sigma-Aldrich) and 98% (Merck) were purchased and used as received. The 98% pure ionic liquid was about double the price of the 95% pure ionic liquid.

### 2.2 Project scope

The main aim of this study was to show the validity in using a lesser pure ionic liquid, [BMIm][$MeSO_4$], for the separation of $SO_2$ and $O_2$. This was achieved by following two approaches concerning the gas separation:

- Testing the temperature influence on the separation capabilities of both a 98% pure and 95% pure [BMIm][$MeSO_4$].
- Testing the influence of total feed gas and partial gas feed pressure on the separation capabilities of the above mentioned ionic liquids.

### 2.3 Temperature and partial pressure influence setup

Fig. 1 shows the process flow diagram for the experimental setup of the temperature influence tests. This figure shows that $SO_2$ and $O_2$ gas first flowed to mass flow controllers (Brooks), where the flows were adjusted to get the required composition for each experiment. The feed composition was set at 0%, 25%, 50%, 75% and 100% $SO_2$, with $O_2$ as the balance. Gas flowed to the absorption chamber from the mass flow controllers. Here, the gas was allowed to bubbled through the ionic liquid while the liquid temperature was controlled by the temperature controller (JCS-33A Shinko) coupled to a pre-calibrated external heater. 3 $cm^3$ of ionic liquid was used in the absorption chamber. The change in ionic liquid mass during gas absorption was measured by a balance (ADAM PGW 753i) and logged on a computer in real time. The excess $SO_2$ and $O_2$ gas exited the absorption chamber to the vent. The vent was configured in such a manner that it could be coupled to an online gas chromatograph (GC) for analyses of the composition thereof. After the ionic liquid had been saturated with $SO_2$ the chamber was heated to 125$^oC$ to desorb the $SO_2$ from the liquid; when desorption was completed and the ionic liquid cooled to room temperature it was ready to be used again.

In this study, the amounts of $SO_2$ that was absorbed, as well as the absorption and desorption rates of $SO_2$ were determined. Absorption was done at four temperatures namely 30ºC, 40$^oC$, 50$^oC$ and 60$^oC$. From these results, the influence of absorption temperature and feed gas composition on the ionic liquid's ability to absorb and desorb $SO_2$ was determined. Furthermore, the absorption and desorption of $O_2$ was investigated in parallel with the previously mentioned experiments.

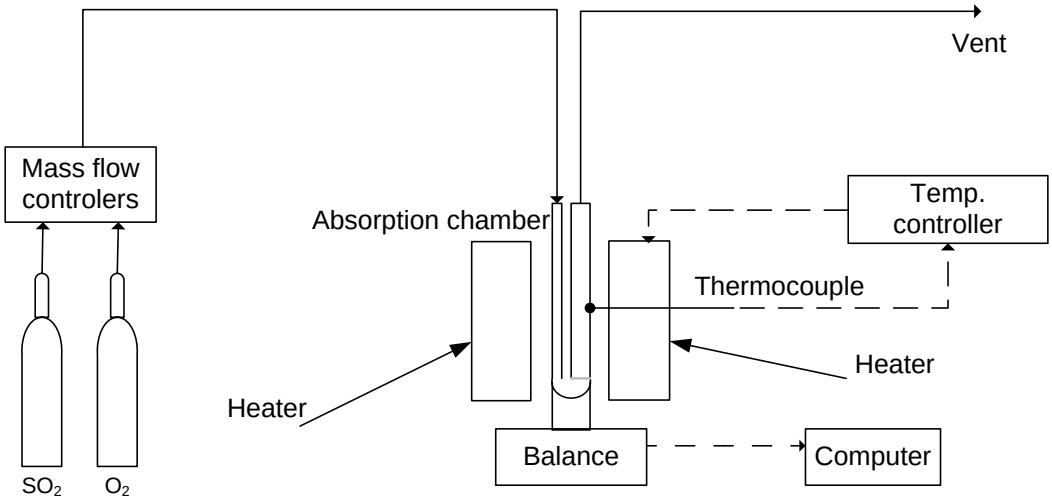


**Fig. 1: Process flow diagram for the temperature change experiment**

### 2.4 Feed pressure influence setup

Fig. 2 shows the process flow diagram of the experimental setup for the pressure influence tests. It can be seen that the gas, either pure $SO_2$ or pure $O_2$, enters the setup through valve V-1. From here the gas flows to the first pressure chamber where the pressure can be read of from pressure gauge 1 (WIKA Pressure gauge). This pressure was varied for the different experiments. Pressures of 1.5, 2.0, 2.5, and 3.0 bar(a) were used for both $SO_2$ and $O_2$, while additional pressures of 6.0 and 7.0 bar(a) were used for only $O_2$. At pressures higher than 3.0 bar(a) $SO_2$ started to liquefy, which is to be expected because the vapour pressure of $SO_2$ at 25$^{o}$C is in the range of 4.0 bar(a) [9]. After the pressure in the first chamber stabilised, the gas flowed through valve V-2 and the needle valve to the second pressure chamber, which was filled with 5 cm$^3$ of ionic liquid. A second pressure gauge was used to determine the gas pressure in this vessel. The amount of gas that was absorbed was determined by calculating the number moles of gas, using the ideal gas law, that was in pressure chamber 1 before the absorption and then comparing that with the number of moles of gas in the system after absorption into the ionic liquid. After the absorption, the excess gas was extracted by the vacuum pump (Edwards vacuum pump) and vented. The ionic liquid was then extracted from pressure chamber 2 and heated to between 130$^{o}$C and 150$^{o}$C to desorb all the gas that was absorbed, where after it was returned to the chamber for reuse.

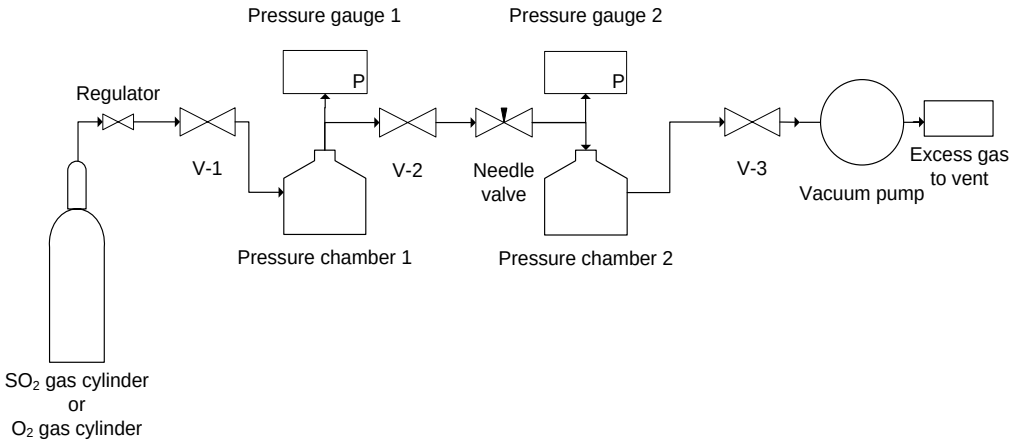


**Fig. 2: Process flow diagram for the pressure change experiment**

## 3. Results and discussion

### 3.1 Temperature and partial pressure influence

In Fig. 3 the influence of the feed gas composition on the maximum absorption of $SO_2$ is given, where graph (a) shows the data for the 95% pure ionic liquid and graph (b) the data for the 98% pure ionic liquid. In the results using 0% $SO_2$ (100% $O_2$) in the feed stream, the 95% pure ionic liquid absorbed 0.080 mol $O_2$/mol IL at 30$^o$C and 0.047 mol $O_2$/mol IL at 40$^o$C. This observation is consistent with the results found when the influence of feed pressure was done, and in the literature, namely that ionic liquids only absorb very small amounts of $O_2$ [10]. Keeping in mind the small amount of $O_2$ absorbed, the y-axis was duly labelled as pure $SO_2$ absorption.

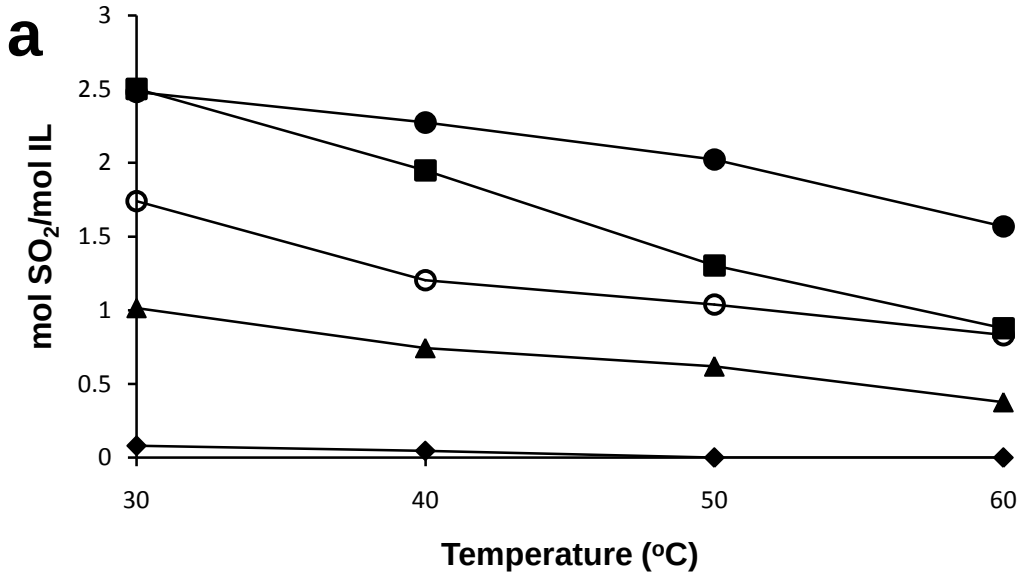

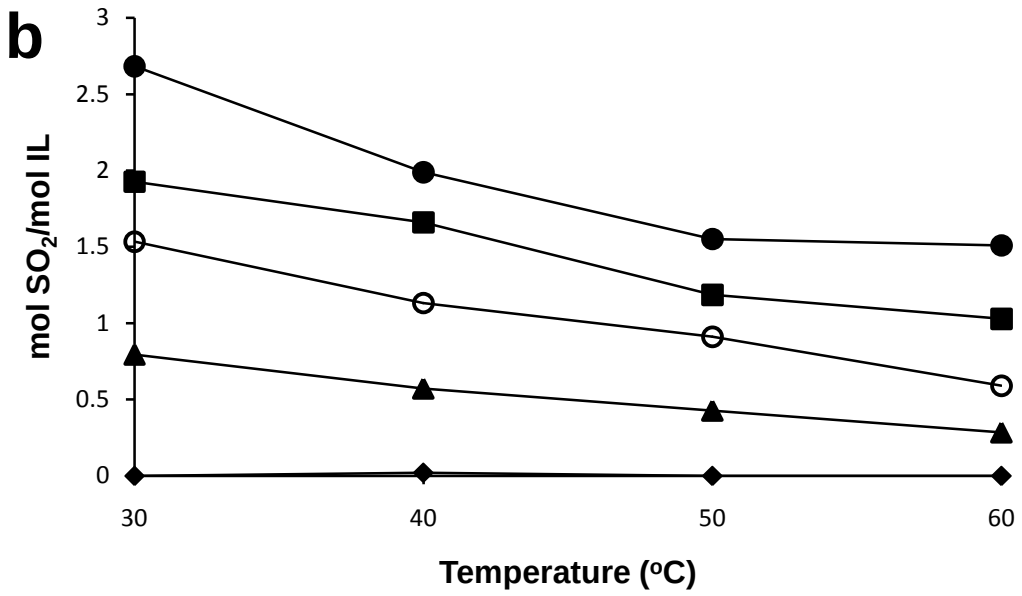


**Fig. 3: Maximum number of moles of $SO_2$ absorbed per mole of ionic liquid at different temperatures and feed compositions for (a) the 95% pure ionic liquid and (b) the 98% pure ionic liquid. -◆- 0% $SO_2$, -▲- 25% $SO_2$, - O - 50% $SO_2$, - ■ - 75% $SO_2$, - ● - 100% $SO_2$. (The lines in the graphs only give a visual indication of the trend of the data and are not a model.)**

From Fig. 3 it may be observed that the temperature of the ionic liquid had a considerable influence on the maximum absorption of the ionic liquid. The highest absorption occurred at 30$^o$C and the lowest at 60$^o$C, which is consistent with results obtained by Lee et al. [6] and Anderson et al. [8]. At 30$^o$C and with the feed gas stream at 100% $SO_2$ the ionic liquid absorbed 2.48 mol $SO_2$/mol IL for the 95% pure ionic liquid and 2.68 mol $SO_2$/mol IL for the 98% pure ionic liquid. It shows a good comparison between the different purity ionic liquids, which serves as a first indication that the lesser pure ionic liquid would be suitable for this separation. Fig. 3 also showed that as the feed percentage of $SO_2$ increased the amount of $SO_2$ absorbed per mole of ionic liquid increased for all temperatures. This is to be expected, because at higher feed percentages of $SO_2$ there is more $SO_2$ to absorb and, therefore, the absorption is higher.

In general it can be observed from Fig. 3 that the 98% pure ionic liquid does absorbs less $SO_2$ than the 95% pure ionic liquid, which implies that it would be better to use the 95% pure ionic liquid to absorb $SO_2$. However, from the data in Fig. 3 it may be noted that the 95% pure ionic liquid absorbed small quantities of $O_2$ while the 98% pure ionic liquid absorbed no $O_2$. It should be noted, however, that for 30$^o$C the 95% pure ionic liquid still absorbed

roughly 30 times more $SO_2$ than $O_2$, which means that even if some $O_2$ was absorbed the selectivity towards $SO_2$ was still very high.

$$\boldsymbol{d}(\ln \boldsymbol{P_{SO2}}) = -\frac{\boldsymbol{\Delta H_{abs}}}{\boldsymbol{R}} \boldsymbol{d}(\frac{\mathbf{1}}{\boldsymbol{T}}) \quad (1)$$

By using the Clausius-Clayperon relationship, Eq. 1, it was possible to determine the state of absorption for $SO_2$ into the ionic liquid. The heat of absorption ($\Delta H_{abs}$) was determined from the slope of the linear plot of $\ln P_{SO2}$ versus 1/T. Table 1 shows this calculated value for both ionic liquids at different absorption amounts. The higher values for the less pure ionic liquid are a general indication of a greater tendency towards absorption, as was confirmed by Fig. 3.

**Table 1: Heat of absorption calculation values.**

| **$SO_2$ absorbed (mol $SO_2$ /mol IL)** | **$\Delta H_{abs}$ (kJ/mol)** | |
|---|---|---|
| | **95% IL** | **98% IL** |
| **0.5** | 28.32 | 27.73 |
| **1.0** | 31.40 | 23.20 |
| **1.5** | 24.38 | 21.17 |

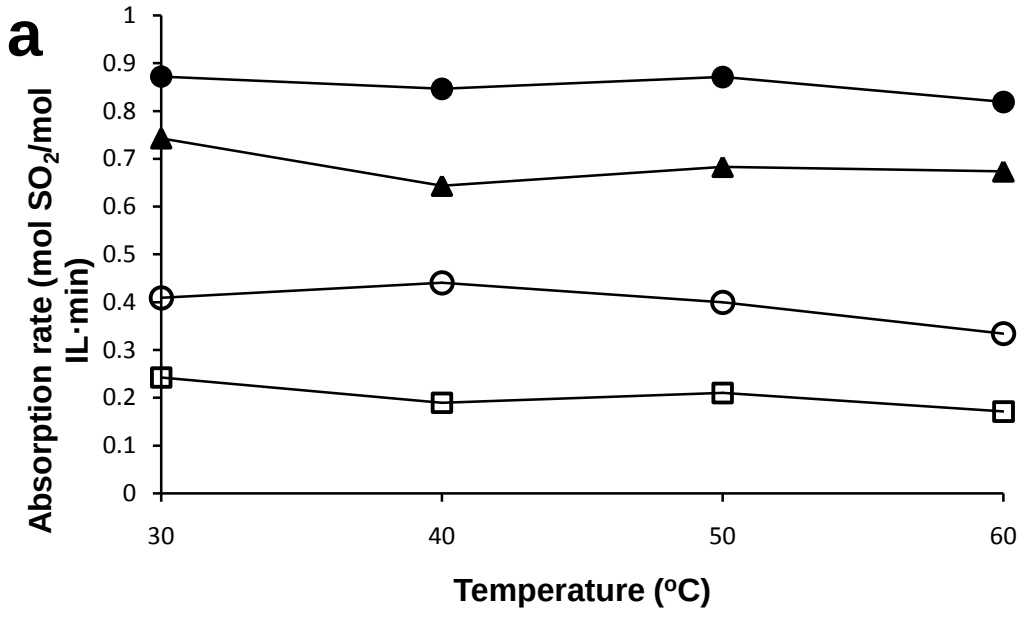

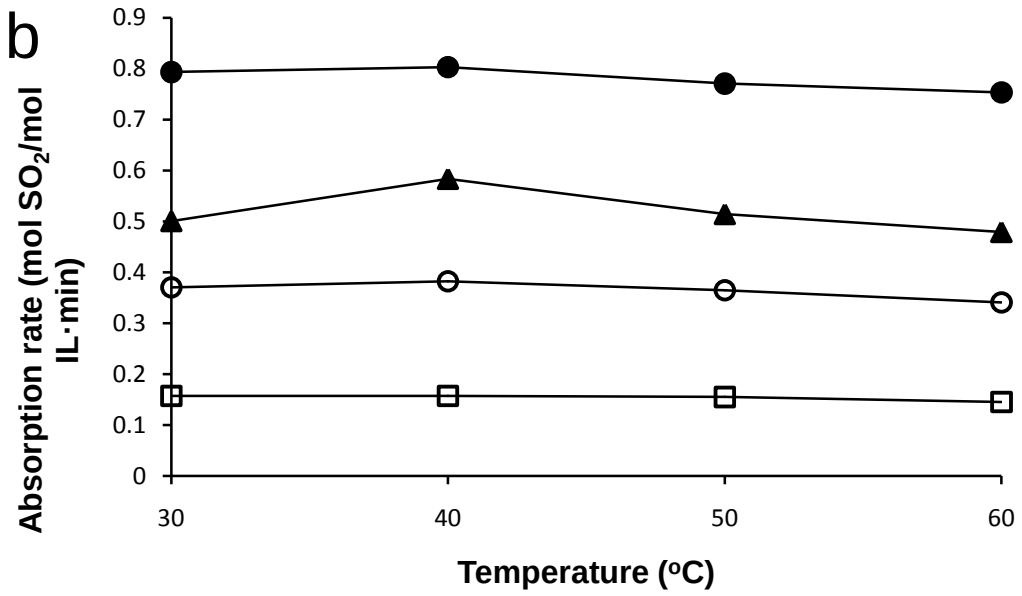


**Fig. 4: Absorption rate of the $SO_2$ into the ionic liquid at different temperatures and feed composition for (a) 95% pure ionic liquid and (b) 98% pure ionic liquid. - □ - 25% $SO_2$, - O - 50% $SO_2$, -▲- 75% $SO_2$, - ● - 100% $SO_2$.** (**The lines in the graphs only give a visual indication of the trend of the data and are not a model.)**

Fig. 4 showed the influence of the feed gas composition on the absorption rate, with Fig. 4(a) showing the data for the 95% pure ionic liquid and Fig. 4(b) the data for the 98% pure ionic liquid. In general, an increase percentage $SO_2$ in the feed led to an increase in the rate of absorption of gas into the ionic liquid. This can be expected since a higher $SO_2$ partial pressure results in an increase in the physical amount $SO_2$ available, which allows the ionic liquid to absorb the gas at a higher rate. However, it is clear to see from Fig. 4 that temperature had no influence on the absorption rate of each of the compositions, evident from the horizontal lines in Fig. 4. It does stand in contrast to the well-documented temperature dependency of the diffusion coefficient in Fick's law. It is believed that the decline in the amount of gas absorbed at higher temperatures by the ionic liquid does influence the rate of absorption at these points, showing the absorption rate to be pseudo independent for this system. When comparing the absorption rates achieved by the 95% pure and 98% pure ionic liquids in Fig. 4(a) and Fig. 4(b) respectively, the 95% pure ionic liquid yielded a higher absorption rate for all feed compositions that the 98% pure ionic liquid. In terms of implementation of the technology in the HyS cycle, the lesser pure ionic liquid outperforms the more pure one, at a fraction of the cost.

The desorption of $SO_2$ from both ionic liquids were done as described in the experimental setup above. Similar levels of desorption were achieved as documented by Lee et al [6], which was close to 100% removal of $SO_2$ from the ionic liquid. Fig. 5 shows the desorption times of the experiments at different feed compositions and temperatures for both ionic liquids. No correlation is visible between either desorption time and feed gas composition, or between desorption time and absorption temperature. There are furthermore no clear difference between the desorption times the different ionic liquids.

For a similar volume of ionic liquid, Lee et al [6] found the desorption time to be independent of the amount of gas absorbed, but highly dependent on the desorption temperature. At a desorption temperature of 130ºC, they found the desorption time to be 600s, similar to the average of Fig. 5. It can therefore be conclude that desorption time is mainly dependent on the desorption temperature, and not by the absorption temperature, feed composition or ionic liquid purity.

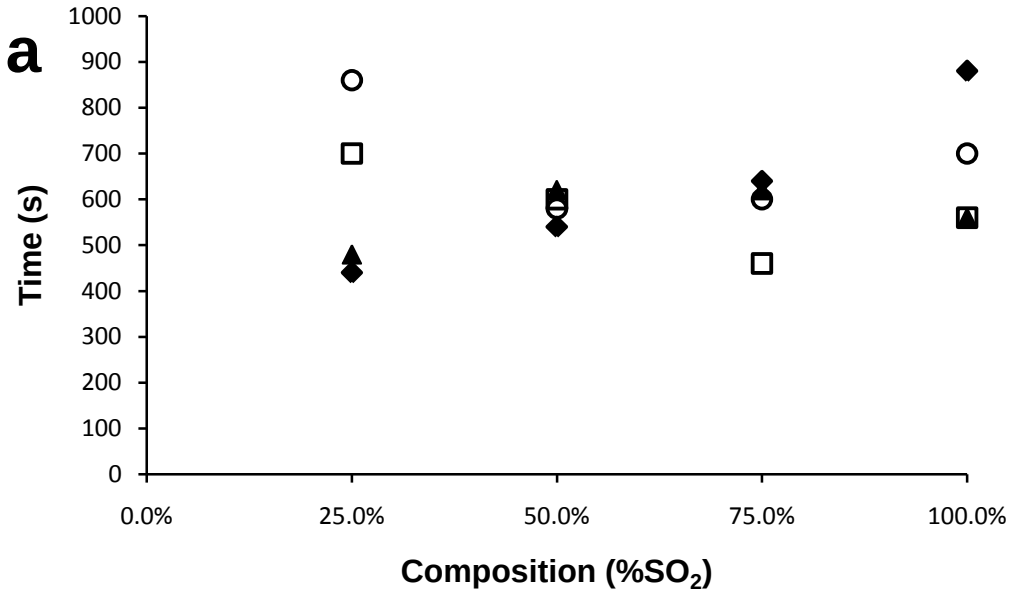

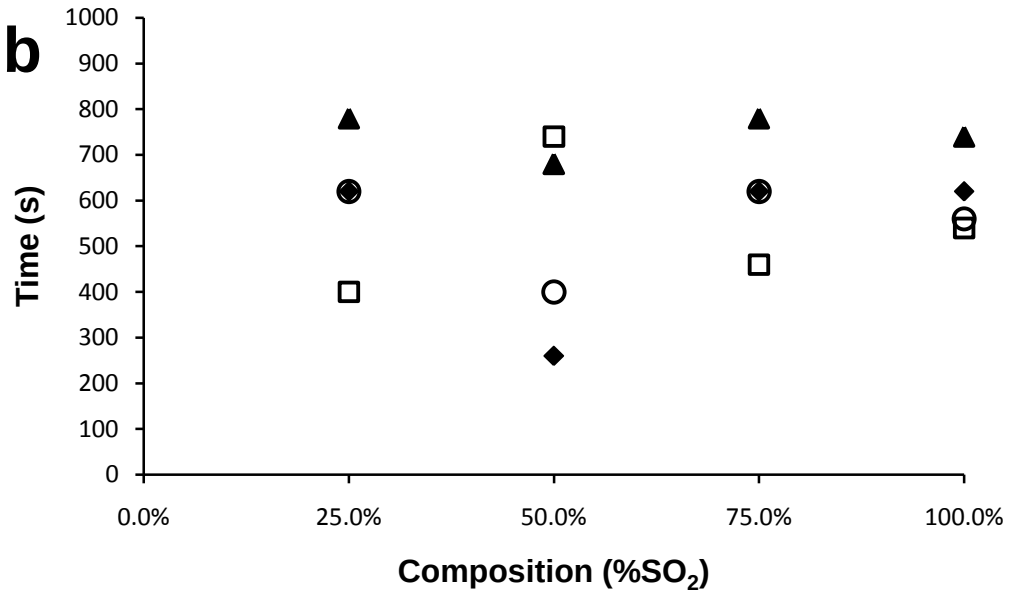


**Fig. 5: Time from the start of the desorption step until complete desorption was reached at different feed compositions and absorption temperatures for (a) the 95% pure ionic liquid and (b) the 98% pure ionic liquid. -▲- 30°C, - □ - 40°C, - ○ - 50°C, -◆- 60°C.**

The Langmuir absorption model was fitted to the data to describe the maximum theoretical absorption possible. The Langmuir equation can be expressed by Eq. 2 [11]:

$$\boldsymbol{x} = \frac{\boldsymbol{x_{max} kP}}{\boldsymbol{1 + kP}} \quad (2)$$

where x is the moles $SO_2$ absorbed per mole ionic liquid, $x_{max}$ is the theoretical maximum moles $SO_2$ absorbed per mole ionic liquid, k is the dissolution constant and P is the partial pressure of $SO_2$ in the feed stream. The fitted model showed a standard deviation of 17.07% calculated by Eq. 3 where SD is the standard deviation, $y_{exp}$ is the experimental value, $y_{calc}$ is the value predicted by the model, N is the number of data points and p is the number of fitted parameters [12].

$$\boldsymbol{SD} = \sqrt{\frac{\sum(\boldsymbol{y_{exp} - y_{calc}})^2}{\boldsymbol{N - p}}} \quad (3)$$

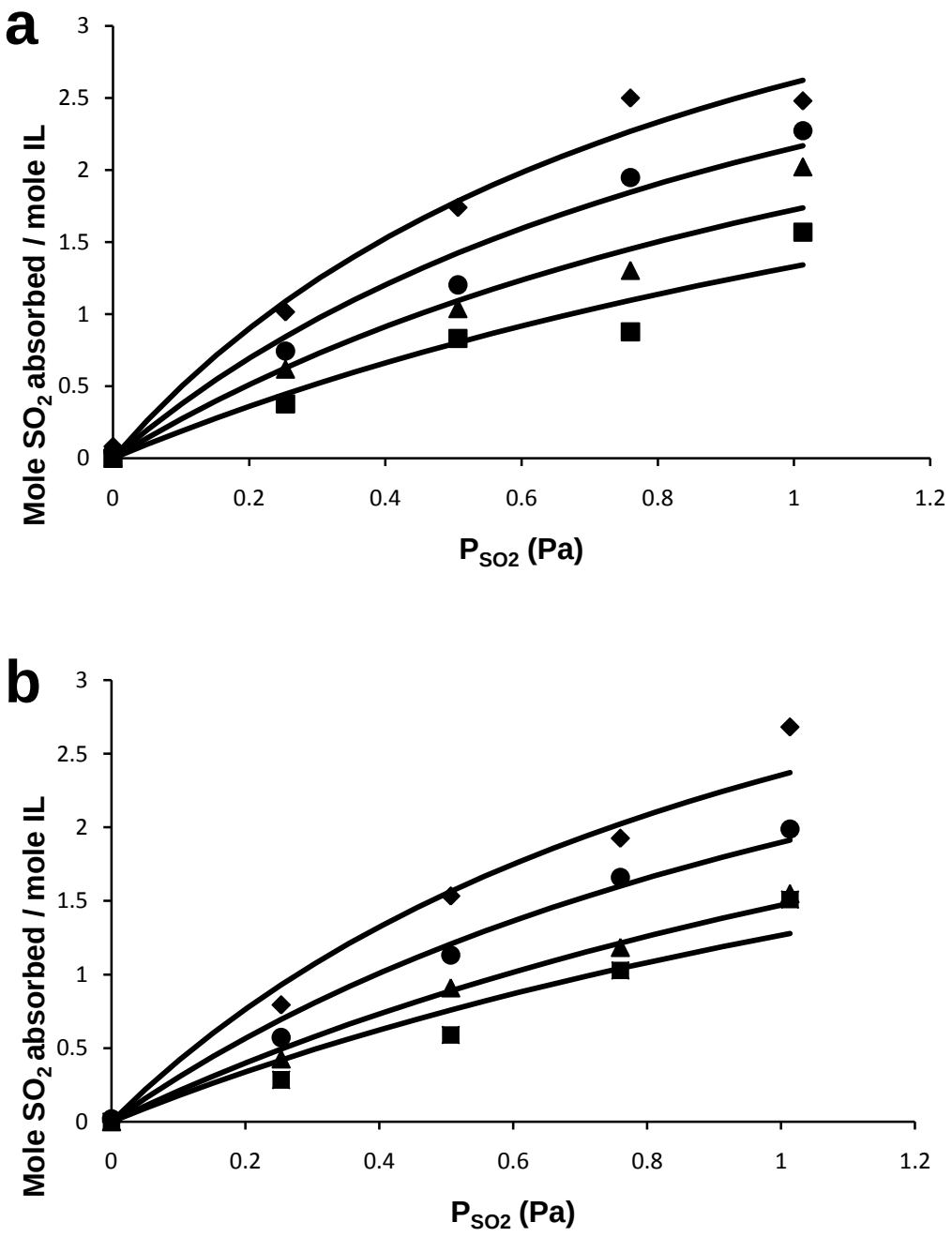


**Fig. 6: Comparison of how well the calculated model data fits the experimental data for (a) 95% pure ionic liquid and (b) 98% pure ionic liquid. -◆- 30°C, - O - 40°C, -▲- 50°C, - □ - 60°C, - model.**

From the fitted Langmuir models, the dissolution constant and theoretical maximum absorption was calculated, and given in Table 2. It clearly shows a higher dissolution constant for both ionic liquids at lower temperatures, and a higher value for the 95% pure ionic liquid at the same temperatures as for the 98% pure ionic liquid. A higher dissolution constant is an indication of a higher absorption rate. This is seconded in Fig 4, which indicated a higher absorption rate for the 95% pure ionic liquid. The maximum theoretical

amount of $SO_2$ absorption ranges from 4 to 5 moles $SO_2$ per mole ionic liquid, with the higher amounts at lower temperatures. There are a high degree of similarity between the different ionic liquid purities, which again increase the plausibility of using the lesser pure one.

**Table 2: Dissolution constants and theoretical maximum absorption.**

| Temperature ($^oC$) | k (1/bar) | | $x_{max}$ (mol $SO_2$/ mol IL) | |
|---|---|---|---|---|
| | 98% IL | 95% IL | 98% IL | 95% IL |
| **30** | 0.92 | 1.11 | 4.91 | 4.94 |
| **40** | 0.70 | 0.90 | 4.60 | 4.54 |
| **50** | 0.49 | 0.69 | 4.49 | 4.23 |
| **60** | 0.46 | 0.48 | 4.05 | 4.08 |

### 3.2 Pressure influence test results

Fig. 7 shows the mole% of the feed gas absorbed by the ionic liquid at each of the feed pressures for the 95% and 98% pure ionic liquid. It was seen that the absorption of $O_2$ into the ionic liquid remained constant over the whole range of feed pressures for both ionic liquids. Absorption between 4 mole% and 5 mole% was achieved. Therefore, it may be concluded that the molar percentage $O_2$ absorbed by the ionic liquid is independent on the feed pressure and ionic liquid purity. During the experiments with $O_2$, it was also observed that the pressure on the pressure gauges stabilised roughly five minutes after valve V-2 was opened to let the gas from the first pressure chamber bleed into the second chamber. This is an indication of the poor absorption rate for $O_2$ into this ionic liquid. After approximately five minutes, the maximum amount of $O_2$ had been absorbed.

For the $SO_2$ experiments, the pressure on the gauges did not stabilise after five minutes (as was observed in the experiments with the $O_2$), but continued changing for an extended period of time. During experimentation, absorption occurred very rapidly for the first ten minutes where after it slowed down as the concentration of the $SO_2$ in the chambers decreased. Because of this rapid decline in the absorption rate of $SO_2$ into the ionic liquid, it was decided to take the pressure reading in the second chamber ten minutes after opening valve V-2. The $SO_2$ data in Fig. 7 show a clear trend for both the 95% and 98% pure ionic

liquids. For the 95% pure ionic liquid, the mole percentage gas absorbed into the ionic liquid increased from 77.64% absorbed at 1.5 bar(a) to 85.87% at 3.0 bar(a). A similar increase was observed for the 98% pure ionic liquid; the absorption increased from 79.67% at 1.5 bar(a) to 87.90% at 3.0 bar(a). These absorption results were obtained after the setup was allowed to reach equilibrium after 10 minutes. The trends observed in Fig. 7 can be explained by Fick's law of diffusion, that is shown in Eq 4 below, where $J_{Az}$ is the molar flux of A in the positive z direction, $D_{AB}$ is the diffusion coefficient and $C_A$ is the molar concentration of A [13]:

$$\boldsymbol{J_{A_z} = -D_{AB}\frac{dc_A}{dz}} \quad (4)$$

Equation 4 shows that the molar flux, and thus the rate of mass transfer of A, or in this case $SO_2$, is influenced by the concentration gradient of $SO_2$. Because it is a closed system the concentration of $SO_2$ will increase when the feed pressure is increased. The fact that the system was allowed 10 minutes to reach equilibrium means that the $SO_2$ absorption will increase when the feed pressure is increased, as were seen from the results in Fig. 7.

From the data in Fig. 7 there is no clear difference between the amount of gas absorbed by the 95% pure ionic liquid and that absorbed by the 98% pure ionic liquid. Based on this data it would be more economically advantageous to use the 95% pure ionic liquid, because it is considerably less expensive than the 98% pure ionic liquid (IL).

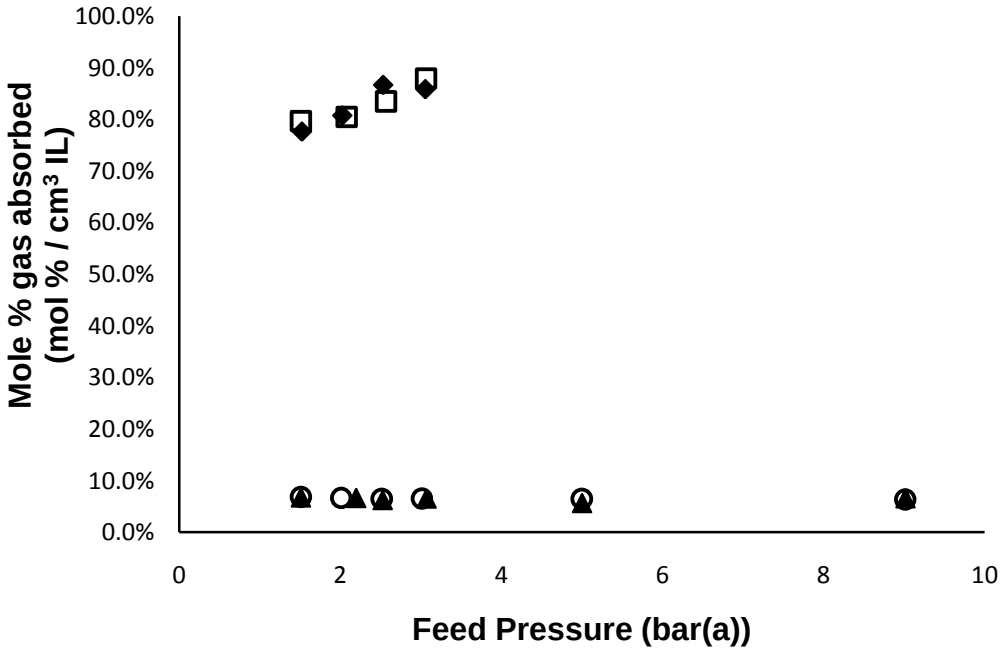

**Fig. 7: Mole% gas fed to the system absorbed by the ionic liquid at different feed pressures for 95% and 98% pure ionic liquid. -◆- % $SO_2$ absorbed in 95% IL, - □ - % $SO_2$ absorbed in 98% IL, -▲- % $O_2$ absorbed in 95% IL, - O - % $O_2$ absorbed in 98% IL.**

## 4. Conclusions

The possibility of using lesser ionic liquid to separate $SO_2$ and $O_2$ in the HyS process was investigated by considering the absorption capability of the different ionic liquids. The influence of feed pressure, absorption temperature, feed gas composition and ionic liquid purity on the ability of the ionic liquid to absorb and desorb $SO_2$ was determined. $SO_2$ absorption results at different temperatures indicated that the amount of gas absorbed increased when the temperature of the ionic liquid decreased, while the absorption rate remained constant over a range of different temperatures. The rate of absorption also increased when the percentage $SO_2$ in the feed stream was increased. The $SO_2$ absorption data was fitted with the Langmuir absorption model, from which dissolution constants and theoretical maximum absorption values were calculated. The dissolution constant showed a reliance on both temperature and ionic liquid purity, favouring lower temperatures as well as the lesser pure ionic liquid. In contrast, the theoretical maximum absorption was found to be dependent only on temperature, again favouring lower temperature. Maximum absorption values between the different liquids were found to be similar. The effect of feed pressure on the $SO_2$ absorption into the ionic liquid showed that when the feed pressure of the $SO_2$ was increased the amount of $SO_2$ absorbed also increased.

The main objective of the study was to determine the influence of the ionic liquid purity on the $SO_2$ absorption capacity of the liquid. For most part, the performance of the two ionic liquids was either very similar, of favoured the lesser pure one. Hence, it can be concluded that even with the $O_2$ that was absorbed it would be economically more advantageous to use the less expensive 95% pure ionic liquid rather than the more expensive 98% pure liquid, because $O_2$ would not influence the performance of the process negatively in the low quantities observed. This would be very beneficial for the commercialisation of the HyS process, due to the fact that ionic liquids are very expensive. This study illustrates that the less expensive 95% pure ionic liquid can be used instead of the more expensive 98% pure ionic liquid whilst still achieving adequate separation of $SO_2$ and $O_2$.

## 5. Acknowledgements

The authors wish to thank the HySA Research Hub for providing the necessary financial support to complete this project, as well as the School of Chemical and Minerals Engineering at the Potchefstroom Campus of the North-West University for supplying the laboratory and equipment used in the study.

## Nomenclature

| Symbol | Unit | Description |
|---|---|---|
| $C_A$ | $Mol/m^3$ | Molar concentration of A |
| $D_{AB}$ | $m^2/s$ | Diffusion coefficient |
| $\Delta H_{abs}$ | kJ/mol | Heat of absorption |
| $J_{Az}$ | $kg/s \cdot m^2$ | Molar flux of A in z direction |
| k | 1/bar | The dissolution constant |
| N | - | Number of data points |
| P | bar | Pressure |
| p | - | Number of fitted parameters |
| x | mol $SO_2$/mol IL | Amount of $SO_2$ absorbed into the ionic liquid |
| $x_{max}$ | mol $SO_2$/mol IL | Maximum amount of $SO_2$ absorbed into the ionic liquid |
| R | J/mol·K | Gas constant |
| T | $^oC$ | Temperature |
| $y_{exp}$ | - | Experimental value |
| $y_{calc}$ | - | Value predicted by the model |

## References

[1] B Johnston, MC Mayo, A Khare. Hydrogen: the energy source for the 21st century, Technovation. 25 (2005) 569-585.

[2] WA Summers, MB Gorensek, MR Buckner, The hybrid sulfur cycle for nuclear hydrogen production, (2005).

[3] MB Gorensek, WA Summers, CO Bolthrunis, EJ Lahoda, DT Allen, R Greyvenstein, Hybrid sulfur process reference design and cost analysis, (2009).

[4] J Leybros, A Saturnin, C Mansilla, T Gilardi, P Carles. Plant sizing and evaluation of hydrogen production costs from advanced processes coupled to a nuclear heat source: Part II: Hybrid-sulphur cycle, Int J Hydrogen Energy. 35 (2010) 1019-1028.

[5] CS Kim, KY Lee, GT Gong, H Kim, BG Lee, GD Jung, Sulfur Dioxide Separation and Recovery with Ionic Liquid Absorbents, 2010 (2008) 5.

[6] KY Lee, GT Gong, KH Song, H Kim, K Jung, CS Kim. Use of ionic liquids as absorbents to separate SO2 in SO2/O2 in thermochemical processes to produce hydrogen, Int J Hydrogen Energy. 33 (2008) 6031-6036.

[7] J Huang, A Riisager, RW Berg, R Fehrmann. Tuning ionic liquids for high gas solubility and reversible gas sorption, Journal of Molecular Catalysis A: Chemical. 279 (2008) 170-176.

[8] JL Anderson, JK Dixon, EJ Maginn, JF Brennecke. Measurement of SO2 solubility in ionic liquids, J Phys Chem B. 110 (2006) 15059-15062.

[9] Air Liquide, Gas Encyclopaedia, 2011 (2009).

[10] J Kumełan, ÁP Kamps, I Urukova, D Tuma, G Maurer. Solubility of oxygen in the ionic liquid [bmim][PF6]: Experimental and molecular simulation results, The Journal of Chemical Thermodynamics. 37 (2005) 595-602.

[11] C Locati, U Lafont, CJ Peters, EM Kelder. Interaction between carbon dioxide and ionic liquids: Novel electrolyte candidates for safer Li-ion batteries, J.Power Sources. 189 (2009) 454-457.

[12] J Ochoa, MC Cassanello, PR Bonelli, AL Cukierman. CO2 gasification of Argentinean coal chars: a kinetic characterization, Fuel Process Technol. 74 (2001) 161-176.

[13] JD Seader, EJ Henley, Separation process principles, 2nd ed., John wiley & Sons inc. 2006.